Year : 2017

EPIGENOME AS A THERAPEUTIC TARGET FOR LYMPHOMA

Bernasconi Elena

UNIL | Université de Lausanne
Faculté de biologie
et de médecine

Département
Institute of Oncology Research

EPIGENOME AS A THERAPEUTIC TARGET FOR LYMPHOMA

Thèse de doctorat ès sciences de la vie (PhD)

présentée à la

Faculté de biologie et de médecine
de l'Université de Lausanne

par

Elena Bernasconi

Master de l'Université de Milano Bicocca, Italie

Jury

Prof. Margot Thome Miazza, Présidente et Rapporteur
MD Francesco Bertoni, Directeur de thèse
Prof. Margot Thome Miazza, Rapporteur
Prof. Antonino Neri, Expert
Prof. Leonardo Scapozza, Expert
Prof. Stephan Dirnhofer, Expert

Lausanne 2017

UNIL | Université de Lausanne
Faculté de biologie
et de médecine

Ecole Doctorale

Doctorat ès sciences de la vie

Imprimatur

Vu le rapport présenté par le jury d'examen, composé de

Président·e	Madame Prof. Margot **Thome-Miazza**
Directeur·rice de thèse	Monsieur Dr Francesco **Bertoni**
Rapporteur·e	Madame Prof. Margot **Thome-Miazza**
Experts·es	Monsieur Prof. Antonio **Neri**
	Monsieur Prof. Stephan **Dirnhofer**
	Monsieur Prof. Leonardo **Scapozza**

le Conseil de Faculté autorise l'impression de la thèse de

Madame Elena Bernasconi

Master en biologie de l'Université de Milan, Italie

intitulée

EPIGENOME AS A THERAPEUTIC TARGET FOR LYMPHOMA

Lausanne, le 17 mars 2017

pour le Doyen
de la Faculté de biologie et de médecine

Thome-Miazza

Prof. Margot Thome-Miazza

INDEX

ABBREVIATIONS LIST

ABC	Activated B-cell like
AITL	Angioimmunoblastic T-cell Lymphoma
ALCL	Anaplastic Large Cell Lymphoma
AML	Acute myeloid leukemia
BD	Bromodomains
BET	Bromodomain and extra-terminal
BL	Burkitt Lymphoma
CLL	Chronic Lymphocytic Leukemia
CTCL	Cutaneous T-cell lymphoma
DLBCL	Diffuse Large B-cell Lymphoma
DZNep	3-deazaneplanocin A
ET	Extra-terminal
EZH2	Enhancer of zeste homolog 2
FDA	Food and Drug Administration
FL	Follicular Lymphoma
GC	Germinal Center
GCB	Germinal Center B-cell like
GEP	Gene Expression Profiling
GI50	Half maximal growth inhibition
GSEA	Gene Set Enrichment Analyis
HAT	Histone acetyltransferases
Hb-HDAC	Hydroxamic acids
HDAC	Histone de acethylase
HKMT	Histone lysine methyltransferases
HMT	Histone methyltransferases
IC50	Half maximal inhibitory concentration
IgH	ImmunoGlobulin Heavy chain
IgHV	ImmunoGlobulin Heavy chain Variable region
IgL	ImmunoGlobulin Light chain
KDM	lysine demethylases
LC50	Half maximal lethal concentration
MALT	Mucosa-Associated Lymphoid Tissue
MCL	Mantle Cell Lymphoma

MHC	Major histocompatibility complex
MM	Multiple myeloma
mTOR	mammalian Target Of Rapamycin
MZL	Marginal Zone Lymphoma
NMC	NUT midline carcinoma
NMZL	Nodal marginal zone lymphoma
P-TEFb	Positive transcription elongation factor b
PCR	Polymerase Chain Reaction
PCR2	Polycomb repression complex 2
PMBL	Primary mediastal B-cell lymphoma
Pol II	RNA polymerase II
PRMT	Protein arginine methyltransferases
PROTACs	Proteolysis Targeting Chimeras
PTCL	Peripheral T-cell Lymphoma
RAG	Recombination activating gene
RT-PCR	Real Time-PCR
SAH	S-adenosylhomocysteine
SAM	S-adenosylmethionine
SHM	Somatic hypermutation
siRNA	Short interfering RNA
SMZL	Splenic marginal zone lymphoma
TGI	Tumor growth inhibition
TLR	Toll like receptor
WHO	World Health Organization
WT	Wild-type

ABSTRACT

Lymphomas are neoplasms derived from lymphoid cells at various stages of development and they are among the ten most frequent types of human cancer. Their incidence has dramatically increased in the past several decades. Although lymphomas are among the most curable tumors, the mortality rate of lymphoma is still very high. Thus, the development of novel treatment strategies and the identification of biological and genetic relevant targets are urgent. Genes involved in chromatin remodeling are very frequently altered in lymphomas, indicating the importance of aberrant epigenetic mechanisms, and providing a rationale to evaluate drugs targeting pathway deregulated in lymphomas.

The aim of this work was to study the anti-lymphoma activity of novel epigenetic drugs, understanding their mechanism of action and identifying biologic and genetic features associated with responses. For this purpose, novel HDAC (ST7612AA1) and BET inhibitors (OTX015/MK-8628, BAY 1238097, BAY-7575 and BAY-5627) were studied in numerous lymphoma preclinical models.

ST7612AA1 is a potent pan-histone deacetylase inhibitor, that targets and consequently inhibits different class I and class II HDACs. Here, *in vitro* and *in vivo* significant antitumor activity in lymphomas was demonstrated, which was linked with an ability to induce transcriptional changes of several genes involved in key biologic processes.

OTX015/MK-8628 is a BET bromodomain inhibitor targeting BRD2-3-4 nuclear kinases and, here, it was tested as single agent and in combination with a series of conventional and targeted anti-lymphoma agents, in mature B-cell lymphomas. OTX015/MK-8628 targeted NFKB/TLR/JAK/STAT signaling pathways, MYC and E2F1-regulated genes, cell cycle regulation, and chromatin structure. OTX015/MK-8628 presented *in vitro* synergism with several anti-cancer agents, especially with mTOR and BTK inhibitors. Gene expression signatures associated with different degree of sensitivity to OTX015/MK-8628 were identified, and it was found that OTX015/MK-8628 induced apoptosis only in a genetically defined subgroup of cells, derived from activated B-cell like DLBCL, bearing WT *TP53*, mutations in *MYD88* and *CD79B* or *CARD11*.

Finally, a set of three novel BET bromodomain inhibitors (BAY-7575, BAY-5627 and remarkably BAY 1238097) showed a wide pre-clinical antitumor activity in lymphoma models. These inhibitors affected important biologic pathways, such as MYC, NFKB, TLR and JAK/STAT.

Through this work, new therapeutic strategies to target the epigenome of the lymphoma cells to possibly increase the curability of lymphoma patients could be developed.

Les lymphomes sont des néoplasmes dérivés de cellules lymphoïdes à diffèrent stades de développement et ils sont entre les dix cancers, les plus fréquents et leur incidence a considérablement augmenté au cours des dernières décennies. Bien que les lymphomes sériant parmi les tumeurs les plus soignable, encore trop de patients succombent pour leur maladie. Ainsi, le développement de nouvelles stratégies de traitement et l'identification de cibles biologiques et génétiques pertinentes sont urgents. Les gènes impliqués dans le remodelage de la chromatine sont très fréquemment altérés dans le lymphomes, ce qui indique l'importance des mécanismes épigénétiques aberrants, et fournit une méthode rationnelle pour évaluer les médicaments ciblant la voie déréglementée dans le lymphomes. Le but de ma thèse était d'étudier l'activité anti-lymphome des nouveaux médicaments épigénétiques, de comprendre leur mécanisme d'action et d'identifier les caractéristiques biologiques et génétiques associées aux réponses. Dans ce but, j'ai étudié les nouveaux inhibiteurs HDAC (ST7612AA1) et BET (OTX015/MK-8628, BAY 1238097, BAY-7575 et BAY-5627) dans de nombreux modèles précliniques de lymphomes.

ST7612AA1 est un puissant inhibiteur de pan-histone désacétylase (HDACi) qui cible et inhibe par conséquent différents HDAC de classe I et de classe II. Ici, j'ai montré *in* vitro et *in vivo* une activité antitumorale significative dans les lymphomes, qui a été apparié avec une capacité à induire des changements de transcription de plusieurs gènes impliqués dans les principaux processus biologiques. OTX015/MK-8628 est un inhibiteur de bromodomane BET ciblant BRD2-3-4 nucléaires kinases et, ici, il a été testé comme agent unique et en combinaison, dans les lymphomes à cellules B matures. OTX015/MK-8628 ciblé NFKB / TLR / JAK / STAT voies de signalisation, MYC et E2F1-gènes régulés, la régulation du cycle cellulaire et la structure de la chromatine. OTX015/MK-8628 a présenté une synergie *in vitro* avec plusieurs agents anticancéreux, et en particulier avec des inhibiteurs mTOR et BTK. Les signatures d'expression génétique associées à un degré différent de sensibilité à OTX015 ont été identifiées et OTX015/MK-8628 a induit l'apoptose uniquement dans un sous-groupe de cellules génétiquement défini, dérivé de lymphocytes B activés comme DLBCL, porteurs de *wtTP53*, de mutations dans *MYD88* et *CD79B* ou *CARD11*.

Enfin, un ensemble de trois nouveaux inhibiteurs du bromodomane BET (BAY 1238097, BAY-7575 et BAY-5627) et en particulier BAY 1238097 ont montré une large activité antitumorale préclinique dans les modèles de lymphomes et ils ont affecté des voies biologiques importantes, telles que MYC, NFKB , Les voies TLR et JAK / STAT.

En conclusion, j'ai identifié de nouvelles stratégies thérapeutiques pour cibler l'épigénome des cellules de lymphome afin d'augmenter éventuellement la guérison des patients atteints de lymphome.

INTRODUCTION

1. Principles of genetics and biology of lymphomas

Lymphomas are a heterogeneous group of neoplasms derived from lymphoid cells. They originate from either mature or immature B-cells, T-cells or natural killer cells. Lymphomas represent the sixth most frequent common cancer [1]. The phenotypic and biologic features of lymphomas derived from B-cells largely mirror the normal development and maturation of B-cells. An important key event in normal and neoplastic B-cells is the genetic rearrangement occurring at the *VDJ* locus, which can lead to chromosomal translocations and also to somatic mutations.

The identification of lymphoma subtypes allows a better evaluation of the pathogenesis and a more accurate therapy. In fact the various types of B-cell lymphoma can have very different clinical behaviors, and therefore require diverse treatment strategies [2].

1.1 Malignant transformation during germinal center (GC) B-cell development

During B-cell development in the bone marrow, recombination of *V, D* and *J* gene segments assembles immunoglobulin *heavy-chain* (*IgH*) and *light-chain* (*IgL*) genes. This process is characterized by the presence of two enzymes encoded by recombinase activating genes (RAG1 and RAG2) that cause breaks in double stranded DNA and the DNA repair processes (non homologous end-joining) that resolve and fix the breaks. However, such breaks can contribute to chromosomal translocations in lymphoma [3]. Naïve B-cells migrate to germinal center, undergo clonal expansion and differentiate into centroblasts in the dark zone. During this proliferation, the process of somatic hypermutation (SHM) introduces base pair changes into the *VDJ* regions and change the amino acid sequence. Centroblasts differentiate into centrocytes and move to the light zone where take place the selection through T-cells and follicular dendritic cells. Centrocytes that have negative selection, then reactive to self, undergo apoptosis. Antigen-selected centrocytes differentiate into memory B-cells or plasma cells.

Most B-cell lymphomas originate from GC as indicated by the presence of somatically mutated *IgV* genes. Moreover, the genomes of these B-cell lymphomas subtypes present distinctive recurrent primary chromosomal translocations and aberrant SHM, due to malfunctions in the immunoglobulin gene remodeling mechanisms [4]. Some of these base pair mutation lead to a change in the amino acid sequence that contribute to the pathogenesis of follicular lymphoma (FL), Burkitt's lymphoma (BL), germinal center diffuse large B-cell lymphoma (GCB-DLBCL), activated B-cell lymphoma (ABC-DLBCL) and Hodgkin's lymphoma.

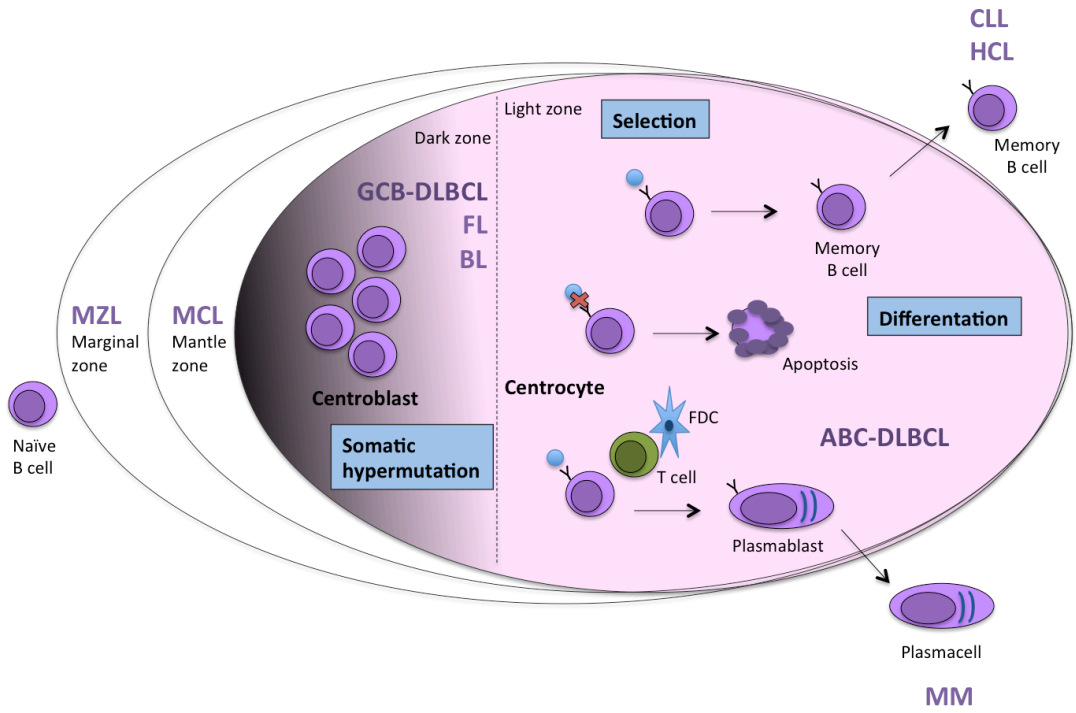

Figure 1. Different B-cell lymphomas arise from different stages in the normal life cycle of a lymphocyte (modified from Kuppers et al, Nat Rev Cancer 2005). Antigen activated B-cells differentiate into centroblasts in the dark zone, undergo clonal expansion and SHM process. Centroblasts differentiate into centrocytes and move to the light zone for selection. Centrocytes undergoes immunoglobulin class-switch recombination. Centrocytes differentiate into memory B-cells or plasma cells [5]. Most B-cell LYMPHOMASs originate from GCB-cells (as it is shown).

1.2 Lymphoma subtypes

Lymphomas comprise many subtypes and here the most common will be briefly presented [6, 7].

Diffuse large B-Cell Lymphoma (DLBCL) is the commonest lymphoma but it is likely to comprise different entities since it is a very heterogeneous disease in term of histological and clinic features. In 30-40% of cases in DLBCL there is a genetic alteration affecting the *BCL6* gene (chromosome 3q27) and in 20% of cases a translocation of the *BCL2* gene with *Ig* locus [8]. At least two major subtypes have been identified: the germinal center B-cell like (GCB-DLBCL) and activated B-cell like (ABC-DLBCL) subgroups. Genes that normally are highly expressed in GC B-cells are strongly expressed in GCB-DLBCL. So probably this subtype is derived from GCB-cell [9]. ABC-DLBCL subtype is characterized by a gene expression signature with features reminiscent of *in vitro* activated B-cells, pointing to a post GCB-cells as the cell of origin of these cases. ABC-DLBCL is characterized by the constitutive

activation of NF-κB pathway. Interestingly, the heterogeneity between the two DLBCL subtypes is also recognizable in terms of genomic aberrations [10, 11].

Primary mediastinal B-cell lymphoma (PMBL) is a relatively rare lymphoma subtype derived from thymic B-cells. Initially, it was classified as DLBCL subtype, but gene expression profiling (GEP) studies demonstrates a significant overlap between PMBL and nodular sclerosing Hodgkin lymphoma and mediastinal gray zone lymphomas [12]. The most common genetic alterations in PMBL are abnormalities on chromosome 9p (75%) and 2p (50%), these subtypes expresses several genes such as *CD30, IL-13* and *TARC* and may arise from thymic B-cells [13, 14].

Follicular Lymphoma (FL) is the most common indolent B-cell lymphomas and accounts for about 30% of all adult Lymphomas and, generally, FL patients present an indolent clinical course. Over time, some FL patients may develop a disease progression or undergo histological transformation to an aggressive lymphoma [15]. FL typically shows the t(14;18)(q32;q21) translocation, detected in approximately 85% of the cases. This translocation juxtaposes the *BCL2* gene on chromosome 18q21 to *IgH* enhancer on chromosome 14, leading to a constitutive expression of *BCL2*.

Mantle Cell Lymphoma (MCL) is an aggressive B-cell lymphomas that comprises about 3-10% of Lymphomas and presents a considerable clinical variability with a generally poor clinical outcome [16]. The cytogenetic peculiarity of MCL is the translocation t(11;14)(q13;q32) that leads to the over expression of *cyclin D1* gene, due to the juxtaposition of the *CCND1* gene on chromosome 11q13 to the *IgH* enhancer [17]. The translocation exhibits its pro-proliferative properties through inhibition of cell-cycle regulators RB1 and CDKN1B [18, 19].

Marginal Zone Lymphomas (MZLs) are divided into three subtypes: extranodal MZLs of mucosa-associated lymphoid tissue (MALT), nodal marginal zone lymphoma (NMZLs) and splenic marginal zone lymphoma (SMZLs) [20]. The incidence is about 12%, but it is difficult to distinguish subtypes because the subgroups share some similarities in histological features as well as some genetic lesions. Gains at 3q and 18q are common in all three subtypes; MALT frequently has specific translocations involving *API2*, *MALT1*, *BCL10*, and *FOXP1*. The commonest genomic aberrations in SMZLs are loss of 7q31 and somatic mutations affecting the *NOTCH2* and *KLF2* genes. Somatic mutations and deletions of *PTPRD* gene are found in NMZLs [21-23].

Burkitt's Lymphoma (BL) is an aggressive B-cell lymphoma. It often presents in extranodal sites. Three clinical variants can be recognized: the endemic, the sporadic and the immunodeficiency-associated cases, each manifesting differences in clinical presentation, morphology and biology. The cytogenetic peculiarity of all variants of BL is the

translocation involving *MYC* gene in chromosome 8q24 and the *IGHV* locus on chromosome 14q32 in more than 80% of cases, or the light chain loci [24]. The consequence of this translocation is the deregulated expression of *MYC*, which is a master regulatory gene. MYC plays a central role in cellular processes such as proliferation, differentiation and apoptosis, and that we will see is affected by treatment with BET Bromodomain inhibitors.

Chronic lymphocytic leukemia (CLL) is a generally indolent disease although some patients face a more aggressive clinical course. The most common genetic alterations include the loss of 13q14.3 *(miR-15a, miR-16-1*; 55% of cases), trisomy 12 (20%) and, less commonly, deletions of 11q22-23 (*ATM*), 17p13 (*TP53*) and 6q21 [25]. The distribution of these variable abnormalities based on the mutational status of *IGHV* gene is associated with different clinical outcomes. CLL had mutations on *NOTCH1* (12.2%), *MYD88* (2.9%)*, XPO* (2.4%) and *KLHL6* (1.8%) genes [26].

The **T-cell lymphomas** are a heterogeneous group of often rare diseases that are divided into two main groups: those arising from precursor cells correspond to the single entity called "lymphoblastic lymphoma", while lymphomas derived from mature lymphocytes are referred to as "peripheral T-cell lymphomas" (PTCLs). The PTCLs represent <15% of all Lymphomas [27]. Their classification is largely based on the presentation of the lymphoma, i.e. disseminated, nodal or extranodal/cutaneous disease.

While in B-cell lymphomas it is possible to identify the cell of origin, the cellular origin of PTCLs remains difficult to determine, although molecular profiling has recently allowed significant progress [28]. Some of the entities recognized by the WHO classification are very rare.

Peripheral T-cell lymphomas, not otherwise specified (PTCL, NOS) are a heterogeneous group of mature T-cell lymphomas, which do not correspond to any of the other specifically defined entities in the current WHO classification [29].

Angioimmunoblastic T-cell Lymphoma (AITL) is an aggressive and rare systemic disease, which represents about 1-2% of all Lymphomas. AITL characterized by consistent association with Epstein Barr virus (EBV), which suggests a pathogenic role for this virus, eliciting chronic antigen-driven T-cell-mediated response.

2. Epigenetic and cancer

Epigenetics is the branch of medicine that study the heritable changes in gene expression that do not involve alterations of the DNA sequence [30]. Epigenetic modulation is a key biological process in cell regulation [31]. The gene regulation occurs in the nucleosome, a very well organized structure in which DNA is packaged with eight histone proteins. Amino acid residues of the aforementioned histones can undergo post-translational modifications such as acetylation, methylation, and phosphorylation [32]. These modifications change the secondary structure in the nucleosome by increasing the distance between DNA and histones and by facilitating the link of transcription factors to gene promoter regions [33]. Chromatin remodeling is a dynamic biological process regulated via several enzymes. The latter can be broadly divided in three classes based on their function: writers, erasers and readers [34]. Writers are epigenetic proteins that promote the addition of post-translational modifications on histone; this family of enzymes contains histone acetyltransferases (HAT), histone methyltransferases (HMT), and kinases. Enzymes that remove these marks (post-translational modifications) are known as erasers and comprise histone deacetylases (HDAC), demethylases, and phosphatases. Epigenetic readers bind these epigenetic marks; to this class of enzymes belonging proteins containing bromodomains, chromodomains and tudor domains. Readers are effector proteins since they can recognize specific marks on histones or nucleotides [35]. While somatic DNA mutations, leading to inactivation of tumor suppressor genes or activation of oncogenes, are irreversible, epigenetic modifications can be reversed [36]. Thus, the latter can be potential targets for antitumor treatment. Indeed, the deregulation of the epigenetic control is common in cancer [37], via aberrant changes in DNA methylation, histone modifications and noncoding RNA expression levels [34, 38]. Also, genes involved in chromatin remodeling (*EZH2, MLL2, MEF2B, EP300, CREBBP*) are very often altered in lymphoma. These features indicate the importance of aberrant epigenetic mechanisms, and providing a rational to evaluate drugs targeting the lymphoma epigenome.

I will now describe the proteins involved in epigenetics regulation and their role in cancer in more detail.

Epigenetic writers are enzymes that catalyze the introduction of the post-translational modifications on target proteins. These dynamic modifications respond rapidly to environmental changes. Histone acetylases (HAT) and histone methyltransferases (HMT) are epigenetic writers that will be more extensively discussed in the following paragraphs.

2.1 Histone methyltransferases (HMTs)

Histone methylation involves two possible amino acid residues: lysine and arginine. Lysines can be monomethylated, dimethylated or trimethylated on their ε-amine group by histone lysine methyltransferases (HKMTs). Arginines can be monomethylated, symmetrically dimethylated or asymmetrically dimethylated on their guanidinyl group by protein arginine methyltransferases (PRMTs) [39]. HMTs transfer a methyl group from the cofactor *S*-adenosylmethionine (SAM) to the terminal amine of specific substrate lysine and/or arginine residues. The catalytic transfer of a methyl group from SAM by using a conserved SET domain, facilitate the SN2 transfer reaction generating *S*-adenosylhomocysteine (SAH) and the methylated histone side chain as products [40]. The transfer of an acetyl-group from the co-factor acetyl-CoA to lysine residues on histone tails neutralizes the positive charge of lysine, and it weakens the affinity of the histone tail for the DNA, reducing chromatin condensation. Methylation is associated with activated euchromatic genes (*H3K4, H3K36* and *H3K79*) or with silenced heterochromatic genes (*H3K9, H3K27* and *H4K20*) [41, 42].

Enhancer of zeste homolog 2 (EZH2) is the catalytic component of polycomb repression complex 2 (PCR2), which is responsible for tri-methylation of histone 3 lysine 27 (H3K27me3) [43]. The human PRC2 includes five subunits: EZH2, EED, SUZ12, RbAp46/48 and AEBP2. An important function of PRC2 is to silence genes involved in cell differentiation [44]. The AEBP2 subunit acts as a cofactor that interacts with the other four subunits by binding to the center of the PRC2 complex and helps the stabilization of PRC2 architecture. The AEBP2 subunit also facilitates the PRC2 complex targeting to specific DNA sites and enhances its methyltransferase activity [44]. In early B-cell development, EZH2 is required for *VDJ* recombination and is then subsequently down regulated in mature B-cells [45]. EZH2 regulates the expression of gene involved in differentiation and inhibitors of cell growth and proliferation such as *CDKN1A, CDKN1B* and *CDKN2* [46]. Polycomb-group proteins have been implicated in several cellular processes, including cell-cycle control, cancer, and senescence [35, 47-50].

Aberrancy in HMTs, such as *EZH2* and *MLL*, plays a role in pathogenesis of FL and DLBCL [46, 51]. Loss of function mutations in *MLL* are detected in 89% of FL and 32% of DLBCL [51], while mutations in *EZH2* are seen in 7–12% of FL, 22% of GCB-DLBCL [52, 53], 7% of BL [54] and in myeloid malignancies [55]. Furthermore, several other Lymphomas, including MCL [56], ALCL [57] and adult T-cell leukemia/lymphoma [58] show strong expression of *EZH2*. Somatic activating mutations in the SET domain of EZH2 have been identified in FL, and DLBCL, leading to increased H3K27me3 [51, 59]. In DLBCL *EZH2* presents several missense mutations in the catalytic SET domain that change a single highly evolutionarily conserved tyrosine residue (Tyr641 or wild-type) to phenylalanine (Y641F),

asparagine (Y641N), histidine (Y641H) or serine (Y641S) [60]. The wild-type (WT) enzyme is more efficient as a mono-methyltransferase and decreases in catalytic efficiency for the second and especially the third methylation reaction. In contrast, all the mutant enzymes, observed in lymphoma cells, are effective in catalyzing the reaction of mono- and di-methyl are very efficient in catalyzing the reaction of di- tri-methyl [61]. In naive B-cells and in GC B-cells, *EZH2* is normally downregulated, but upregulated in actively proliferating GC B-cells [62, 63]. In DLBCL, EZH2 is important for G2/S transition and represses cell-cycle of tumor suppressor genes through tri-methylation of H3K27 [62]. Based on these data EZH2 appeared as a good therapeutic target.

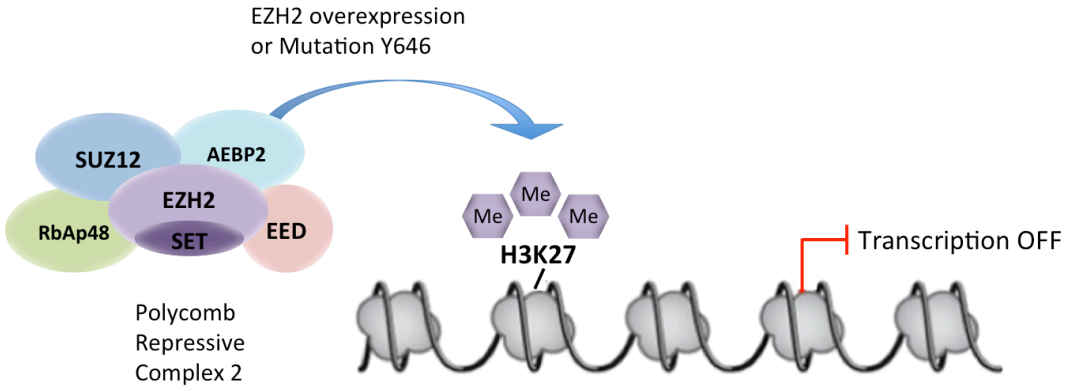

Figure 2. The interaction and effect of EZH2 in regulation of transcriptional repression (adapted from Martinez-Garcia, 2010). PRC2 exerts methyltransferase activity to H3K27 via the SET domain of the EZH2 subunit [42].

2.1.1 HMT inhibitors

HMT inhibitors are a new class of drugs that target epigenetic and in particular EZH2 [64]. 3-deazaneplanocin A (DZNep) is the cyclopentanyl analog of 3-deazaadenosine, an inhibitor of SAH hydrolase. DZNep inhibits and induce the degradation of the PRC2 complex [61], with loss of H3K27me3. Also, it induces the F-box protein FBXO32, a component of the SCF ubiquitin protein E3 ligase complex, associated with apoptosis of cancer cells [65]. In MCL cell lines DZNep induces cell-cycle arrest and apoptosis [66]. Depletion of EZH2 by short interfering RNA (siRNA) also induces the levels of p16, p21, p27, and FBXO32, which indicate that DZNep-mediated depletion of EZH2 is responsible for modulating these protein levels and growth inhibition in MCL cells [66]. DZNep is not a specific inhibitor of EZH2, and it can affect the methylation status of chromatin marks other than H3K27 [67].

Different EZH2 inhibitors are now under active preclinical and clinical investigation [68]. GSK126, used in the work presented in this thesis, is a specific EZH2 inhibitor [69]. GSK126 significantly increases cell death in non-small cell lung cancer, prostate cancer [70], skin cancer [71], colorectal cancer [72] and lymphoma cell lines [73]. Importantly, GSK126 inhibits both mutant Y641 EZH2 and WT GSK126 induces in DLBCL cell lines a 50% loss of H3K27me3 levels in both WT and mutant and induces transcriptional activation of EZH2 target genes in sensitive cell lines [73].

2.1.2 Histone acetyltransferases (HATs)

HATs use acetyl-CoA as a cofactor and catalyze the transfer of an acetyl-group to the ε-amino group of lysine side chains on the histone protein. This process causes the neutralization of the positive charge of lysine and reduced the affinity of the histone tail that protrudes from the nucleosome core of DNA. As final result, chromatin relaxes and by modifying its structure allow the recruitment of proteins and initiation of transcription [40]. Type A HATs are nuclear proteins that acetylate chromatin-associated proteins and histones, comprise three families of enzymes GNATs, EP300/CREBBP and MYST. Type B HATs are located in the nucleus and the cytoplasm, where they acetylate newly synthesized cytoplasmic histones to promote their nuclear localization and deposition onto nascent DNA chains [74]. KAT1 is the only HAT in the type B group.

Mutations affecting the chromatin have been detected in genes coding for HATs CREBBP and EP300 [75] and HAT-recruiting protein MEF2B [51]. CREBBP and EP300 proteins are co-activators of transcription factors and acetylate many proteins including P53, Hsp90, and NF-kB [67, 76, 77]. EP300 is a direct target of BCL6. In DLBCL, BCL6 inhibitors can stimulate EP300 protein function *in vivo* and *in vitro*, leading to activation of tumor-suppressor activity [77]. Deletions and/or somatic mutations of CREBBP or EP300 are detected in approximately 39% of DLBCL, 41% of FL [78], 13% of GCB-DLBCL and 15% of FL displayed recurrent point mutations in the MADS box or MEF2 domains of the *MEF2B* gene [51, 79, 80]. Mutations affecting the HAT activity of CREBBP and EP300 promote the activation of BCL6 and Hsp90 while destabilizing P53 [77, 78]. The balance between HATs and HDACs can be pharmacologically manipulated using HDAC inhibitors and preclinical studies suggest that DLBCL with CREBBP and/or EP300 mutations may be resistant to this strategy [77].

2.2 Epigenetic erasers in cancer

The overexpression of several HDACs have been implicated as an important oncogenic mechanism in different types of cancers, including ovarian, gastric, lung, breast, pancreatic, colorectal, prostate cancer, myeloid leukaemia and lymphoma [4, 81-86].

HDACs 1 and 2 are critical for B-cell development and are required for proliferation induced by mitogens in mature B-cells [87]. In primary ABC- and GCB-DLBCL samples the expression of HDACs 1 and 2 has been found to be elevated relative to normal lymphoid tissue [88, 89]. In DLCBL and PTCL HDAC1, 2 and 6 were found to be highly expressed [88], while in cutaneous T-cell lymphoma (CTCL) HDAC2 have a prognostic significance [90]. HDACs inhibition induces cell differentiation, transcriptional control and arrest of cell growth or prevention of tumor development in animal models [91]. HDAC3 is implicated in STAT3-positive DLBCL, as a direct interaction partner of STAT3, important for STAT3 phosphorylation and activity [92].

2.2.1 HDAC inhibitors

Epigenetic erasers remove epigenetic marks (post-translational modifications), and they comprise HDACs, lysine demethylases (KDMs) and phosphatases [41]. HATs acetylate ε-amino lysine residues located in the NH_2-terminal, creating a tail of core histones open chromatin conformation associated with transcriptional activation. Conversely, HDACs catalyze the deacetylation of α-acetyl lysine residues through creating a closed chromatin conformation that is associated with transcriptional repression [93-95]. HDACs remove acetyl-groups from the ε-amino group of lysine side chains of the histones H2A, H2B, H3, and H4, thus reconstituting the positive charge on the lysine. HDACs affect several substrates, including transcription factors, signal transcription mediators, DNA repair enzymes, chaperones and structural proteins [96]. HDACs can be classified into four classes:

class I: are predominantly localized in the nucleus and comprise HDAC1, HDAC2, HDAC3 and HDAC8;

class II: are subdivided into class IIa (HDAC4, HDAC5, HDAC7 and HDAC9) and class IIb (HDAC6 and HDAC10), shuttle between the nucleus and cytoplasm;

class III: comprise the Sirtuins, mainly localized in the nucleus and mitochondrion. Differently from the zinc-dependent HDACs in the other three classes, Sirtuins require NAD^+ as a co-factor to carry out deacetylase activity. Importantly, since they have a different catalytic mechanism, they do respond to classical HDAC inhibitors.

Class IV contains HDAC11, a nuclear protein [3, 97, 98].

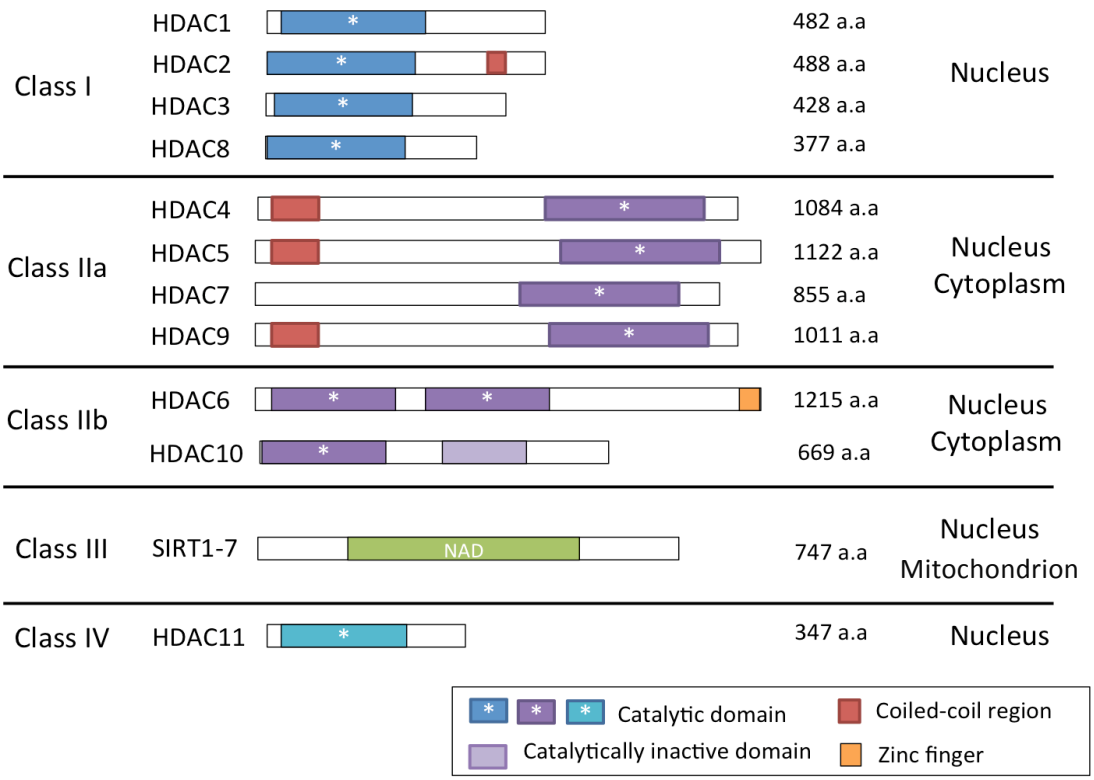

Figure 3. The histone deacetylase family (modified from Dell'Aversana et al, 2012 and Shirakawa et al, 2013). Schematic representations of class I (HDAC1, 2, 3, and 8), class II (HDAC4, 5, 6, 7, 9 and 10), class III (SIRT1) and class IV (HDAC11). Structure and Length of HDACs are shown. The total number of amino acid residues is depicted on the right, next to each HDAC.

HDAC inhibitors bind to the catalytic pocket of HDACs, preventing substrate binding to the enzyme and accessibility of promoter regions to transcription factors [99, 100]. HDAC inhibitors kill cells through upregulation of death receptors, cell-cycle checkpoint disruption [101], upregulation of pro-apoptotic proteins, induction of oxidative injury [102], and interference with Hsp90 function. HDAC inhibitors are considered transcriptional activators [103]. Natural and synthetic HDAC inhibitors can be structurally divided into four classes: hydroxamic acids (Hb-HDACs), small molecular weight carboxylates, benzamides, cyclic peptides and short-chain fatty acids [32]. Hb-HDAC inhibitors typically contain a metal-binding moiety represented by the hydroxamic acid group [19]. The catalytic pocket of the HDAC enzyme consists in the hydroxamic acid group able to chelate the Zn^{2+} metal ions, an aliphatic linker, and a capping group that interacts with the residues at the entrance of the active site. Each of structure differently interacts with the catalytic pocket [33]. By inserting in the HDAC catalytic pocket, Hb-HDAC inhibitors block the substrate access to the enzyme,

inhibiting its activity with the consequence of an accumulation of acetylated histone and non-histone proteins [19, 104]

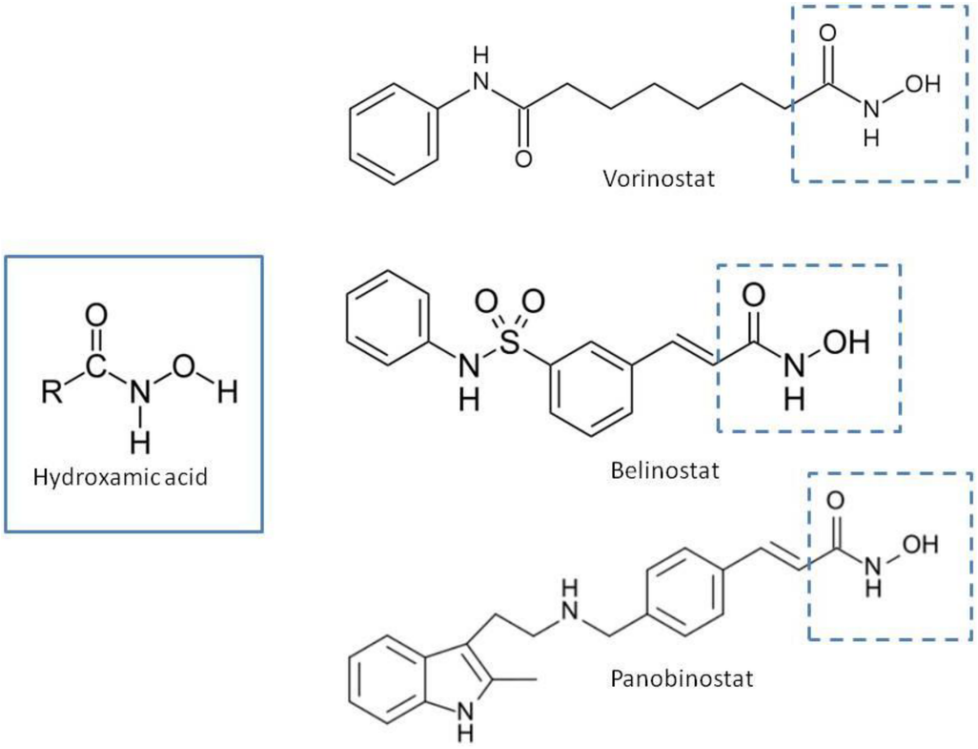

Figure 4. Chemical structures of Hb-HDAC inhibitors (from Grassadonia, et al., 2013). Chemical structure of vorinostat, belinostat and panobinostat are shown. In the square is represented the hydroxamic acid group, that characterizes this class of HDAC inhibitors. It is responsible for the binding of these compounds to the Zn^{2+} located into the catalytic domain of the enzyme [19].

Several HDAC inhibitors are under clinical development in leukemia, lymphoma, and myelodysplastic syndrome [105, 106]. HDAC inhibitors, such as vorinostat for the treatment of CTCL [107], panobinostat (previously called LBH589) for the treatment of CTCL and multiple myeloma (MM) [108], romidepsin [109] for the treatment of CTCL and PTCL, and belinostat [110] for the treatment of PTCL have been approved by the FDA (Food and Drug Administration) [109, 111, 112]. HDAC1 mutations have been associated with a sensitization of cells to the HDAC inhibitor panobinostat [113] suggesting that HDAC mutations could be used as predictive biomarkers [114].

Panobinostat is a non-selective HDAC inhibitors and it is a cinnamic hydroxamic acid analogue. It has shown antitumor activity in patients with Hodgkin's lymphoma, MM and acute myeloid leukemia (AML) [115]. *In vitro*, panobinostat induces acetylation of histone

H3 and H4, increase p21 levels, affect the function of Hsp90, and induce cell-cycle G1-phase accumulation and apoptosis of acute leukemia cells [116].

Romidepsin is a cyclic peptide that has activity against class I-III HDACs [97, 117]. Romidepsin has been shown to induce cell differentiation, cell-cycle arrest, and apoptosis. This agent also inhibits hypoxia-induced angiogenesis and depletes several Hsp90-dependent oncoproteins [46].

Belinostat is a hydroxamic acid HDAC inhibitors, that has pro-apoptotic activity and growth-inhibitory at low concentrations in several cancer types [60, 118]. It down regulates several kinase, like aurora kinase, vascular endothelial growth factor (VEGF), epidermal growth factor receptor (EGFR), and up regulates cyclin A [119]. Since HDAC inhibitors are generally well tolerated and show selectivity toward tumor cells, there is interest in combining them with other therapeutics to increase effectiveness against DLBCL [120-122].

2.2.2 Preclinical antitumor activity of ST7612AA1: a new oral thiol-based histone deacetylase (HDAC) inhibitor.

ST7612AA1 (property of Sigma-Tau, Italy), a thioacetate-ω (γ-lactam amide) derivative, is a potent, second generation, oral pan HDAC inhibitors. Pan HDAC inhibitors inhibit HDACs from class I, II and IV, while class specific HDAC inhibitors only inhibit HDACs from either class I or class II. The hydroxamates are able to target and affect all classes of HDACs, thus exerting nonspecific HDAC inhibition activity [123-125]. ST7612AA1 is a prodrug of ST7464AA1, selected within lactam carboxamide inhibitors.

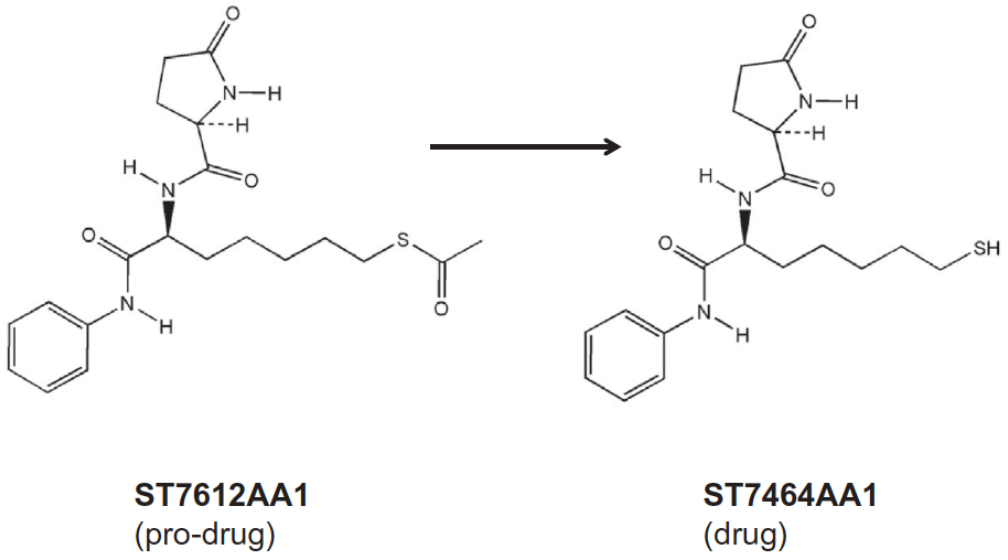

Figure 5. Chemical structure of the prodrug ST7612AA1 and its drug ST7464AA1 (from Vesci et al., 2015).

The active drug, ST7464AA1 revealed the maximum potency on HDAC3 and 6 (mean of IC_{50}= 4 nM), and then on HDAC1, 10 and 11 (mean of IC_{50}=13 nM) and HDAC2 (IC_{50}=78 nM). The minor potency was observed on HDAC8 (IC_{50}=281 nM) [126].

2.3 Epigenetic readers in cancer

Readers are a class of proteins scaffolds that recognize covalent modifications of histone proteins or DNA. The ε-N-acetylation of lysine residues on histone tails is associated with an open chromatin architecture and transcriptional activation [127]. The bromodomain and extra-terminal (BET) family (BRD2, BRD3, BRD4 and BRDT) shares a common domain architecture comprising two N-terminal bromodomains, which exhibit high levels of sequence conservation, and a more divergent C-terminal recruitment domain [72]. The name of these proteins arises from the presence of two bromodomains BD1 and BD2 and the extra-terminal region in the C-terminal moiety [128]. The bromodomain is a 110 amino acid motif comprised of four anti-parallel α-helices with two connecting loops that form a binding pocket for ε-acetyl-lysines of histones present in nucleosomal chromatin [129, 130]. Human genome encodes 61 bromodomains present in 46 different proteins [131]. The differences lie in the amino acid residues around the acetyl-lysine binding site. BET proteins are found in the cell nucleus, where they bind via their two bromodomains to acetylated proteins, including histones H3 and H4 [131]. BET proteins are part of large nuclear complexes that have been implicated in transcriptional networks, such as replication, transcription processes and chromatin remodeling [132]. Accordingly, BET proteins also are involved in inflammation, adipogenesis, post-mitotic memory, virus episomal persistence, latency and memory [133-137]. BET family comprises four members: BRD2, BRD3, BRD4, and BRDT. Mammalian BET proteins have been implicated in proliferation and mitosis process [138-140].

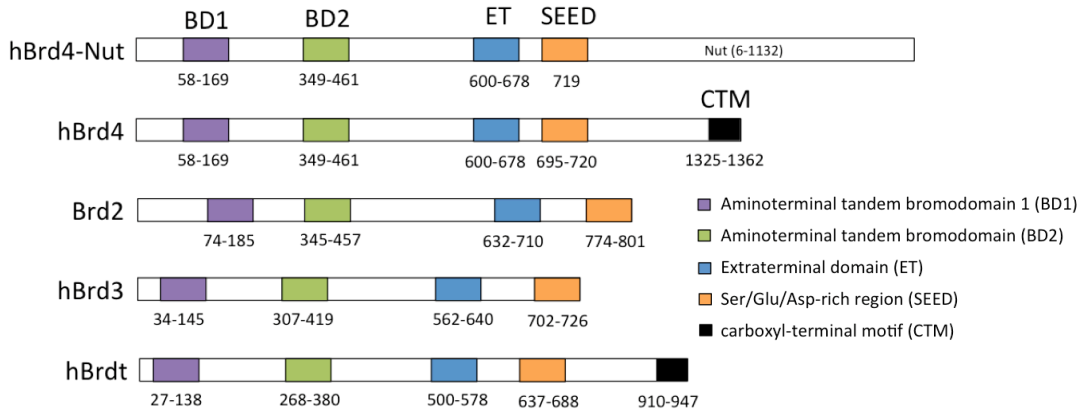

Figure 6. The evolutionarily conserved domains found in bromodomain containing protein 4 (BRD4) and the other BET family proteins include bromodomain 1 (BD1), bromodomain 2 (BD2), extraterminal (ET) (modified from Chiang, 2009). Numbers indicate the amino acid boundaries of each protein derived from human (h). The short form of human BRD4 (hBRD4) is also shown for comparison. Alignment of amino acid sequences and the accession number for each protein-coding gene are based on the information described by Wu and Chiang [128].

BRD2 is a nuclear transcriptional regulator, that mediate recruitment of histone acetyltransferase and E2 promoter binding factors (E2Fs) [141]. BRD2 expression drives *cyclin A*, *cyclin D1, cyclin E* transcription and cell-cycle progression [142]. BRD2 also is involved in the recruitment of HDACs, histone H4 specific acetyltransferase (HAT) and proteins involved in chromatin remodeling [98, 143].

BRD3 plays a role in the regulation of erythropoiesis, interact with acetylated GATA1 and promotes chromatin occupancy of this transcription factor at target genes [144, 145]. Interestingly, RNA polymerase II (Pol II) need BRD2 and BRD4 for its transcription [143].

BRD4 is a super-enhancer protein that plays an important role in regulating gene expression by recruiting transcription modulators to specific genomic promoters. BRD4 regulates oncogenes such as *MYC, BCL6, BCL-xL* [146-148]. Its BD2 domain interacts with the acetylated region of *cyclin T1* [149]. Cyclin T1 and CDK9 are included in the heterodimeric complex of the active form of the positive transcription elongation factor b (P-TEFb). The recruitment of active P-TEFb is important for the sustained presence of Pol II in active genes and for transcription initiation and elongation [150-152]. In fact it is crucial for the expression of cell-proliferation supporting genes, including MYC and its target genes [153].

The ET domain of BRD4 is able to recruit the arginine demethylase JMJD6 and the lysine methyltransferase NSD3 and CHD4, a catalytic component of the NuRD nucleosome

complex [154, 155]. Active P-TEFb phosphorylates Pol II during promoter clearance at the start of transcription elongation [156].

Finally, BRDT is expressed only in testis, where it plays a role in spermatogenesis by regulating several genes important during and after meiosis [157, 158]. BRDT is involved in the post-meiotic organization and remodeling of chromatin that takes place during spermiogenesis [159, 160].

Somatic mutations, amplifications and translocations in genes that encode for chromatin-related proteins are frequent in cancer. The epigenetic proteins represent several targets for the discovery of new active drugs. BRDs are interesting targets for drug development for the large number of diseases that are caused by aberrant acetylation of lysine residues [161]. BET proteins have two amino-terminal bromodomains that facilitate binding to hyperacetylated promoter/enhancer regions [131, 162] and a distal carboxyl terminal binding site for the P-TEFb [163]. BRD2 expression drives *cyclin A, cyclin D1, cyclin E* transcription and cell-cycle progression, [142] which promotes lymphoid malignancy [164]. Constitutive expression of BRD2 in the lymphoid lineage of mice transcriptionally co-activates *cyclin A* [103], thus eventually leading to B-cell malignancy [98, 164]. BRD3 down-regulates the RB-E2F pathway in most cancers and especially in nasopharyngeal carcinoma cells [98]. BRD4 is regulating gene expression by recruiting relevant transcription modulators to specific genomic loci. The recruitment of P-TEFb and Pol II by BRD4 regulates the expression of cell-proliferation supporting genes, including *MYC* [153]. Functional studies suggested that BRD4 regulates growth-associated genes by retaining P-TEFb at the promoters of key regulatory genes throughout mitosis [149, 165]. In cancer, BET bromodomains promote M to G1 cell-cycle progression [149] and contribute to mitotic memory [140, 146]. Chimeric proteins of the N-terminal BRDs of BRD4 or BRD3 with the protein NUT (nuclear protein in testis) cause NUT midline carcinoma (NMC), an incurable subtype of squamous carcinoma [166].

2.3.1 Bromodomain inhibitors

Bromodomain inhibitors mimic the binding mode of acetylated lysine by forming hydrogen bonds with the conserved asparagine residue. These inhibitors also competitively inhibit the binding of acetylated lysine containing peptides to bromodomains. Inhibitors that belong to this class include the thienodiazepines [167]. These inhibitors directly interact with the acetyl-lysine-binding BD1 and BD2 pockets of all BET proteins. Bromodomain inhibitors displace the BET protein from chromatin, which alters the transcriptional activity of the target genes. The discovery that MYC regulates promoter proximal pause release of Pol II, also through the recruitment of P-TEFb [153], established a rationale for targeting BET bromodomains to inhibit MYC dependent transcription [90]. For this main reason BET inhibitors have been

proposed for therapeutic treatment in MM [90], BL [168], acute lymphoblastic lymphoma [59], DLBCL [169] and AML [170]. BET inhibitors block the assembly of a functional protein complex and disturb the interaction of the bromodomain with the acetylated residue. BET inhibitors (JQ1, I-BET151, I-BET762, OTX015/MK-8628, TEN-010, CPI-0610 and BAY 1238097) have been developed for the treatment of hematopoietic malignancies, solid tumor and the rare NMC disease [132, 150, 171]. Four BET inhibitors are currently in clinical trials for cancer patients: OTX015/MK-8628 is tested in patients with hematological and solid malignancies (NCT01949883, NCT02698189 NCT01587703, NCT01713582, NCT01987362, NCT02259114, NCT02698176); I-BET762 (GSK525762) is investigated in solid tumors and in refractory hematological malignancies (NCT02964507, NCT01943851); CPI-0610 is being evaluated in Phase I studies in patients with AML, MM and progressive lymphoma (NCT02158858, NCT02157636, NCT01949883) and TEN-010 is administered subcutaneously to patients with hematological or solid tumors (NCT02308761, NCT01987362). A clinical study for testing BAY 1238097 orally in patients with solid and hematological tumors has recently been terminated [172]. Inhibition of BRD4 by JQ1 or specific siRNA treatment resulted in the downregulation of *BCL6* expression and impaired activation of NF-kB signaling pathway in primary activated B-cells and B-cell lymphoma [173]. Also it induces the suppression of *MYC* expression [59, 90, 168]. I-BET suppresses induction of a subset of TLR4-induced genes in mouse macrophages and suppresses inflammation in mouse models [174].

BRD4 is essential for maintenance of AML and JQ1 cause the same effects of RNA interference of BRD4 [170, 175]. JQ1 showed anti-proliferative effect in other hematological malignancies and solid organ tumors including glioblastoma, prostate cancer, and neuroblastoma [59, 176-179]. Another study shows that combination of JQ1 with rituximab desensitizes resistant DLBCL cell lines to this drug [180]. Finally, synergy with the HDAC inhibitor vorinostat was reported for RVX2135 in a MYC-dependent mouse lymphoma model [181].

PROTACs (Proteolysis Targeting Chimeras) are chimeric molecules with one small moiety binding a desired target protein that is connected by a flexible polyethylene glycol linker with a ligand for the E3 ubiquitin ligase. Thus, the PROTAC technology had the goal to induce the degradation of their target proteins through the ubiquitin proteasome system [182]. ARV-825 contains OTX015/MK-8628 moiety to binding BRD4, and a ligand for the E3 ubiquitin ligase cereblon (pomalidomide). ARV-825 actively recruits BRD4 to cereblon, resulting in the rapid and efficient degradation of the former via the proteasome [183].

2.3.2 The BET Bromodomain inhibitor OTX015 affects pathogenetic pathways in preclinical B-cell tumor models and synergizes with targeted drugs.

OTX015/MK-8628 (Merck, Germany) is a BET bromodomain inhibitor in early clinical development, has shown preclinical activity against a wide range of hematologic malignancies [184] as well as both pediatric and adult solid tumors. [29]

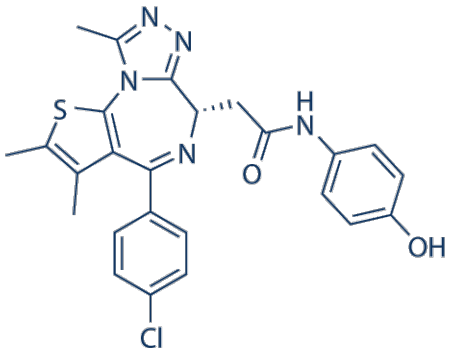

Figure 7. Chemical structure of the OTX015/MK-8628.

OTX015/MK-8628, like JQ1 and I-BET151, is able to induce growth inhibition, block of cell-cycle G1-S transition and causes apoptosis in acute leukemia cell lines and patient-derived leukemic samples [132, 175]. OTX015/MK-8628 inhibits BRD proteins in several preclinical models and shows significant *in vitro* and *in vivo* antitumor activity with cell-cycle arrest and downregulation of *MYC* in a number of hematologic malignancy models [185], including leukaemia [168], lymphomas [186], anaplastic large T-cell lymphoma and MM [50] as well as in solid tumor models like triple-negative breast cancer [187] and non-small cell lung carcinoma [188].

2.3.3 BAY 1238097, BAY-7575 and BAY-5627 are novel BET Bromodomain inhibitors with anti-lymphoma activity.

BAY 1238097, BAY-7575 and BAY-5627 are a novel BET inhibitors developed by Bayer, Germany. Most BET inhibitors are derived from diazepine and azepine scaffolds and, recently, from quinazolinones and isoxazoles. BAY 1238097 is derived from a new scaffold identified by Bayer. In particular, BAY 1238097 is a potent inhibitor of BET binding to histones that showed selectivity for BRD4 and strong anti-proliferative activity in AML and MM models. This novel compound has shown strong BRD4-BrD1 bromodomain inhibitory activity *in vitro*. A strong reduction of MYC transcript and protein levels are observed in treated MOLM-13 (AML) and MOLP-8 (MM) cell lines. *In vivo*, BAY 1238097 shows strong efficacy in the AML models THP-1, MOLM-13 and KG-1 [189].

BAY 1238097 underwent clinical investigation in patients with Lymphomas and solid tumors (NCT02369029) to determine the safety, tolerability and maximum tolerated dose of BAY1238097. Unfortunately, the study was closed due to toxicity (severe and unexpected headaches, vomit and back pain) [172].

3 Aim of the study

Aim of this thesis is to study new epigenetic drugs as novel anti-lymphoma agents, understand their mechanism of action and identify biological and genetic features associated with responses.

RESULTS

In summary, I focused my PhD work on the study of modalities to target the epigenome of lymphomas. I had the opportunity to work with novel epigenetic drugs, such as HDAC and BET inhibitors studying their anti-proliferative and pro-apoptotic role in several lymphoma models and also the changes at RNA and protein levels induced by these compounds. In most cases, the studies were completed with *in vivo* proof of efficacy in lymphoma models.

Article 1

My first work was the study of a novel HDAC inhibitor, ST7612AA1 (SigmaTau, Italy). ST7612AA1 is a pan-HDAC inhibitor, targeting HDAC1-2-3-6-8-10-11, that was studied as follow. Established human cell lines derived from DLBCL (n=11), MCL (n=4), and SMZL (n=3) were exposed to increasing concentrations of ST7612AA1 and the MTT assay was performed after 72 hours to determine its effect on lymphoma proliferation. All cell lines were sensitive to ST7612AA1 without differences among histological subtypes. ST7612AA1 induced moderate apoptosis in 3/8 lymphoma cell lines. ST7612AA1 presented both nuclear and cytoplasmic anti-deacetylase activity as demonstrated by Western blotting analysis showing increased levels of both acetylated histone H3 and acetyl-α-tubulin. To obtain a global view of the transcriptional changes after ST7612AA1 treatment, GEP was done with the Illumina HumanHT-12 Expression BeadChips on two sensitive cell lines (TMD8 and DOHH-2) treated with ST7612AA1 or DMSO for 8h. Differential expression analysis was performed with LIMMA, GSEA and Metacore. The most down-regulated genes are oncogenes or involved in lymphoma pathogenesis such as *IRAK1*, *MYD88*, *MYC*, *MYB*, *CCND2, BLK, CDK4, IKZF1* or *TNFRSF17* (*BCMA*). The up-regulated ones comprised tumor suppressor genes (*CDKN2C*, *CDKN1A*, *CDKN2D*) or genes involved in immune response (*HLA*, *CD69*). Validation of GEP results was obtained by real-time PCR analysis, confirming the upregulation of *CDKN1A* and downregulation of *MYC*, *IRAK4*, *MYD88*, *STAT3*, and, in the ABC-DLBCL cell line, also of *IRAK1*. DOHH-2 cells were injected s.c. in NOD-SCID mice, then mice were treated with ST7612AA1 (40mg/Kg, p.o.) or its vehicle control. ST7612AA1 determined a significant delay in tumor progression ($p = 0.0449$).

Article 2

The second work was on the study of the first-in-class clinical BET inhibitor, OTX015/MK-8628 (Merck, Germany). OTX015/MK-8628 targets BRD2-3-4 and it was mainly tested in DLBCL and in MCL. 33 lymphomas cell lines were exposed to increasing concentrations of OTX015/MK-8628 and the MTT assay was performed after 72 hours. The median IC50 value for the whole series was 240 nmol/L (range, 70 nmol/L–15 μmol/L). OTX015/MK-8628 showed cytostatic activity in 29/33, induced cell-cycle arrest with G1 accumulation and

decreased S-phase and apoptosis in 3/22. GEP was done on two sensitive cell lines (SU-DHL-6 and SU-DHL-2) treated with DMSO or with OTX015/MK-8628 for 1, 2, 4, 8, and 12 hours. Most up-regulated genes were histones. MYC target genes were highly significantly enriched among all OTX015/MK-8628 regulated transcripts and MYC was the most frequently down-regulated gene. OTX015/MK-8628 also down-regulated *MYD88, IRAK1, TLR6, IL6, STAT3*, and *TNFRSF17*, members of the NFKB, TLR and JAK/STAT pathways. Real-time PCR showed that there was a significant downregulation of *MYC*, *IL6*, *TLR6*, *TNFSRF17* and, although not reaching the statistical significance, of *IRAK1*, *IRF4*, and *STAT3*. Immunoblotting and immunohistochemistry showed a reduction of transcriptionally active pSTAT3 in 2 ABC-DLBCL cell lines, and a reduction in nuclear localization of p50 (NFKB1), indicating an inhibitory effect of OTX015/MK-8628 on the canonical NFKB pathway. GEP suggested combination study using a series of conventional and targeted anti-lymphoma agents in a panel of five DLBCL cell lines. Strong synergism was observed with everolimus (CI=0.11) and ibrutinib (CI=0.04); moderate synergism with idelalisib (CI=0.5), vorinostat (CI=0.5), rituximab (CI=0.5), decitabine (CI=0.6), lenalidomide (CI=0.7). Additive effect with romidepsin (CI=1.08), bendamustine (CI=0.63) and doxorubicin (CI=0.83). Baseline GEP were obtained in 14 cell lines with an IC50 lower than 500 nmol/L and eight with a higher IC50. Transcripts positively associated with OTX015/MK-8628 sensitivity were significantly enriched of genes involved in IFN, IL6 and IL10 signaling genes, TLR and JAK/STAT signaling, STAT3 targets, genes involved in glucose metabolism, and hypoxia-regulated genes. Transcripts associated with lower sensitivity to OTX015/MK-8628 were significantly enriched of E2F target genes, genes involved in cell-cycle regulation, DNA repair, P53 signa<ling, chromatin structure, and apoptosis. NOD-SCID mice were treated with OTX015/MK-8628 (25 mg/kg, p.o) or its vehicle control. OTX015/MK-8628 induced a reduced growth of the lymphoma xenografts, the median tumor volumes for the control and for the experimental arm were 600 mm3 (95% CI, 550–684) and 239 mm3 (95% CI, 0–582), respectively ($p = 0.001$).

I performed the combination study of OTX015/MK-8628 with a series of conventional and targeted anti-lymphoma agents (Figure 5), I prepared samples for GEP analysis and I validated several genes by real-time PCR (Figure 3A and Figure 4A).

Article 3

The third work was aimed to the study and evaluation of three novel BET inhibitors, BAY 1238097, BAY-7575 and BAY-5627 (Bayer, Germany), BAY 1238097 mainly targeting BRD4. BAY 1238097, BAY-7575 and BAY-5627 resulted very active *in vitro* models of Lymphomas and BAY 1238097 resulted active also *in vivo*. BAY 1238097, BAY-7575 and

BAY-5627 showed anti-proliferative activity in 51 lymphomas cell lines treated, the median IC50 values of 208 nM (157-260), 100 nM (75-120) and 70 nM (54-90 nM) respectively, with a very similar pattern of activity. The antitumor activity was mainly cytostatic. Cell lines presented LC50 values more similar to their IC50 exposed to the compounds for 72h or 96h underwent apoptosis. Baseline GEP showed that sensitive cell lines had high expression levels of genes involved in the JAK/STAT, IFN and BCR signaling. Sensitive cell lines had high incidence of mutation in *EZH2* and *MYD88*. Chromatin Immunoprecipitation assay shown that treatment with BAY 1238097 reduced BRD4 binding to the *EZH2* upstream regulatory region, indicating a direct effect of BAY 1238097 on the regulation of the EZH2 mRNA. GEP suggested combination study using EZH2, BTK and mTOR inhibitors. BAY 1238097 was combined with two different EZH2 inhibitors, DZNep and GSK126. Synergistic effects were seen in 3/5 cell lines harbouring *EZH2* mutation, while additive effects or not benefits were detected in 3/3 WT *EZH2* cell lines. We assessed changes at protein levels of EZH2, total histone H3 and H3K27me3 after exposure to BAY 1238097 single agent and in combination with the GSK126 or DZNep. BAY 1238097 determined a downregulation of EZH2, Histone 3 and H3K27me3, which apparently led to a stronger downregulation of H3K27me3 levels after the BAY 1238097/GSK126 combination. BAY 1238097 was combined with the BTK inhibitor ibrutinib for 72 h. Synergism was observed in 2/2 ABC-DLBCL cell lines harboring L265P-*MYD88* mutation (OCI-LY-10, TMD8). No benefit was observed in 2/2 ABC-DLBCL with WT *MYD88* (SU-DHL-2, U-2932). BAY 1238097 was combined with the mTOR inhibitor everolimus, leading to synergism in 2/2 ABC-DLBCL (U-2932, TMD8) and in 5/6 GCB-DLBCL (KARPAS-422, SU-DHL-6, DOHH-2, SU-DHL-8, Toledo) and additive in the remaining WSU-DLCL2. The treatment of two DLBCL cell lines with single BAY 1238097 induced a downregulation of pAKT protein levels, maintained in the cell lines exposed to both compounds. BAY 1238097 affected the growth of both GCB-DLBCL (SU-DHL-8) and ABC-DLBCL (OCI-LY-3) xenografts: treated tumors resulted 6-8 fold smaller in volume respect to controls.

DISCUSSION

Lymphomas are a heterogeneous group of neoplasms derived from lymphoid cells at various stages of development and they are among the ten most frequent human cancers. Treatment of lymphomas patients that are resistant/refractory to standard chemotherapy is in need for new drugs therapeutic and approaches.

Epigenetic modulation is a dynamic and reversible process. Somatic mutations, amplifications and translocations in genes that encode for chromatin-related proteins are frequent in cancer, providing interesting targets for epigenetic drugs [190, 191]. Different classes of protein are involved, mainly divided in epigenetic writers, epigenetic erasers and epigenetic readers [34, 114, 192].

Histone deacetylation induces transcriptional repression in closed-chromatin configuration. On the converse, histone acetylation induces transcriptional activation and relaxing chromatin [193, 194]. The acetylation status of the histone is a dynamic process and depends on the balance between these two conditions. Thus, compounds targeting the histone deacetylation - HDAC inhibitors - are generally considered to be transcriptional activators. Several HDAC inhibitors are under clinical development in various malignancies, many of them of hematological origin, such as multiple myeloma, leukemia, lymphoma and myelodysplastic syndrome [105, 106]. Recently, a systematic study of medicinal chemistry aimed at identifying a new generation of HDAC inhibitors identified a new class of thiol-based potent pan-HDAC inhibitors [126]. ST7612AA1 (property of Sigma-Tau, Italy) is a thioacetate-ω (γ-lactam amide) derivative, first synthetic thiol-derivative, potent oral pan-HDAC inhibitor. This is a prodrug of ST7464AA1, which has exquisite potency toward class I and class IIb HDACs. In agreement with the powerful inhibition of class I HDACs, here, we show that ST7612AA1 had a broad spectrum anti-proliferative activity on cell lines derived from lymphoma. We evaluated the activity of ST7612AA1 on a panel of 17 lymphoma cell lines. The median IC_{50} was 375 nM (range, 46-2664) for all the cell lines without significant differences among histological subtypes or between GCB- and ABC-DLBCL. ST7612AA1 presented both nuclear and cytoplasmic anti-deacetylase activity as demonstrated by Western blotting analysis showing increased protein levels of both acetylated histone H3 and acetyl-α tubulin. GEP was performed on two sensitive cell lines (DOHH-2 and TMD8) treated with ST7612AA1, important oncogenes and tumor suppressor genes were affected. The most down-regulated genes were related to TLR and NF-κB pathways, such as *TNFRSF17 (BCMA), MYC, IRAK1, MYD88, BLK, CDK4, IKZF1, BID*, while the up-regulated transcripts comprised cell-cycle genes (*CDKN2C (p18), CDKN1A (p21), CDKN2D (p19),* genes coding histones, MHC-I, MHC-II and metallothioneins). Our validations by real-time PCR confirmed the upregulation of *CDKN1A* and downregulation of *MYC*, *IRAK4*, *MYD88*, *STAT3*. ST7612AA1 by affecting NF-κB pathway and cell-cycle. All these genes are relevant

not only in cancer therapy but also in the inflammatory diseases [195]. Since ST7612AA1 can down-regulate MYC target genes and NF-κB pathway, it is also of interest for DLBCL. Indeed, the *in vivo* activity of ST7612AA1 was observed against a DLBCL cell line characterized by both *MYC* and *BCL2* gene translocations with a significant delay tumor progression was observed.
In one study, we reported that this novel HDAC inhibitor inhibited cell growth/proliferation in not only in lymphoma cell lines but also in tumor cell lines from solid tumors.

Epigenetic readers facilitate transcriptional activation by recognizing specific histone acetylated lysine residues and recruiting specific transcription factors (BET bromodomain proteins) [150]. Inhibition of epigenetic readers looks an interesting option for the treatment of human cancer. In several pre-clinical lymphoma models BET bromodomain inhibitors have shown antitumor activity [180, 181, 186, 196] and, interestingly, efficacy have been observed in phase I studies [197-199]. We evaluated the activity of OTX015/MK-8628, a new oral BET bromodomain inhibitor in pre-clinical lymphoma models and showed its proliferative activity on 33 cell lines derived from mature B-cell lymphoid tumors. DLBCL cells treated with OTX015/MK-8628 underwent cell-cycle arrest with G1 accumulation and decreased S-phase. OTX015/MK-8628 appeared to induce a senescence-like phenotype, compatible with described "senescence with incomplete growth arrest" [200], also observed after treatment of DLBCL cells with demethylating agents [201]. Baseline GEP showed that sensitivity to the OTX015/MK-8628 were significantly enriched of genes involved in interferon, interleukin signaling genes, TLR and JAK/STAT signaling, STAT3 targets, genes involved in glucose metabolism, and hypoxia-regulated genes. Transcripts associated with lower sensitivity to OTX015/MK-8628 were significantly enriched of E2F target genes, genes involved in cell-cycle regulation, DNA repair, P53 signaling, chromatin structure, and apoptosis. MYC, E2F1 targets and genes involved in NFKB/TLR/JAK/STAT pathways were down-regulated by OTX015/MK-8628 and other BRD-inhibitors [59, 90, 168, 176, 196].
MYC plays an important role in the pathogenesis and in the progression of most of the lymphoma subtypes. In particular, some DLBCL cases carry chromosomal translocations of both *MYC* and *BCL2* genes ("double hit lymphomas") and others express, albeit in the absence of chromosomal translocations, express both MYC and BCL2 proteins ("double expressors"), and both groups of patients present inferior outcome when compared with the remaining DLBCL cases [202]. Thus, compounds that can target MYC appear very interesting for their potential clinical implication [202-204].
We performed combination study by using OTX015/MK-8628 with a series of conventional and targeted anti-lymphoma agents. Strong synergistic effects were observed with the mTOR

inhibitor everolimus and with the BTK inhibitor ibrutinib. The mTOR is central to a signaling cascade leading to cell growth and proliferation, and mTOR inhibitors are approved for treatment of relapsed MCL [205]. Ibrutinib is more active in ABC-DLBCL cases with *CD79B*/*CD79A, CARD11* and *MYD88* mutated genes [206, 207]. Moderate synergism were observed with PI3K-delta inhibitor idelalisib that is clinically active in B-cell lymphomas [208], with anti-CD20 monoclonal antibody rituximab and with the immunomodulant lenalidomide, as also recently reported for another BET bromodomain inhibitor in MCL [209]. OTX015/MK-8628 presented synergism with the demethylating agent decitabine and the HDAC inhibitor vorinostat at concentrations pharmacologically achievable in clinical use [210], in accordance with the similarities here observed at the level of gene expression signatures, and also with published data obtained with other BET bromodomain inhibitors [181]. Additive effects were observed for combinations with class I HDAC inhibitor romidepsin, chemotherapy agent bendamustine and chemotherapy agent doxorubicin.

HDACs of both classes I and II were associated with a lower sensitivity to OTX015/MK-8628 as single agent and indeed the synergism appeared stronger with the class I and IIa/b HDAC inhibitor vorinostat than that seen with the class I HDAC inhibitor romidepsin suggesting that the synergism might be class dependent.

Further pre-clinical studies with OTX015/MK-8628 will help to understand the mechanism of action of the molecule and to optimize its use as an anti-lymphoma agent.

An article “in preparation” will report new *in vitro* and *in vivo* data on OTX015/MK-8628 in MCL (Bernasconi, Gaudio et al., in preparation). GEP was performed on MCL cell lines after treatment with OTX015/MK-8628 and genetic features associated with sensitivity and resistance. We report also the pre-clinical activity of OTX015/MK-8628 combinations that might overcome adaptive resistance mechanisms.

OTX015/MK-8628 is in clinical trials, including patients with hematologic malignancies such as lymphoma, MM, AML, myelodysplastic syndrome and show clinical activity [197, 199, 211, 212]. A recent study shows that OTX015/MK-8628 induces a rapid tumor regression in two patients affected by NMC [198] and OTX015/MK-8628 has been initiated in patients with selected solid tumors and glioblastoma multiforme. The trials suggest the use of OTX015/MK-8628 combated with other compounds and can help to identify therapeutic target.

Finally, we have evaluated the activity of three new novel BET bromodomain inhibitors (BAY 1238097, BAY-7575 and BAY-5627) in pre-clinical models of mature B-cell lymphoid tumors, correlating the sensitivity to genetic and biologic features.

These BET bromodomain inhibitors showed anti-proliferative activity in most of the lymphoma cell lines tested, with no differences in sensitivity among the histologic subtypes.

The antitumor activity of BAY 1238097 was also conformed in two DLBCL xenograft models. Strong efficacy was demonstrated when giving the compound orally using either a daily or a twice weekly schedule. BAY 1238097 induced a block in cell-cycle with G1 accumulation and decreased S-phase as observed with other BET bromodomain inhibitors [213, 214] Few cell lines derived from ABC-DLBCL, GCB-DLBCL and MCL underwent apoptosis after 72h of drug exposure, how observed in OTX015/MK-8628 activity.

Baseline GEP is a strategy to identify mutations and features associated with response to a compound and to suggest possible combinatorial schemes.

Transcripts associated with highest sensitivity to BAY 1238097 were significantly enriched of genes involved in the JAK/STAT, IFN and BCR signaling. The less sensitive GCB-DLBCL had higher expression of genes involved in cell cycle, chromatin structure, and E2F1 targets. Baseline GEP signature of BAY 1238097 were overlap with that of OTX015/MK-8628. In fact transcripts positively associated with OTX015/MK-8628 sensitivity were significantly enriched of genes involved in interferon, IL6 and IL10 signaling genes, TLR and JAK/STAT signaling, STAT3 targets, genes involved in glucose metabolism, and hypoxia-regulated genes. While transcripts associated with lower sensitivity to OTX015/MK-8628 were significantly enriched of E2F target genes, genes involved in cell cycle regulation, DNA repair, P53 signaling, chromatin structure, and apoptosis.

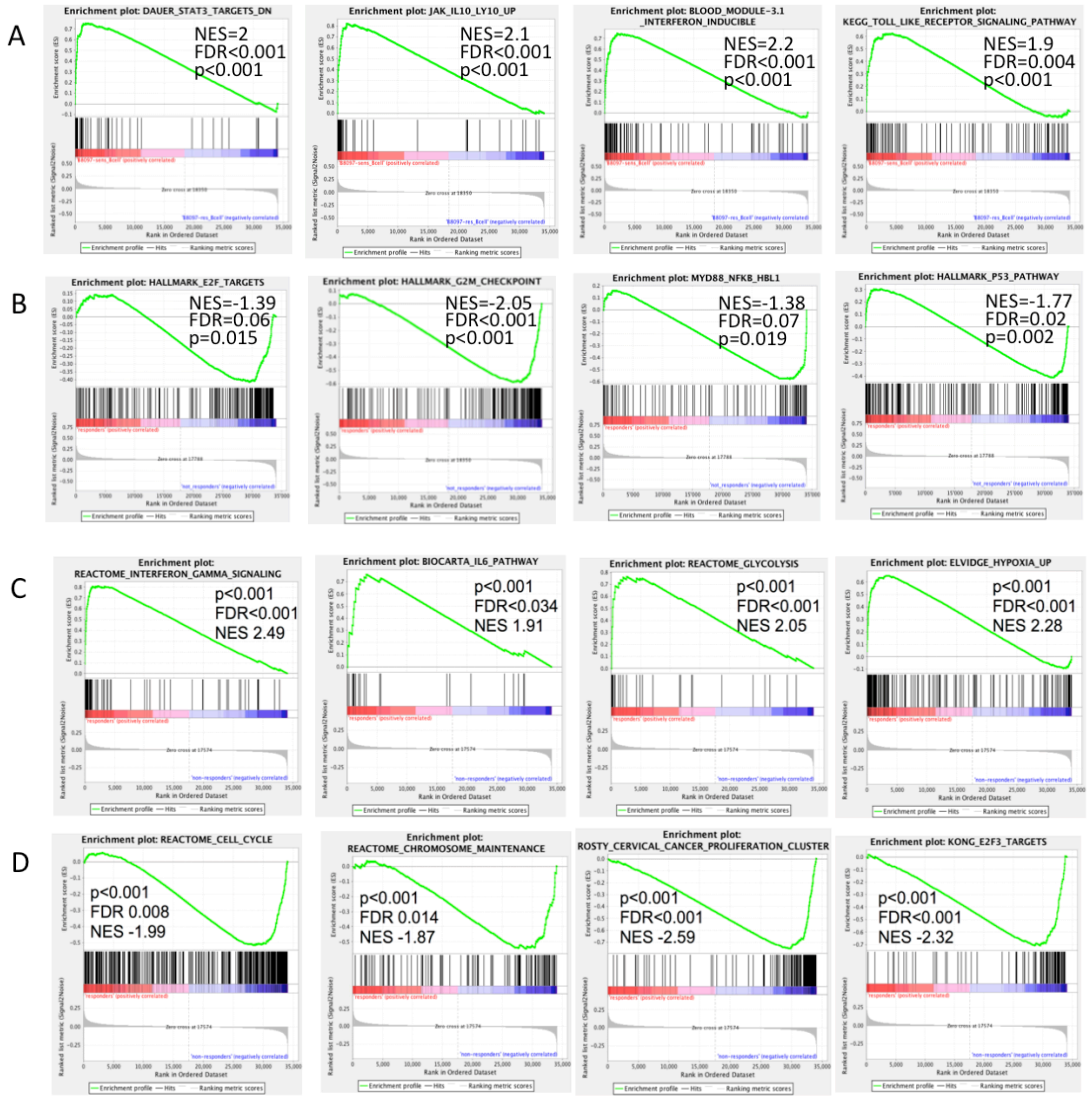

Figure 8. Representative GSEA plots illustrating: (A) the enrichment of genes involved in JAK/STAT, IFN and BCR signaling among the transcripts associated with a higher BAY 1238097 sensitivity; (B) the enrichment of genes involved in cell cycle, chromatin structure, and E2F1 targets among the transcripts associated with a lower sensitivity to BAY 1238097; (C) the enrichment of genes involved in interferon and IL6 signaling, in glucose metabolism, and in hypoxia among the transcripts associated with a higher OTX015/MK-8628 sensitivity; (D) the enrichment of genes involved in cell cycle regulation and chromatin structure and of E2F targets among the transcripts associated with a lower sensitivity to OTX015/MK-8628. FDR, false discovery rate; NES, normalized enrichment score.

Mutations of EZH2 occur frequently in DLBCL and in FL and EZH2 signature from FL patients with or without mutated *EZH2* [215] was associated with higher sensitivity in GCB-DLBCL cell lines. Treatment with BAY 1238097 reduced BRD4 binding to the *EZH2*

upstream regulatory region, indicating a direct effect of BET bromodomain inhibitors on the regulation of the EZH2 mRNA. Based on this data and our previous data with the BET inhibitor OTX015/MK-8628 [186], we perform combination study using EZH2, BTK and mTOR inhibitors. DZNep induce a synergistic or additive effect in GCB-DLBCL with mutated *EZH2*, while it did not present any benefit in cell lines with WT *EZH2* tested.

To obtain a global view of the transcriptional changes after BAY 1238097 treatment, GEP study was done on the cell line DOHH-2 exposed to DMSO or BAY 1238097 for 8, 12 or 24 hours. The up-regulated transcripts were mainly represented by histones. The up-regulated genes included *CCL5, CDKN2C, CD69, JUN,* and *MKNK2*.

BAY 1238097 decreased target genes of MYC, NOTCH and E2F, members of NFKB/MYD88 and mTOR/AKT signaling. *BTK, CCDC86, CCND2, CCRL1, CD19, CD27, FAIM, FAIM3, IL7R, IRAK1, MAPK13, MLKL, MYB, MYC, PDE4B, PTPN22, PVRIG, TNFRSF13B, TNFRSF17, VPREB3* were among the top down-regulated genes.

BAY 1238097 gene expression signature overlapped with HDAC, highly overlapped with the signatures obtained with other BET inhibitors JQ1, with OTX015/MK-8628 [179, 186, 196, 216, 217]. In fact, GEP was done on two sensitive cell lines (TMD8 and DOHH-2) treated with the HDAC inhibitor ST7612AA1 or DMSO for 8h. The up-regulated genes comprised tumor suppressor genes or genes involved in immune response. The most down-regulated genes were genes known as oncogenes or involved in lymphoma pathogenesis such as *IRAK1*, *MYD88*, *MYC*, *MYB*, *CCND2*, *BLK*, *CDK4*, *IKZF1* or *TNFRSF17* (*BCMA*). Furthermore GEP was done on two sensitive cell lines (SU-DHL-6 and SU-DHL-2) treated with DMSO or with BET Bromodomain inhibitor OTX015/MK-8628 for 1, 2, 4, 8, and 12 hours. Most up-regulated genes were histones. Most down-regulated genes were *MYD88, IRAK1, TLR6, IL6, STAT3*, and *TNFRSF17*, members of the NFKB, TLR and JAK/STAT pathways.

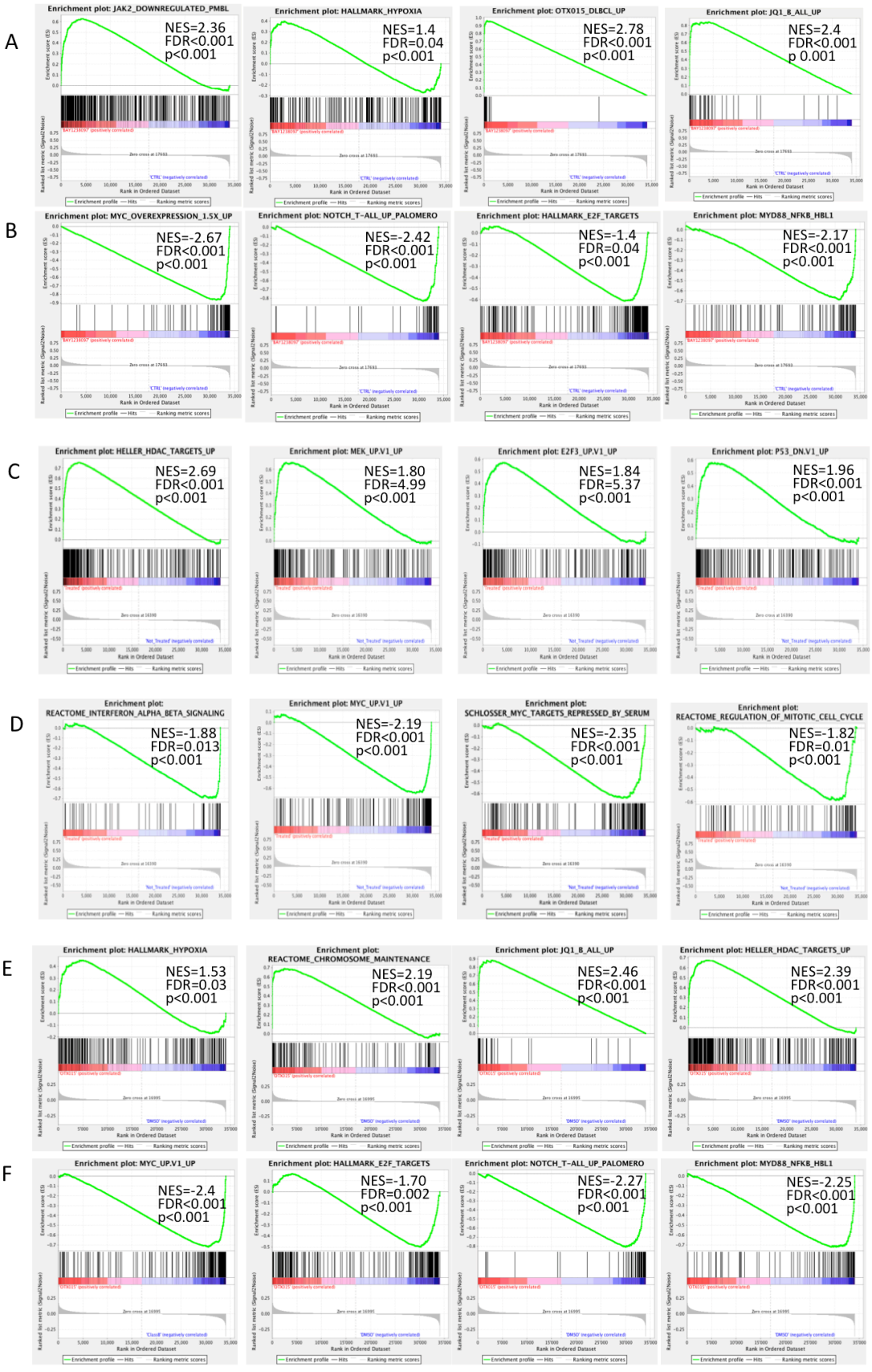
A
Enrichment plot: JAK2_DOWNREGULATED_PMBL
NES=2.36
FDR<0.001
p<0.001
Enrichment plot: HALLMARK_HYPOXIA
NES=1.4
FDR=0.04
p<0.001
Enrichment plot: OTX015_DLBCL_UP
NES=2.78
FDR<0.001
p<0.001
Enrichment plot: JQ1_B_ALL_UP
NES=2.4
FDR<0.001
p 0.001
B
Enrichment plot: MYC_OVEREXPRESSION_1.5X_UP
NES=-2.67
FDR<0.001
p<0.001
Enrichment plot: NOTCH_T-ALL_UP_PALOMERO
NES=-2.42
FDR<0.001
p<0.001
Enrichment plot: HALLMARK_E2F_TARGETS
NES=-1.4
FDR=0.04
p<0.001
Enrichment plot: MYD88_NFKB_HBL1
NES=-2.17
FDR<0.001
p<0.001
C
Enrichment plot: HELLER_HDAC_TARGETS_UP
NES=2.69
FDR<0.001
p<0.001
Enrichment plot: MEK_UP.V1_UP
NES=1.80
FDR=4.99
p<0.001
Enrichment plot: E2F3_UP.V1_UP
NES=1.84
FDR=5.37
p<0.001
Enrichment plot: P53_DN.V1_UP
NES=1.96
FDR<0.001
p<0.001
D
Enrichment plot: REACTOME_INTERFERON_ALPHA_BETA_SIGNALING
NES=-1.88
FDR=0.013
p<0.001
Enrichment plot: MYC_UP.V1_UP
NES=-2.19
FDR<0.001
p<0.001
Enrichment plot: SCHLOSSER_MYC_TARGETS_REPRESSED_BY_SERUM
NES=-2.35
FDR<0.001
p<0.001
Enrichment plot: REACTOME_REGULATION_OF_MITOTIC_CELL_CYCLE
NES=-1.82
FDR=0.01
p<0.001
E
Enrichment plot: HALLMARK_HYPOXIA
NES=1.53
FDR=0.03
p<0.001
Enrichment plot: REACTOME_CHROMOSOME_MAINTENANCE
NES=2.19
FDR<0.001
p<0.001
Enrichment plot: JQ1_B_ALL_UP
NES=2.46
FDR<0.001
p<0.001
Enrichment plot: HELLER_HDAC_TARGETS_UP
NES=2.39
FDR<0.001
p<0.001
F
Enrichment plot: MYC_UP.V1_UP
NES=-2.4
FDR<0.001
p<0.001
Enrichment plot: HALLMARK_E2F_TARGETS
NES=-1.70
FDR=0.002
p<0.001
Enrichment plot: NOTCH_T-ALL_UP_PALOMERO
NES=-2.27
FDR<0.001
p<0.001
Enrichment plot: MYD88_NFKB_HBL1
NES=-2.25
FDR<0.001
p<0.001

Figure 9. Representative GSEA plots illustrating the gene-set enrichment in genes up-regulated (A) and down-regulated (B) in DOHH-2 cell line after BAY 1238097 exposure; GEP shows transcripts with higher expression (C) and lower expression (D) in two sensitive cell lines (TMD8 and DOHH-2) treated with ST7612AA1; up-regulated gene-set (E) and down-regulated gene-set (F) in two sensitive cell lines (SU-DHL-6 and SU-DHL-2) after OTX015/MK-8628 exposure. FDR, false discovery rate; NES, normalized enrichment score.

BAY 1238097 in combination with ibrutinib was synergistic in ABC-DLBCL cell lines harboring L265P-*MYD88* and of no benefit in ABC-DLBCL with WT *MYD88*. Similarly to what seen with OTX015/MK-8628 [213], the combination of BAY 1238097 with everolimus was very beneficial, both in ABC- and in GCB-DLBCL cells. Immunoblotting data suggested that the synergism could be due to decreased levels of pAKT after BET inhibitor, which might attenuate the negative feedback observed after mTOR inhibitors alone [218].
BAY 1238097 underwent clinical investigation in patients with solid tumors (NCT02369029), but unfortunately, the study was closed due to toxicity (severe and unexpected headaches, vomit and back pain) [172].

In conclusion, the epigenetic compounds studied in this PhD work represents promising new anti-lymphoma agents with anti-proliferative activity in the clear majority of the examined pre-clinical models. They are able to modulate important signaling pathways that are commonly deregulated in lymphomas. It will be important to properly move these drugs to the clinics as single agents and in combination.

REFERENCES

1. Siegel, R.L., K.D. Miller, and A. Jemal, *Cancer statistics, 2016.* CA Cancer J Clin, 2016. **66**(1): p. 7-30.
2. Lenz, G., et al., *Stromal gene signatures in large-B-cell lymphomas.* N Engl J Med, 2008. **359**(22): p. 2313-23.
3. Jung, D., et al., *Mechanism and control of V(D)J recombination at the immunoglobulin heavy chain locus.* Annu Rev Immunol, 2006. **24**: p. 541-70.
4. Saji, S., et al., *Significance of HDAC6 regulation via estrogen signaling for cell motility and prognosis in estrogen receptor-positive breast cancer.* Oncogene, 2005. **24**(28): p. 4531-9.
5. Kuppers, R., *Mechanisms of B-cell lymphoma pathogenesis.* Nat Rev Cancer, 2005. **5**(4): p. 251-62.
6. Swerdlow, S.H., et al., *The 2016 revision of the World Health Organization classification of lymphoid neoplasms.* Blood, 2016. **127**(20): p. 2375-90.
7. Swerdlow, S.H., et al., eds. *WHO Classification of Tumours of Haematopoietic and Lymphoid Tissues.* 2008, IARC Press: Lyon, France. 439.
8. Lossos, I.S., *Molecular pathogenesis of diffuse large B-cell lymphoma.* J Clin Oncol, 2005. **23**(26): p. 6351-7.
9. Lenz, G., et al., *Molecular subtypes of diffuse large B-cell lymphoma arise by distinct genetic pathways.* Proc Natl Acad Sci U S A, 2008. **105**(36): p. 13520-5.
10. Tilly, H., et al., *Diffuse large B-cell lymphoma (DLBCL): ESMO Clinical Practice Guidelines for diagnosis, treatment and follow-up.* Ann Oncol, 2012. **23 Suppl 7**: p. vii78-82.
11. Testoni, M., et al., *Genetic lesions in diffuse large B-cell lymphomas.* Ann Oncol, 2015. **26**(6): p. 1069-80.
12. Grant, C., et al., *Primary mediastinal large B-cell lymphoma, classic Hodgkin lymphoma presenting in the mediastinum, and mediastinal gray zone lymphoma: what is the oncologist to do?* Curr Hematol Malig Rep, 2011. **6**(3): p. 157-63.
13. Raia, V., et al., *Dynamic mathematical modeling of IL13-induced signaling in Hodgkin and primary mediastinal B-cell lymphoma allows prediction of therapeutic targets.* Cancer Res, 2011. **71**(3): p. 693-704.
14. Dunleavy, K. and W.H. Wilson, *Primary mediastinal B-cell lymphoma and mediastinal gray zone lymphoma: do they require a unique therapeutic approach?* Blood, 2015. **125**(1): p. 33-9.
15. Horning, S.J., *Follicular lymphoma: have we made any progress?* Ann Oncol, 2000. **11 Suppl 1**: p. 23-7.
16. Swerdlow, S.H. and M.E. Williams, *From centrocytic to mantle cell lymphoma: a clinicopathologic and molecular review of 3 decades.* Hum Pathol, 2002. **33**(1): p. 7-20.
17. Li, J.Y., et al., *Detection of translocation t(11;14)(q13;q32) in mantle cell lymphoma by fluorescence in situ hybridization.* Am J Pathol, 1999. **154**(5): p. 1449-52.
18. Kelly, W.K., et al., *Phase I study of an oral histone deacetylase inhibitor, suberoylanilide hydroxamic acid, in patients with advanced cancer.* J Clin Oncol, 2005. **23**(17): p. 3923-31.
19. Grassadonia, A., et al., *Role of Hydroxamate-Based Histone Deacetylase Inhibitors (Hb-HDACIs) in the Treatment of Solid Malignancies.* Cancers (Basel), 2013. **5**(3): p. 919-42.
20. Rinaldi, A., et al., *Genome-wide DNA profiling of marginal zone lymphomas identifies subtype-specific lesions with an impact on the clinical outcome.* Blood, 2011. **117**(5): p. 1595-604.
21. Thieblemont, C., T. Molina, and F. Davi, *Optimizing therapy for nodal marginal zone lymphoma.* Blood, 2016. **127**(17): p. 2064-71.
22. Arcaini, L., D. Rossi, and M. Paulli, *Splenic marginal zone lymphoma: from genetics to management.* Blood, 2016. **127**(17): p. 2072-81.

23. Spina, V., et al., *The genetics of nodal marginal zone lymphoma.* Blood, 2016. **128**(10): p. 1362-73.
24. Hummel, M., et al., *A biologic definition of Burkitt's lymphoma from transcriptional and genomic profiling.* N Engl J Med, 2006. **354**(23): p. 2419-30.
25. Dohner, H., et al., *Genomic aberrations and survival in chronic lymphocytic leukemia.* N Engl J Med, 2000. **343**(26): p. 1910-6.
26. Bergsagel, P.L. and W.M. Kuehl, *Comprehensive identification of somatic mutations in chronic lymphocytic leukemia.* Cancer Cell, 2011. **20**(1): p. 5-7.
27. O'Leary, H.M. and K.J. Savage, *Update on the World Health Organization classification of peripheral T-cell lymphomas.* Curr Hematol Malig Rep, 2009. **4**(4): p. 227-35.
28. de Leval, L., et al., *The gene expression profile of nodal peripheral T-cell lymphoma demonstrates a molecular link between angioimmunoblastic T-cell lymphoma (AITL) and follicular helper T (TFH) cells.* Blood, 2007. **109**(11): p. 4952-63.
29. Henssen, A., et al., *Targeting MYCN-Driven Transcription By BET-Bromodomain Inhibition.* Clin Cancer Res, 2016. **22**(10): p. 2470-81.
30. Kelly, T.K., D.D. De Carvalho, and P.A. Jones, *Epigenetic modifications as therapeutic targets.* Nat Biotechnol, 2010. **28**(10): p. 1069-78.
31. Jones, R.S., *Epigenetics: reversing the 'irreversible'.* Nature, 2007. **450**(7168): p. 357-9.
32. Drummond, D.C., et al., *Clinical development of histone deacetylase inhibitors as anticancer agents.* Annu Rev Pharmacol Toxicol, 2005. **45**: p. 495-528.
33. Chen, P.C., et al., *Synthesis and structure-activity relationship of histone deacetylase (HDAC) inhibitors with triazole-linked cap group.* Bioorg Med Chem, 2008. **16**(9): p. 4839-53.
34. Dawson, M.A., T. Kouzarides, and B.J. Huntly, *Targeting epigenetic readers in cancer.* N Engl J Med, 2012. **367**(7): p. 647-57.
35. Lalonde, M.E., X. Cheng, and J. Cote, *Histone target selection within chromatin: an exemplary case of teamwork.* Genes Dev, 2014. **28**(10): p. 1029-41.
36. Simo-Riudalbas, L. and M. Esteller, *Targeting the histone orthography of cancer: drugs for writers, erasers and readers.* Br J Pharmacol, 2015. **172**(11): p. 2716-32.
37. Baylin, S.B. and P.A. Jones, *A decade of exploring the cancer epigenome - biological and translational implications.* Nat Rev Cancer, 2011. **11**(10): p. 726-34.
38. Jiang, Y., K. Hatzi, and R. Shaknovich, *Mechanisms of epigenetic deregulation in lymphoid neoplasms.* Blood, 2013. **121**(21): p. 4271-9.
39. Li, K.K., et al., *Chemical and biochemical approaches in the study of histone methylation and demethylation.* Med Res Rev, 2012. **32**(4): p. 815-67.
40. Arrowsmith, C.H., et al., *Epigenetic protein families: a new frontier for drug discovery.* Nat Rev Drug Discov, 2012. **11**(5): p. 384-400.
41. Falkenberg, K.J. and R.W. Johnstone, *Histone deacetylases and their inhibitors in cancer, neurological diseases and immune disorders.* Nat Rev Drug Discov, 2014. **13**(9): p. 673-91.
42. Martinez-Garcia, E. and J.D. Licht, *Deregulation of H3K27 methylation in cancer.* Nat Genet, 2010. **42**(2): p. 100-1.
43. Stimson, L. and N.B. La Thangue, *Biomarkers for predicting clinical responses to HDAC inhibitors.* Cancer Lett, 2009. **280**(2): p. 177-83.
44. Tan, J.Z., et al., *EZH2: biology, disease, and structure-based drug discovery.* Acta Pharmacol Sin, 2014. **35**(2): p. 161-74.
45. Kapoor, S., *Inhibition of HDAC6-dependent carcinogenesis: emerging, new therapeutic options besides belinostat.* Int J Cancer, 2009. **124**(2): p. 509.
46. Campas-Moya, C., *Romidepsin for the treatment of cutaneous T-cell lymphoma.* Drugs Today (Barc), 2009. **45**(11): p. 787-95.
47. Lessard, J. and G. Sauvageau, *Bmi-1 determines the proliferative capacity of normal and leukaemic stem cells.* Nature, 2003. **423**(6937): p. 255-60.

48. Sparmann, A. and M. van Lohuizen, *Polycomb silencers control cell fate, development and cancer.* Nat Rev Cancer, 2006. **6**(11): p. 846-56.
49. Bracken, A.P., et al., *The Polycomb group proteins bind throughout the INK4A-ARF locus and are disassociated in senescent cells.* Genes Dev, 2007. **21**(5): p. 525-30.
50. Boi, M., et al., *Therapeutic efficacy of the bromodomain inhibitor OTX015/MK-8628 in ALK-positive anaplastic large cell lymphoma: an alternative modality to overcome resistant phenotypes.* Oncotarget, 2016.
51. Morin, R.D., et al., *Frequent mutation of histone-modifying genes in non-Hodgkin lymphoma.* Nature, 2011. **476**(7360): p. 298-303.
52. Morin, R.D., et al., *Somatic mutations altering EZH2 (Tyr641) in follicular and diffuse large B-cell lymphomas of germinal-center origin.* Nat Genet, 2010. **42**(2): p. 181-5.
53. Bodor, C., et al., *EZH2 Y641 mutations in follicular lymphoma.* Leukemia, 2011. **25**(4): p. 726-9.
54. Love, C., et al., *The genetic landscape of mutations in Burkitt lymphoma.* Nat Genet, 2012. **44**(12): p. 1321-5.
55. Nikoloski, G., et al., *Somatic mutations of the histone methyltransferase gene EZH2 in myelodysplastic syndromes.* Nat Genet, 2010. **42**(8): p. 665-7.
56. Visser, H.P., et al., *The Polycomb group protein EZH2 is upregulated in proliferating, cultured human mantle cell lymphoma.* Br J Haematol, 2001. **112**(4): p. 950-8.
57. Eckerle, S., et al., *Gene expression profiling of isolated tumour cells from anaplastic large cell lymphomas: insights into its cellular origin, pathogenesis and relation to Hodgkin lymphoma.* Leukemia, 2009. **23**(11): p. 2129-38.
58. Sasaki, D., et al., *Overexpression of Enhancer of zeste homolog 2 with trimethylation of lysine 27 on histone H3 in adult T-cell leukemia/lymphoma as a target for epigenetic therapy.* Haematologica, 2011. **96**(5): p. 712-9.
59. Ott, C.J., et al., *BET bromodomain inhibition targets both c-Myc and IL7R in high-risk acute lymphoblastic leukemia.* Blood, 2012. **120**(14): p. 2843-52.
60. Gimsing, P., *Belinostat: a new broad acting antineoplastic histone deacetylase inhibitor.* Expert Opin Investig Drugs, 2009. **18**(4): p. 501-8.
61. Knutson, S.K., et al., *A selective inhibitor of EZH2 blocks H3K27 methylation and kills mutant lymphoma cells.* Nat Chem Biol, 2012. **8**(11): p. 890-6.
62. Velichutina, I., et al., *EZH2-mediated epigenetic silencing in germinal center B cells contributes to proliferation and lymphomagenesis.* Blood, 2010. **116**(24): p. 5247-55.
63. van Galen, J.C., et al., *Distinct expression patterns of polycomb oncoproteins and their binding partners during the germinal center reaction.* Eur J Immunol, 2004. **34**(7): p. 1870-81.
64. Hassler, M.R., A.I. Schiefer, and G. Egger, *Combating the epigenome: epigenetic drugs against non-Hodgkin's lymphoma.* Epigenomics, 2013. **5**(4): p. 397-415.
65. Tan, J., et al., *Pharmacologic disruption of Polycomb-repressive complex 2-mediated gene repression selectively induces apoptosis in cancer cells.* Genes Dev, 2007. **21**(9): p. 1050-63.
66. Fiskus, W., et al., *Superior efficacy of a combined epigenetic therapy against human mantle cell lymphoma cells.* Clin Cancer Res, 2012. **18**(22): p. 6227-38.
67. Miranda, T.B., et al., *DZNep is a global histone methylation inhibitor that reactivates developmental genes not silenced by DNA methylation.* Mol Cancer Ther, 2009. **8**(6): p. 1579-88.
68. Kim, K.H. and C.W. Roberts, *Targeting EZH2 in cancer.* Nat Med, 2016. **22**(2): p. 128-34.
69. Takeshima, H., et al., *Identification of coexistence of DNA methylation and H3K27me3 specifically in cancer cells as a promising target for epigenetic therapy.* Carcinogenesis, 2015. **36**(2): p. 192-201.

70. Kirk, J.S., et al., *Top2a identifies and provides epigenetic rationale for novel combination therapeutic strategies for aggressive prostate cancer.* Oncotarget, 2015. **6**(5): p. 3136-46.
71. Adhikary, G., et al., *Survival of skin cancer stem cells requires the Ezh2 polycomb group protein.* Carcinogenesis, 2015. **36**(7): p. 800-10.
72. Maryan, N., et al., *Regulation of the expression of claudin 23 by the enhancer of zeste 2 polycomb group protein in colorectal cancer.* Mol Med Rep, 2015. **12**(1): p. 728-36.
73. McCabe, M.T., et al., *EZH2 inhibition as a therapeutic strategy for lymphoma with EZH2-activating mutations.* Nature, 2012. **492**(7427): p. 108-12.
74. Ruiz-Carrillo, A., L.J. Wangh, and V.G. Allfrey, *Processing of newly synthesized histone molecules.* Science, 1975. **190**(4210): p. 117-28.
75. Yuan, Z.L., et al., *Stat3 dimerization regulated by reversible acetylation of a single lysine residue.* Science, 2005. **307**(5707): p. 269-73.
76. Rothgiesser, K.M., M. Fey, and M.O. Hottiger, *Acetylation of p65 at lysine 314 is important for late NF-kappaB-dependent gene expression.* BMC Genomics, 2010. **11**: p. 22.
77. Cerchietti, L.C., et al., *BCL6 repression of EP300 in human diffuse large B cell lymphoma cells provides a basis for rational combinatorial therapy.* J Clin Invest, 2010. **120**(12): p. 4569-82.
78. Pasqualucci, L., et al., *Inactivating mutations of acetyltransferase genes in B-cell lymphoma.* Nature, 2011. **471**(7337): p. 189-95.
79. Lohr, J.G., et al., *Discovery and prioritization of somatic mutations in diffuse large B-cell lymphoma (DLBCL) by whole-exome sequencing.* Proc Natl Acad Sci U S A, 2012. **109**(10): p. 3879-84.
80. Ying, C.Y., et al., *MEF2B mutations lead to deregulated expression of the oncogene BCL6 in diffuse large B cell lymphoma.* Nat Immunol, 2013. **14**(10): p. 1084-92.
81. Khabele, D., et al., *Drug-induced inactivation or gene silencing of class I histone deacetylases suppresses ovarian cancer cell growth: implications for therapy.* Cancer Biol Ther, 2007. **6**(5): p. 795-801.
82. Song, J., et al., *Increased expression of histone deacetylase 2 is found in human gastric cancer.* APMIS, 2005. **113**(4): p. 264-8.
83. Bartling, B., et al., *Comparative application of antibody and gene array for expression profiling in human squamous cell lung carcinoma.* Lung Cancer, 2005. **49**(2): p. 145-54.
84. Mariadason, J.M., *HDACs and HDAC inhibitors in colon cancer.* Epigenetics, 2008. **3**(1): p. 28-37.
85. Abbas, A. and S. Gupta, *The role of histone deacetylases in prostate cancer.* Epigenetics, 2008. **3**(6): p. 300-9.
86. Melnick, A. and J.D. Licht, *Histone deacetylases as therapeutic targets in hematologic malignancies.* Curr Opin Hematol, 2002. **9**(4): p. 322-32.
87. Yamaguchi, T., et al., *Histone deacetylases 1 and 2 act in concert to promote the G1-to-S progression.* Genes Dev, 2010. **24**(5): p. 455-69.
88. Marquard, L., et al., *Histone deacetylase 1, 2, 6 and acetylated histone H4 in B- and T-cell lymphomas.* Histopathology, 2009. **54**(6): p. 688-98.
89. Gloghini, A., et al., *Expression of histone deacetylases in lymphoma: implication for the development of selective inhibitors.* Br J Haematol, 2009. **147**(4): p. 515-25.
90. Delmore, J.E., et al., *BET bromodomain inhibition as a therapeutic strategy to target c-Myc.* Cell, 2011. **146**(6): p. 904-17.
91. Richon, V.M., et al., *Histone deacetylase inhibitor selectively induces p21WAF1 expression and gene-associated histone acetylation.* Proc Natl Acad Sci U S A, 2000. **97**(18): p. 10014-9.
92. Gupta, M., et al., *Regulation of STAT3 by histone deacetylase-3 in diffuse large B-cell lymphoma: implications for therapy.* Leukemia, 2012. **26**(6): p. 1356-64.

93. Dokmanovic, M., C. Clarke, and P.A. Marks, *Histone deacetylase inhibitors: overview and perspectives.* Mol Cancer Res, 2007. **5**(10): p. 981-9.
94. Yang, X.J. and E. Seto, *HATs and HDACs: from structure, function and regulation to novel strategies for therapy and prevention.* Oncogene, 2007. **26**(37): p. 5310-8.
95. Glozak, M.A. and E. Seto, *Histone deacetylases and cancer.* Oncogene, 2007. **26**(37): p. 5420-32.
96. Peng, L. and E. Seto, *Deacetylation of nonhistone proteins by HDACs and the implications in cancer.* Handb Exp Pharmacol, 2011. **206**: p. 39-56.
97. Lue, J.K., J.E. Amengual, and O.A. O'Connor, *Epigenetics and Lymphoma: Can We Use Epigenetics to Prime or Reset Chemoresistant Lymphoma Programs?* Curr Oncol Rep, 2015. **17**(9): p. 40.
98. Belkina, A.C. and G.V. Denis, *BET domain co-regulators in obesity, inflammation and cancer.* Nat Rev Cancer, 2012. **12**(7): p. 465-77.
99. Sasakawa, Y., et al., *Effects of FK228, a novel histone deacetylase inhibitor, on tumor growth and expression of p21 and c-myc genes in vivo.* Cancer Lett, 2003. **195**(2): p. 161-8.
100. Lin, H.Y., et al., *Targeting histone deacetylase in cancer therapy.* Med Res Rev, 2006. **26**(4): p. 397-413.
101. Burgess, A., et al., *Histone deacetylase inhibitors specifically kill nonproliferating tumour cells.* Oncogene, 2004. **23**(40): p. 6693-701.
102. Ruefli, A.A., et al., *The histone deacetylase inhibitor and chemotherapeutic agent suberoylanilide hydroxamic acid (SAHA) induces a cell-death pathway characterized by cleavage of Bid and production of reactive oxygen species.* Proc Natl Acad Sci U S A, 2001. **98**(19): p. 10833-8.
103. Peng, J., et al., *Brd2 is a TBP-associated protein and recruits TBP into E2F-1 transcriptional complex in response to serum stimulation.* Mol Cell Biochem, 2007. **294**(1-2): p. 45-54.
104. Witter, D.J., et al., *Benzo[b]thiophene-based histone deacetylase inhibitors.* Bioorg Med Chem Lett, 2007. **17**(16): p. 4562-7.
105. Lane, A.A. and B.A. Chabner, *Histone deacetylase inhibitors in cancer therapy.* J Clin Oncol, 2009. **27**(32): p. 5459-68.
106. Prince, H.M., M.J. Bishton, and S.J. Harrison, *Clinical studies of histone deacetylase inhibitors.* Clin Cancer Res, 2009. **15**(12): p. 3958-69.
107. West, A.C. and R.W. Johnstone, *New and emerging HDAC inhibitors for cancer treatment.* J Clin Invest, 2014. **124**(1): p. 30-9.
108. Giles, F., et al., *A phase I study of intravenous LBH589, a novel cinnamic hydroxamic acid analogue histone deacetylase inhibitor, in patients with refractory hematologic malignancies.* Clin Cancer Res, 2006. **12**(15): p. 4628-35.
109. Piekarz, R.L., et al., *Phase II multi-institutional trial of the histone deacetylase inhibitor romidepsin as monotherapy for patients with cutaneous T-cell lymphoma.* J Clin Oncol, 2009. **27**(32): p. 5410-7.
110. McDermott, J. and A. Jimeno, *Belinostat for the treatment of peripheral T-cell lymphomas.* Drugs Today (Barc), 2014. **50**(5): p. 337-45.
111. Whittaker, S.J., et al., *Final results from a multicenter, international, pivotal study of romidepsin in refractory cutaneous T-cell lymphoma.* J Clin Oncol, 2010. **28**(29): p. 4485-91.
112. Coiffier, B., et al., *Results from a pivotal, open-label, phase II study of romidepsin in relapsed or refractory peripheral T-cell lymphoma after prior systemic therapy.* J Clin Oncol, 2012. **30**(6): p. 631-6.
113. Masica, D.L. and R. Karchin, *Collections of simultaneously altered genes as biomarkers of cancer cell drug response.* Cancer Res, 2013. **73**(6): p. 1699-708.
114. Ryan, R.J. and B.E. Bernstein, *Molecular biology. Genetic events that shape the cancer epigenome.* Science, 2012. **336**(6088): p. 1513-4.

115. Prince, H.M., M.J. Bishton, and R.W. Johnstone, *Panobinostat (LBH589): a potent pan-deacetylase inhibitor with promising activity against hematologic and solid tumors.* Future Oncol, 2009. **5**(5): p. 601-12.
116. George, P., et al., *Combination of the histone deacetylase inhibitor LBH589 and the hsp90 inhibitor 17-AAG is highly active against human CML-BC cells and AML cells with activating mutation of FLT-3.* Blood, 2005. **105**(4): p. 1768-76.
117. Sandor, V., et al., *Phase I trial of the histone deacetylase inhibitor, depsipeptide (FR901228, NSC 630176), in patients with refractory neoplasms.* Clin Cancer Res, 2002. **8**(3): p. 718-28.
118. Plumb, J.A., et al., *Pharmacodynamic response and inhibition of growth of human tumor xenografts by the novel histone deacetylase inhibitor PXD101.* Mol Cancer Ther, 2003. **2**(8): p. 721-8.
119. Martinet, N. and P. Bertrand, *Interpreting clinical assays for histone deacetylase inhibitors.* Cancer Manag Res, 2011. **3**: p. 117-41.
120. Dasmahapatra, G., et al., *The pan-HDAC inhibitor vorinostat potentiates the activity of the proteasome inhibitor carfilzomib in human DLBCL cells in vitro and in vivo.* Blood, 2010. **115**(22): p. 4478-87.
121. Kalac, M., et al., *HDAC inhibitors and decitabine are highly synergistic and associated with unique gene-expression and epigenetic profiles in models of DLBCL.* Blood, 2011. **118**(20): p. 5506-16.
122. Bots, M. and R.W. Johnstone, *Rational combinations using HDAC inhibitors.* Clin Cancer Res, 2009. **15**(12): p. 3970-7.
123. Marks, P.A., *The clinical development of histone deacetylase inhibitors as targeted anticancer drugs.* Expert Opin Investig Drugs, 2010. **19**(9): p. 1049-66.
124. Schneider-Stock, R. and M. Ocker, *Epigenetic therapy in cancer: molecular background and clinical development of histone deacetylase and DNA methyltransferase inhibitors.* IDrugs, 2007. **10**(8): p. 557-61.
125. Vesci, L., et al., *Preclinical antitumor activity of ST7612AA1: a new oral thiol-based histone deacetylase (HDAC) inhibitor.* Oncotarget, 2015. **6**(8): p. 5735-48.
126. Giannini, G., et al., *ST7612AA1, a thioacetate-omega(gamma-lactam carboxamide) derivative selected from a novel generation of oral HDAC inhibitors.* J Med Chem, 2014. **57**(20): p. 8358-77.
127. Marushige, K., *Activation of chromatin by acetylation of histone side chains.* Proc Natl Acad Sci U S A, 1976. **73**(11): p. 3937-41.
128. Wu, S.Y. and C.M. Chiang, *The double bromodomain-containing chromatin adaptor Brd4 and transcriptional regulation.* J Biol Chem, 2007. **282**(18): p. 13141-5.
129. Dhalluin, C., et al., *Structure and ligand of a histone acetyltransferase bromodomain.* Nature, 1999. **399**(6735): p. 491-6.
130. Owen, D.J., et al., *The structural basis for the recognition of acetylated histone H4 by the bromodomain of histone acetyltransferase gcn5p.* EMBO J, 2000. **19**(22): p. 6141-9.
131. Filippakopoulos, P., et al., *Histone recognition and large-scale structural analysis of the human bromodomain family.* Cell, 2012. **149**(1): p. 214-31.
132. Dawson, M.A., et al., *Inhibition of BET recruitment to chromatin as an effective treatment for MLL-fusion leukaemia.* Nature, 2011. **478**(7370): p. 529-33.
133. Xiao, Y., et al., *Bromodomain and extra-terminal domain bromodomain inhibition prevents synovial inflammation via blocking IkappaB kinase-dependent NF-kappaB activation in rheumatoid fibroblast-like synoviocytes.* Rheumatology (Oxford), 2016. **55**(1): p. 173-84.
134. Goupille, O., et al., *Inhibition of the acetyl lysine-binding pocket of bromodomain and extraterminal domain proteins interferes with adipogenesis.* Biochem Biophys Res Commun, 2016. **472**(4): p. 624-30.
135. Voigt, P. and D. Reinberg, *BRD4 jump-starts transcription after mitotic silencing.* Genome Biol, 2011. **12**(11): p. 133.

136. You, J., et al., *Kaposi's sarcoma-associated herpesvirus latency-associated nuclear antigen interacts with bromodomain protein Brd4 on host mitotic chromosomes.* J Virol, 2006. **80**(18): p. 8909-19.
137. Korb, E., et al., *BET protein Brd4 activates transcription in neurons and BET inhibitor Jq1 blocks memory in mice.* Nat Neurosci, 2015. **18**(10): p. 1464-73.
138. Dey, A., et al., *A bromodomain protein, MCAP, associates with mitotic chromosomes and affects G(2)-to-M transition.* Mol Cell Biol, 2000. **20**(17): p. 6537-49.
139. Maruyama, T., et al., *A Mammalian bromodomain protein, brd4, interacts with replication factor C and inhibits progression to S phase.* Mol Cell Biol, 2002. **22**(18): p. 6509-20.
140. Dey, A., et al., *The double bromodomain protein Brd4 binds to acetylated chromatin during interphase and mitosis.* Proc Natl Acad Sci U S A, 2003. **100**(15): p. 8758-63.
141. Denis, G.V., B.S. Nikolajczyk, and G.R. Schnitzler, *An emerging role for bromodomain-containing proteins in chromatin regulation and transcriptional control of adipogenesis.* FEBS Lett, 2010. **584**(15): p. 3260-8.
142. Sinha, A., D.V. Faller, and G.V. Denis, *Bromodomain analysis of Brd2-dependent transcriptional activation of cyclin A.* Biochem J, 2005. **387**(Pt 1): p. 257-69.
143. LeRoy, G., B. Rickards, and S.J. Flint, *The double bromodomain proteins Brd2 and Brd3 couple histone acetylation to transcription.* Mol Cell, 2008. **30**(1): p. 51-60.
144. Lamonica, J.M., et al., *Bromodomain protein Brd3 associates with acetylated GATA1 to promote its chromatin occupancy at erythroid target genes.* Proc Natl Acad Sci U S A, 2011. **108**(22): p. E159-68.
145. Gamsjaeger, R., et al., *Structural basis and specificity of acetylated transcription factor GATA1 recognition by BET family bromodomain protein Brd3.* Mol Cell Biol, 2011. **31**(13): p. 2632-40.
146. Zhao, R., et al., *Gene bookmarking accelerates the kinetics of post-mitotic transcriptional re-activation.* Nat Cell Biol, 2011. **13**(11): p. 1295-304.
147. Ceribelli, M., et al., *Blockade of oncogenic IkappaB kinase activity in diffuse large B-cell lymphoma by bromodomain and extraterminal domain protein inhibitors.* Proc Natl Acad Sci U S A, 2014. **111**(31): p. 11365-70.
148. Klein, U. and R. Dalla-Favera, *Germinal centres: role in B-cell physiology and malignancy.* Nat Rev Immunol, 2008. **8**(1): p. 22-33.
149. Yang, Z., N. He, and Q. Zhou, *Brd4 recruits P-TEFb to chromosomes at late mitosis to promote G1 gene expression and cell cycle progression.* Mol Cell Biol, 2008. **28**(3): p. 967-76.
150. Filippakopoulos, P. and S. Knapp, *Targeting bromodomains: epigenetic readers of lysine acetylation.* Nat Rev Drug Discov, 2014. **13**(5): p. 337-56.
151. Chen, R., et al., *Brd4 and HEXIM1: multiple roles in P-TEFb regulation and cancer.* Biomed Res Int, 2014. **2014**: p. 232870.
152. Itzen, F., et al., *Brd4 activates P-TEFb for RNA polymerase II CTD phosphorylation.* Nucleic Acids Res, 2014. **42**(12): p. 7577-90.
153. Rahl, P.B., et al., *c-Myc regulates transcriptional pause release.* Cell, 2010. **141**(3): p. 432-45.
154. Liu, W., et al., *Brd4 and JMJD6-associated anti-pause enhancers in regulation of transcriptional pause release.* Cell, 2013. **155**(7): p. 1581-95.
155. Rahman, S., et al., *The Brd4 extraterminal domain confers transcription activation independent of pTEFb by recruiting multiple proteins, including NSD3.* Mol Cell Biol, 2011. **31**(13): p. 2641-52.
156. Bres, V., S.M. Yoh, and K.A. Jones, *The multi-tasking P-TEFb complex.* Curr Opin Cell Biol, 2008. **20**(3): p. 334-40.
157. Shang, E., et al., *The first bromodomain of Brdt, a testis-specific member of the BET sub-family of double-bromodomain-containing proteins, is essential for male germ cell differentiation.* Development, 2007. **134**(19): p. 3507-15.

158. Matzuk, M.M., et al., *Small-molecule inhibition of BRDT for male contraception.* Cell, 2012. **150**(4): p. 673-84.
159. Pivot-Pajot, C., et al., *Acetylation-dependent chromatin reorganization by BRDT, a testis-specific bromodomain-containing protein.* Mol Cell Biol, 2003. **23**(15): p. 5354-65.
160. Dhar, S., A. Thota, and M.R. Rao, *Insights into role of bromodomain, testis-specific (Brdt) in acetylated histone H4-dependent chromatin remodeling in mammalian spermiogenesis.* J Biol Chem, 2012. **287**(9): p. 6387-405.
161. Muller, S., P. Filippakopoulos, and S. Knapp, *Bromodomains as therapeutic targets.* Expert Rev Mol Med, 2011. **13**: p. e29.
162. Zhang, W., et al., *Bromodomain-containing protein 4 (BRD4) regulates RNA polymerase II serine 2 phosphorylation in human CD4+ T cells.* J Biol Chem, 2012. **287**(51): p. 43137-55.
163. Bisgrove, D.A., et al., *Conserved P-TEFb-interacting domain of BRD4 inhibits HIV transcription.* Proc Natl Acad Sci U S A, 2007. **104**(34): p. 13690-5.
164. Greenwald, R.J., et al., *E mu-BRD2 transgenic mice develop B-cell lymphoma and leukemia.* Blood, 2004. **103**(4): p. 1475-84.
165. Dey, A., et al., *Brd4 marks select genes on mitotic chromatin and directs postmitotic transcription.* Mol Biol Cell, 2009. **20**(23): p. 4899-909.
166. French, C.A., *Pathogenesis of NUT midline carcinoma.* Annu Rev Pathol, 2012. **7**: p. 247-65.
167. Filippakopoulos, P., et al., *Selective inhibition of BET bromodomains.* Nature, 2010. **468**(7327): p. 1067-73.
168. Mertz, J.A., et al., *Targeting MYC dependence in cancer by inhibiting BET bromodomains.* Proc Natl Acad Sci U S A, 2011. **108**(40): p. 16669-74.
169. Trabucco, S.E., et al., *Inhibition of bromodomain proteins for the treatment of human diffuse large B-cell lymphoma.* Clin Cancer Res, 2015. **21**(1): p. 113-22.
170. Zuber, J., et al., *RNAi screen identifies Brd4 as a therapeutic target in acute myeloid leukaemia.* Nature, 2011. **478**(7370): p. 524-8.
171. French, C.A., *NUT midline carcinoma.* Cancer Genet Cytogenet, 2010. **203**(1): p. 16-20.
172. Postel-Vinay, S., et al., *First-in-human phase I dose escalation study of the Bromodomain and Extra-Terminal motif (BET) inhibitor BAY 1238097 in subjects with advanced malignancies.* European Journal of Cancer. **69**: p. S7-S8.
173. Gao, F., et al., *BRAD4 plays a critical role in germinal center response by regulating Bcl-6 and NF-kappaB activation.* Cell Immunol, 2015. **294**(1): p. 1-8.
174. Nicodeme, E., et al., *Suppression of inflammation by a synthetic histone mimic.* Nature, 2010. **468**(7327): p. 1119-23.
175. Herrmann, H., et al., *Small-molecule inhibition of BRD4 as a new potent approach to eliminate leukemic stem- and progenitor cells in acute myeloid leukemia AML.* Oncotarget, 2012. **3**(12): p. 1588-99.
176. Zhao, X., et al., *Disruption of the MYC-miRNA-EZH2 loop to suppress aggressive B-cell lymphoma survival and clonogenicity.* Leukemia, 2013. **27**(12): p. 2341-50.
177. Tolani, B., et al., *Targeting Myc in KSHV-associated primary effusion lymphoma with BET bromodomain inhibitors.* Oncogene, 2014. **33**(22): p. 2928-37.
178. Gao, L., et al., *Androgen receptor promotes ligand-independent prostate cancer progression through c-Myc upregulation.* PLoS One, 2013. **8**(5): p. e63563.
179. Cheng, Z., et al., *Inhibition of BET bromodomain targets genetically diverse glioblastoma.* Clin Cancer Res, 2013. **19**(7): p. 1748-59.
180. Emadali, A., et al., *Identification of a novel BET bromodomain inhibitor-sensitive, gene regulatory circuit that controls Rituximab response and tumour growth in aggressive lymphoid cancers.* EMBO Mol Med, 2013. **5**(8): p. 1180-95.

181. Bhadury, J., et al., *BET and HDAC inhibitors induce similar genes and biological effects and synergize to kill in Myc-induced murine lymphoma.* Proc Natl Acad Sci U S A, 2014. **111**(26): p. E2721-30.
182. Sakamoto, K.M., et al., *Protacs: chimeric molecules that target proteins to the Skp1-Cullin-F box complex for ubiquitination and degradation.* Proc Natl Acad Sci U S A, 2001. **98**(15): p. 8554-9.
183. Lu, J., et al., *Hijacking the E3 Ubiquitin Ligase Cereblon to Efficiently Target BRD4.* Chem Biol, 2015. **22**(6): p. 755-63.
184. Coude, M.M., et al., *BET inhibitor OTX015 targets BRD2 and BRD4 and decreases c-MYC in acute leukemia cells.* Oncotarget, 2015. **6**(19): p. 17698-712.
185. Noel, J.K., et al., *Development of the BET bromodomain inhibitor OTX015.* Proceeding of the 2013 AACR- NCI-EORTC Molecular Targets and Cancer Therapeutics Conference, 2013: p. 414-414.
186. Boi, M., et al., *The BET Bromodomain Inhibitor OTX015 Affects Pathogenetic Pathways in Preclinical B-cell Tumor Models and Synergizes with Targeted Drugs.* Clin Cancer Res, 2015. **21**(7): p. 1628-38.
187. Vazquez, R., et al., *The bromodomain inhibitor OTX015 (MK-8628) exerts anti-tumor activity in triple-negative breast cancer models as single agent and in combination with everolimus.* Oncotarget, 2016.
188. Riveiro, M.E., et al., *OTX015 (MK-8628), a novel BET inhibitor, exhibits antitumor activity in non-small cell and small cell lung cancer models harboring different oncogenic mutations.* Oncotarget, 2016.
189. Lejeune, P., et al., *Abstract 3524: BAY 1238097, a novel BET inhibitor with strong efficacy in hematological tumor models.* Cancer Research, 2015. **75**(15 Supplement): p. 3524.
190. Marks, P.A. and R. Breslow, *Dimethyl sulfoxide to vorinostat: development of this histone deacetylase inhibitor as an anticancer drug.* Nat Biotechnol, 2007. **25**(1): p. 84-90.
191. Cerchietti, L. and J.P. Leonard, *Targeting the epigenome and other new strategies in diffuse large B-cell lymphoma: beyond R-CHOP.* Hematology Am Soc Hematol Educ Program, 2013. **2013**: p. 591-5.
192. Shih, A.H., et al., *The role of mutations in epigenetic regulators in myeloid malignancies.* Nat Rev Cancer, 2012. **12**(9): p. 599-612.
193. de Ruijter, A.J., et al., *Histone deacetylases (HDACs): characterization of the classical HDAC family.* Biochem J, 2003. **370**(Pt 3): p. 737-49.
194. Bolden, J.E., M.J. Peart, and R.W. Johnstone, *Anticancer activities of histone deacetylase inhibitors.* Nat Rev Drug Discov, 2006. **5**(9): p. 769-84.
195. Dekker, F.J., T. van den Bosch, and N.I. Martin, *Small molecule inhibitors of histone acetyltransferases and deacetylases are potential drugs for inflammatory diseases.* Drug Discov Today, 2014. **19**(5): p. 654-60.
196. Chapuy, B., et al., *Discovery and characterization of super-enhancer-associated dependencies in diffuse large B cell lymphoma.* Cancer Cell, 2013. **24**(6): p. 777-90.
197. Berthon, C., et al., *Bromodomain inhibitor OTX015 in patients with acute leukaemia: a dose-escalation, phase 1 study.* Lancet Haematol, 2016. **3**(4): p. e186-95.
198. Stathis, A., et al., *Clinical Response of Carcinomas Harboring the BRD4-NUT Oncoprotein to the Targeted Bromodomain Inhibitor OTX015/MK-8628.* Cancer Discov, 2016. **6**(5): p. 492-500.
199. Amorim, S., et al., *Bromodomain inhibitor OTX015 in patients with lymphoma or multiple myeloma: a dose-escalation, open-label, pharmacokinetic, phase 1 study.* Lancet Haematol, 2016. **3**(4): p. e196-204.
200. Sherman, M.Y., et al., *Oncogenes induce senescence with incomplete growth arrest and suppress the DNA damage response in immortalized cells.* Aging Cell, 2011. **10**(6): p. 949-61.

201. Clozel, T., et al., *Mechanism-Based Epigenetic Chemosensitization Therapy of Diffuse Large B-Cell Lymphoma.* Cancer Discov, 2013. **3**(9): p. 1002-1019.
202. Thieblemont, C. and J. Briere, *MYC, BCL2, BCL6 in DLBCL: impact for clinics in the future?* Blood, 2013. **121**(12): p. 2165-6.
203. Aukema, S.M., et al., *Double-hit B-cell lymphomas.* Blood, 2011. **117**(8): p. 2319-31.
204. Ott, G., A. Rosenwald, and E. Campo, *Understanding MYC-driven aggressive B-cell lymphomas: pathogenesis and classification.* Blood, 2013. **122**(24): p. 3884-91.
205. Reeder, C.B. and S.M. Ansell, *Novel therapeutic agents for B-cell lymphoma: developing rational combinations.* Blood, 2011. **117**(5): p. 1453-62.
206. Staudt, L.M., *II. Therapy of DLBCL based on genomics.* Hematol Oncol, 2013. **31 Suppl 1**: p. 26-8.
207. Honigberg, L.A., et al., *The Bruton tyrosine kinase inhibitor PCI-32765 blocks B-cell activation and is efficacious in models of autoimmune disease and B-cell malignancy.* Proc Natl Acad Sci U S A, 2010. **107**(29): p. 13075-80.
208. Gopal, A.K., et al., *PI3Kdelta inhibition by idelalisib in patients with relapsed indolent lymphoma.* N Engl J Med, 2014. **370**(11): p. 1008-18.
209. Moros, A., et al., *Synergistic antitumor activity of lenalidomide with the BET bromodomain inhibitor CPI203 in bortezomib-resistant mantle cell lymphoma.* Leukemia, 2014. **28**(10): p. 2049-59.
210. Smith, M.A. and P. Houghton, *A proposal regarding reporting of in vitro testing results.* Clin Cancer Res, 2013. **19**(11): p. 2828-33.
211. Mottamal, M., et al., *Histone deacetylase inhibitors in clinical studies as templates for new anticancer agents.* Molecules, 2015. **20**(3): p. 3898-941.
212. Odore, E., et al., *Phase I Population Pharmacokinetic Assessment of the Oral Bromodomain Inhibitor OTX015 in Patients with Haematologic Malignancies.* Clin Pharmacokinet, 2016. **55**(3): p. 397-405.
213. Boi, M., et al., *The BET Bromodomain Inhibitor OTX015 Affects Pathogenetic Pathways in Preclinical B-cell Tumor Models and Synergizes with Targeted Drugs.* Clinical Cancer Research, 2015. **21**(7): p. 1628-38.
214. Ezell, S.A., et al., *Synergistic induction of apoptosis by combination of BTK and dual mTORC1/2 inhibitors in diffuse large B cell lymphoma.* Oncotarget, 2014. **5**(13): p. 4990-5001.
215. Guo, S., et al., *EZH2 mutations in follicular lymphoma from different ethnic groups and associated gene expression alterations.* Clin Cancer Res, 2014. **20**(12): p. 3078-86.
216. Gupta, S.S., et al., *Bromo- and extraterminal domain chromatin regulators serve as cofactors for murine leukemia virus integration.* J Virol, 2013. **87**(23): p. 12721-36.
217. Picaud, S., et al., *PFI-1, a highly selective protein interaction inhibitor, targeting BET Bromodomains.* Cancer Res, 2013. **73**(11): p. 3336-46.
218. Gupta, M., et al., *Inhibition of histone deacetylase overcomes rapamycin-mediated resistance in diffuse large B-cell lymphoma by inhibiting Akt signaling through mTORC2.* Blood, 2009. **114**(14): p. 2926-35.

ARTICLES

ARTICLE 1

www.impactjournals.com/oncotarget/ Oncotarget, Advance Publications 2014

Preclinical antitumor activity of ST7612AA1: a new oral thiol-based histone deacetylase (HDAC) inhibitor

Loredana Vesci[1,*], Elena Bernasconi[2,*], Ferdinando Maria Milazzo[1], Rita De Santis[1], Eugenio Gaudio[2], Ivo Kwee[2,3], Andrea Rinaldi[2], Silvia Pace[1], Valeria Carollo[4], Giuseppe Giannini[1] and Francesco Bertoni[2,5]

[1] Research & Development, Sigma-Tau, Pomezia, Italy

[2] Lymphoma and Genomics Research Program, IOR Institute of Oncology Research, Bellinzona, Switzerland

[3] Dalle Molle Institute for Artificial Intelligence (IDSIA), Manno, Switzerland

[4] Hysto-Cyto Service srl, Rome, Italy

[5] Lymphoma Unit, IOSI Oncology Institute of Southern Switzerland, Bellinzona, Switzerland

[*] These two Authors equally contributed to this work

***Correspondence to**: Loredana Vesci, **email**: loredana.vesci@sigma-tau.it*

*Correspondence to: Francesco Bertoni, **email**: frbertoni@mac.com*

Keywords: histone deacetylase inhibitor, anti-tumor, oral, preclinical, tumor models

***Received**: November 12, 2014 **Accepted**: December 24, 2014 **Published**: December 25, 2014*

ABSTRACT

ST7612AA1 (property of Sigma-Tau), a thioacetate-ω (γ-lactam amide) derivative, is a potent, second generation, oral pan-histone deacetylase inhibitor (HDACi). Aim of the study was to assess the efficacy of ST7612AA1 in solid and haematological tumors, and to characterize its mechanism of action. *In vitro*, ST7612AA1 potently inhibited different class I and class II HDACs, leading to restore the balance of both histone and non-histone protein acetylation. *In vivo*, it induced significant anti-tumor effects in xenograft models of lung, colon, breast and ovarian carcinomas, leukemia and lymphoma. This was likely due to the modulation of different HDAC substrates and induction of transcriptional changes with respect to several genes involved in key processes, such as cell cycle regulation, DNA damage checkpoints, immune response, cell adhesion and epithelial-to-mesenchymal transition. PK analysis confirmed the pro-drug nature of ST7612AA1, which is rapidly absorbed and converted to ST7464AA1 after a single oral dose in mice. ST7612AA1 was selected from a novel generation of oral HDAC inhibitors. Its high efficacy correlated with its potent and selective inhibitory activity of HDAC and was combined with a favorable pharmacodynamics profile. These aspects support a clinical development of ST7612AA1 towards a broad spectrum of human solid and haematologic malignancies.

INTRODUCTION

Epigenetic mechanisms result in changes in gene expression without altering the DNA sequence per se. These changes involve DNA methylation and histone modifications (such as acetylation), which are potentially reversible. Due to this property, modulation of epigenetic gene suppression has become a very attractive model to treat cancer [1]. The expression of histone deacetylases (HDAC) is frequently altered in several malignancies [2], thus histone deacetylase inhibitors (HDACis) able to bind with high affinity to HDACs and to severely affect their enzymatic activity, have emerged as a promising new class of multifunctional anticancer drugs [3, 4]. In fact, HDACis have been previously shown to reduce multiple epigenetic pathways exerting pro-tumorigenic activity. In addition to regulate gene expression and transcription through chromatin remodelling, HDACis can also modulate a variety of cellular functions including growth, differentiation, and survival [5, 6], by enhancing acetylation of a wide variety of proteins, including

transcription factors, modular chaperones, and structural components [3, 7]. Specifically, HDACis have been shown to induce several down-stream effects in tumor cell lines, including: cell cycle arrest, induction of apoptosis, inhibition of angiogenesis, activation or inactivation of tumor suppressor genes or oncogenes, and decrease of invasion and metastasis [3, 4, 8]. Interestingly, tumor cells appear much more sensitive to the induction of apoptosis by HDAC inhibitors than normal cells, probably linked to the disturbed chromatin structure in cancer cells [9] and to the induction of double-strand DNA breaks [10]. The classical HDAC inhibitors inhibit the function of one or more of the 11 known zinc-containing HDAC enzymes. The zinc-containing HDAC enzymes can be classified into several Classes: Class I HDAC (HDAC1, 2, 3, 8), Class IIA (HDAC4, 5, 7, 9), Class IIB (HDAC6, 10) and Class IV (HDAC11) [11]. Class III HDACs or Sirtuins, have a different catalytic mechanism and are not a target for the classical HDAC inhibitors. Generally, pan-HDAC inhibitors inhibit HDACs from Class I, II and IV, while Class specific-HDAC inhibitors only inhibit HDACs from either Class I or Class II. At the present, three HDACis – vorinostat (suberoylanilide hydroxamic acid, Zolinza) orally delivered, depsipeptide (romidepsin, Istodax) and belinostat (Beleodaq) intravenously delivered– have received approval from the US Food and Drug Administration (FDA) for treatment of refractory cutaneous T-cell lymphoma (CTCL), and more recently, depsipeptide has gained FDA approval for peripheral T-cell lymphoma (PTCL) [12-14]. Several HDAC inhibitors are under clinical development in various malignancies, many of them of haematological origin, such as leukemia, lymphoma, and myelodysplastic syndrome [2, 15]. Broadly, HDACis can be classified into different structural groups: the hydroxamic acids, cyclic peptides, benzimides and short-chain fatty acids. Although HDAC inhibitors preferentially targeting a single HDAC have been recently developed [16], it is noteworthy that the hydroxamates are able to target and affect all classes of HDACs, thus exerting nonspecific HDAC-inhibition activity [17, 18].

We previously identified a highly potent HDAC inhibitor, named ST7612AA1 as prodrug of ST7464AA1 (Figure 1A), showing oral antitumor activity in human tumor-bearing mice. This thioacetyl derivative, selected within a lactam carboxamide inhibitors screening project, showed a high cytotoxic activity on NCI-H460 (NSCLC) and HCT116 (colon carcinoma) cell lines and associated to strong induction of tubulin and histone H4 acetylation in cellular assays [19]. The active drug, ST7464AA1 revealed the maximum potency on HDAC3 and 6 (mean of IC_{50}= 4 nM), and then on HDAC1, 10 and 11 (mean of IC_{50}=13 nM) and HDAC2 (IC_{50}=78 nM). The minor potency was observed on HDAC8 (IC_{50}=281 nM) [19].

In this study, the ability of ST7612AA1 in different pre-clinical cancer models characterized by specific protein-overexpression or mutation was determined to better define the pharmacological profile of the drug. Here we report that this novel HDAC inhibitor potently inhibited cell growth/proliferation in human tumor cell lines from both solid and hematologic origin, and significantly suppressed tumor growth in several xenograft models after oral daily delivery, thus suggesting a putative application against some tumor subsets in patients. Furthermore, the drug-dependent modulation of some transcripts involved in immune response and in key pathogenetic pathways, such NF-κB pathway and epithelial-mesenchymal transition, would suggest a relevant implication not only in cancer therapy but also in the inflammatory diseases.

RESULTS

ST7612AA1 reduces HDACs activity

We have previously shown that ST7464AA1 (the active drug of ST7612AA1) is a very potent HDAC inhibitor, displaying activity against different HDAC isoforms in the low nanomolar range [19]. Here, we assessed the ability of ST7612AA1 to affect *in vitro* acetylation of tubulin and histone H4 substrates, which is mainly dependent on HDAC6 and class I HDACs respectively, through Western Blot analysis on NCI-H460 NSCLC cells. As shown in Figure 1B, ST7612AA1 was 40-fold more potent in increasing the acetylation of histone H4 (IC_{50} = 4.8 nM) than of tubulin (IC_{50} = 200 nM). Results and details of the densitometry analysis are shown in Supplementary Figure 1. ST7612AA1 was very effective at increasing histone acetylation at concentrations lower than those determining cytotoxicity on the same cell line, thus confirming the ability of its drug (once released within the cell) to bind with a very high affinity to the catalytic site of different HDAC isoforms.

ST7612AA1 affects proliferation and induces apoptosis in human tumor cell lines

ST7612AA1 showed a high potency in terms of antiproliferative effects in a first broad panel of human tumor cell lines from both solid and hematologic origin. As indicated in Table 1, ST7612AA1 inhibited proliferation in cell lines derived from epithelial cancers (lung, breast, colon, ovarian) and from leukemias and lymphomas, with IC_{50} values ranging from 43 to 500 nmol/L. ST7612AA1 also inhibited the proliferation with comparable potency of different mature B cell lymphomas with a median IC_{50} of 375 nM (range, 46-2664 nM). There were no significant differences among histological subtypes or between germinal center B cell like (GCB) and the activated B cell like (ABC) type –DLBCL: ABC-DLBCL

Table 1: Antiproliferative activity of ST7612AA1 on different human tumor cell lines.

Tumor cell line	IC_{50} (μM)
Ovarian cancer	
A2780	0.043±0.01
SKOV-3	0.38±0.003
Breast cancer	
MDA-MB436	0.18±0.01
MDA-MB231	0.23±0.009
MCF-7	0.19±0.02
NSCLC	
NCI-H460	0.066±0.01
NCI-H1975	0.50±0.05
Colon cancer	
HCT116	0.075±0.01
Acute myeloid leukemia	
MV4;11	0.19±0.02
U937	0.049±0.005
T-cell lymphoma	
HUT78	0.48±0.02
Chronic myeloid leukemia	
K562	0.19±0.02
Diffuse large B-cell lymphoma of the germinal center B-cell type	
DOHH2	0.046±0.01
OCI-Ly8	0.24±0.01
OCI-Ly7	0.56±0.02
SUDHL-6	0.63±0.02
SUDHL-4	0.98±0.01
VAL	2.36±0.1
Karpas422	2.66±0.2
Diffuse large B-cell lymphoma of the activated B-cell like type	
TMD8	0.10±0.03
OCI-Ly10	0.26±0.01
U2932	0.80±0.02
Splenic marginal zone lymphoma	
K1718	0.10±0.01
VL51	0.12±0.09
SSK41	0.26±0.05
Mantle cell lymphoma	
Jeko-1	0.25±0.01
MAVER1	0.39±0.02
Granta-519	0.47±0.05
REC-1	0.55±0.02

Tumor cells were treated for 72 h at different concentrations to evaluate IC_{50} values. IC_{50} values were determined using ALLFIT program, a sigmoidal dose response model. Results are the means ± S.E.M. of three independent experiments.

257 nM (101-805 nM); GCB-DLBCL 597 nM (46-2664 nM); mantle cell lymphoma (MCL) 433 nM (248-553 nM); splenic marginal zone lymphoma (SMZL) 119 nM (102-257 nM). As shown in Supplementary Figure 2, the ST7612AA1 anti-proliferative activity was both time and dose-dependent. Exposure to ST7612AA1 (250 nM) for 72 hrs induced moderate apoptosis in three out of eight lymphoma cell lines (Figure 1C). Differently from what observed regarding on the anti-proliferative activity, the apoptosis was apparently restricted to cell lines bearing a wild type TP53.

ST7612AA1 affects key molecular pathways in DLBCL *in vitro* models

To obtain a global view of the transcriptional changes after ST7612AA1 treatment, we performed GEP (Gene Expression Profiling) on two sensitive cell lines, one derived from GCB-DLBCL (DOHH2) and one from ABC-DLBCL (TMD8). We first confirmed the anti-deacetylase activity of ST7612AA1 in the two cell lines (Figure 2A). Then, the tumor cells were exposed to DMSO or to ST7612AA1 (300 nM) for 8 hours. (Figure 2B). ST7612AA1 importantly affected the gene

expression profile of the two DLBCL cell lines: applying stringent criteria (genes showing fold change > 1.5, with an adjusted p-value < 0.005, were considered as differentially expressed) 674 genes were up-regulated and 563 down-regulated (Supplementary Table 4). Among the most down-regulated genes there were genes known as oncogenes or involved in lymphoma pathogenesis such as *IRAK1*, *MYD88*, *MYC*, *MYB*, *CCND2*, *BLK*, *CDK4*, *IKZF1* or *TNFRSF17* (*BCMA*). Conversely, the up-regulated ones comprised tumor suppressor genes (*CDKN2C*, *CDKN1A*, *CDKN2D*) or genes involved in immune response (*HLA*, *CD69*). Validation of GEP results was obtained by real-time PCR analysis, confirming the up-regulation of *CDKN1A* and down-regulation of *MYC*, *IRAK4*, *MYD88*, *STAT3*, and, in the ABC-DLBCL cell line, also of *IRAK1* (Supplementary Figure 3). Further insights on the pathways affected by exposure to the HDACi were provided by applying the GSEA algorithm (Supplementary Table 5). Functional analysis highlighted that the down-regulated genes were significantly enriched of MYC targets, E2F targets, transcripts coding proteins involved in cell cycle, RNA processing, G1/S transition, DNA damage checkpoint, genes down-regulated in hypoxia, by other HDACis, or by mTOR inhibitor rapamycin. Up-regulated genes were significantly enriched of genes involved in packaging of telomeres, in meiosis, in RNA polymerase I promoter opening, in autophagy regulation, genes coding components of lysosome, cell adhesion molecules, genes up-regulated by other HDACi, genes of the DLBCL prognostically favorable stromal signature. Figure 2C shows some of the gene sets significantly enriched among down- and up-regulated genes.

ST7612AA1 causes growth inhibition of different tumor xenografts

Following the observed potent *in vitro* inhibition of tumor cell proliferation by ST7612AA1, we subsequently investigated whether these properties translated into tumor growth inhibition in preclinical *in vivo* models. Oral ST7612AA1 (60 mg/10 mL/kg, qdx5/w, for 2-4 weeks), strongly inhibited the growth of different pre-established tumor xenografts. In particular, as shown in Table 2, ST7612AA1 inhibited tumor volume by 77% (P<0.01 vs vehicle treated group) in the colon carcinoma model HCT116, consistently with the antiproliferative effect achieved *in vitro* against the same tumor cell line. Analogously, a potent and significant antitumor activity of ST7612AA1 was also shown against other solid tumor xenografts, such as the NSCLC model NCI-H1975 (TVI=65%, P<0.001), the ovarian carcinoma model SKOV-3 (TVI=59%, P<0.01) and the breast cancer model

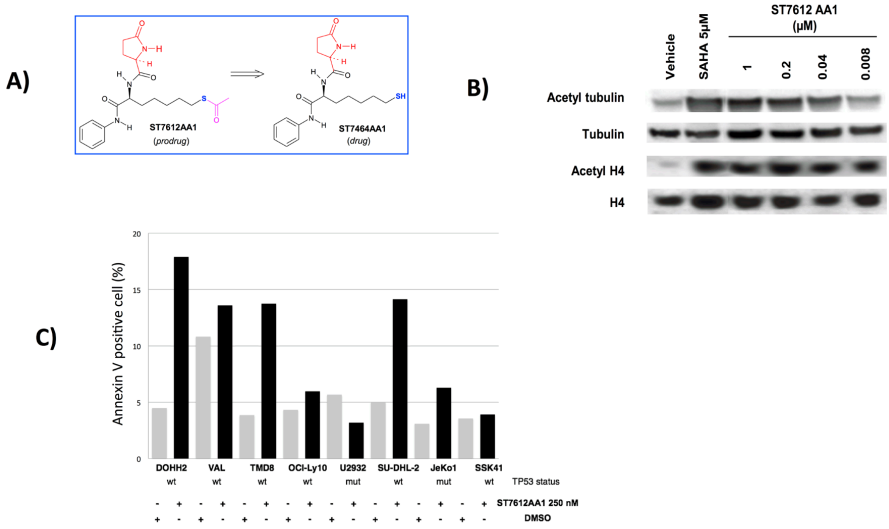

Figure 1: ST7612AA1 reduces HDAC activity and induces apoptosis of human cancer cells. A) Chemical structure of the prodrug ST7612AA1 and its drug ST7464AA1. B) Assessment of a dose-dependent effect of ST7612AA1 on acetylation of alpha-tubulin and histone H4 in NCI-H460 NSCLC cells after 3 h exposure. SAHA 5 μM was used as internal positive reference. To control for equal loading, blots were stripped and reprobed with antibodies against tubulin and histone H4. C) Assessment of ST7612AA1-induced apoptosis in lymphoma cell lines. Y-axis, percentage of Annexin V positive cells after exposure to ST7612AA1 (250 nM) for 72 hrs. The TP53 gene status of each cell line was shown below the X-axis.

Table 2: Antitumor activity of ST7612AA1 against different human tumor cell xenografts in nude mice.

Tumor cells	DT	Treatment schedule	TVI%	BWL% max	Lethal toxicity
Colon cancer HCT-116	5.9	Qdx5/wx3w (3-7, 10-14, 17-21)	**77	1	0/8
NSCLC NCI-H1975	3.5	Qdx5/wx2w (5-9, 12-16)	***65	4	0/8
Ovarian cancer SKOV-3	7.9	Qdx5/wx4w (3-7, 10-14, 17-21, 24-28)	**59	1	0/8
Breast cancer MDA-MB436	9.5	Qdx5/wx4w (6-10, 13-17, 20-24, 27-31)	*35	4	0/8
Acute myeloid leukemia MV4;11	6.6	Qdx5/wx3w (11-15, 18-22, 25-29)	**70	4	0/8

Mice bearing subcutaneously implanted tumor cells were orally administered with ST7612AA1 (60 mg/10 mL/kg) every day according to a schedule Qdx5/w. TVI was calculated 8-10 days after the end of treatment. n=8 mice/group.
DT, Doubling Time. TVI, tumor volume inhibition. BWL%, maximum body weight loss during the experimental period.
Lethal toxicity: Number of mice dead from toxicity/total number of mice. The statistic comparison was performed between the mean of tumor lesions of drug-treated group and the mean of tumors of vehicle-treated group.
*P<0.05 vs vehicle (Mann-Whitney test). **P<0.01 vs vehicle (Mann-Whitney test). ***P<0.001 vs vehicle (Mann-Whitney test).

MDA-MB436 orthotopically implanted in mammary fat pad (TVI=35%, P<0.05). Finally, *in vivo* antitumor efficacy of ST7612AA1 was also observed against hematological tumor models, as shown by the potent antitumor activity (TVI=70%, *P*<0.01) in the AML model MV4;11 (Table 2) and in the GCB-DLBCL model DOHH2 bearing both MYC and BCL2 chromosomal rearrangement in which a significant delay in tumor progression (*P*<0.05) was observed (Supplementary Figure 4).

ST7612AA1 affects key molecular pathways in colon cancer *in vivo* model

Western Blot analysis of the HCT116 tumor xenografts collected 24 h after the last oral administration of ST7612AA1 revealed a strong induction of pan H3 acetylation (Figure 3A). Besides restoring histone acetylation through inhibition of class I HDACs, ST7612AA1 was also effective in targeting HDAC6, as shown by the increased levels of acetylated α-tubulin and by the dramatic decrease of HSP90 protein levels (this effect likely due to hyperacetylation of the chaperone), paralleled by a significant increase of HSP70 levels. Moreover, treatment of HCT116 tumor-bearing mice with ST7612AA1 resulted in up-regulation of P21 and ATF3 proteins, also confirmed at the transcriptional level in Figure 3B, thus suggesting that molecular pathways, activated by DNA damage events (TP53-mediated or not), or associated to a putative ER-stress response, might be involved. This evidence is further supported by qPCR data, showing increased mRNA levels of several genes associated to DNA-damage (*gadd45α*), TP53-mediated pro-apoptotic events (*Noxa*, *P53AIP1*, *stratifin*) and ER-stress response (*gadd153/CHOP*). Treatment with ST7612AA1 also resulted in down-modulation of NF-κB gene (Figure 3B), whereas no effect was observed on the expression of genes involved in DNA replication, such as *TYMS* and *AURK-A*, although the last one was moderately down-modulated at the protein level (Figure 3A). Finally, because HDACis have been shown to counteract the EMT process in different tumor models [20, 21], we next assessed the effects of ST7612AA1 on epithelial/mesenchymal markers in HCT116 tumor xenografts. As shown in Figure 3B, ST7612AA1 induced a significant overexpression of several genes (*e-cadherin*, *keratins 4/18*, *TJP1*, *PDE4D*, *claudin 1*) coding typical epithelial markers and a concomitant down-modulation of genes associated to mesenchymal phenotype, such as *ACTA2*, *syndecan-1* and *vimentin* (the last one being dramatically down-regulated also at the protein level, as depicted in Figure 3A). Overall, biochemical data suggest that reversion of the EMT process might contribute to the *in vivo* antitumor activity of the drug.

ST7612AA1 is *in vivo* rapidly converted to ST7464AA1

The PK profile of ST7612AA1 (pro-drug) and ST7464AA1 (drug) in healthy mice was determined after a single dose of 120 mg/kg of compound administered by oral route. As expected, ST7612AA1 was not detected in plasma after oral administration in mice, confirming its pro-drug properties. Conversely, ST7464AA1 rapidly appeared in plasma being quantifiable at the first blood sampling time (0.25 h). ST7464AA1 reached the C_{max} of 1577 ± 478 ng/mL (as mean ± SEM) 0.5 h post dosing; then its plasma concentration declined according to a bi-exponential profile (Figure 4) being still quantifiable

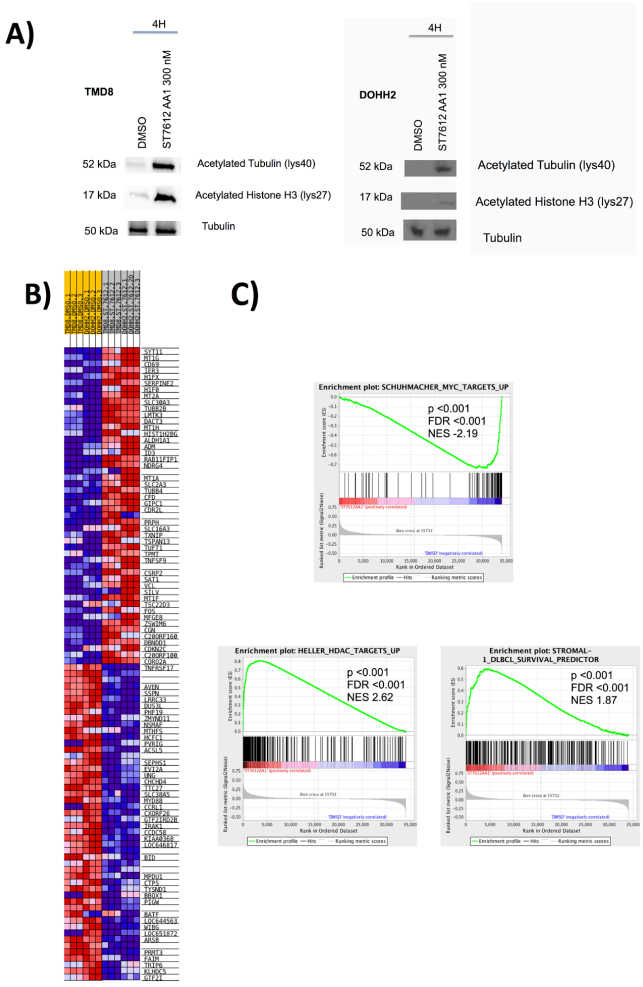

Figure 2: ST7612AA1 affects key molecular pathways in DLBCL. A) ST7612AA1 determines acetylation of alpha-tubulin and histone H3 in DOHH2 and TMD8 DLBCL after 4 h exposure. To control for equal loading, blots were probed with antibodies against tubulin. B) Heat map of the top 50 up- top 50 down-regulated rank ordered genes according to GSEA in DOHH2 and TMD8 DLBCL cells exposed to ST7612AA1 (300 nM) for 8 hrs. Expression values are represented as colors, where the range of colors (red, pink, light blue, dark blue) shows the range of expression values (high, moderate, low, lowest). C) GSEA plot illustrating the enrichment of different biologically relevant gene-sets in DOHH2 and TMD8 DLBCL cells exposed to ST7612AA1 as above. FDR, false discovery rate; NES, normalized enrichment score.

Table 3: **Pharmacokinetic parameters for ST7464AA1 in CD1 mice receiving a single oral dose of 120 mg/kg of ST7612AA1 derived from the plasma concentration vs time data according to a model independent approach for sparse data sampling.**

T_{max} (h)	C_{max}* (ng/mL)	T_{last} (h)	C_{last} (ng/mL)	AUC_{last}* (h* ng/mL)	AUC_{INF} (h*ng/mL)	CL/F (mL/h/kg)	Vz/F (mL/kg)	$T_{1/2}$ (h)
0.5	1577±478	6.0	303	3747±299	5506	21795	119340	3.8

C_{max}: maximum plasma concentration; T_{max}: time of C_{max}; C_{last}: last quantifiable concentration; T_{last}: time of C_{last}; AUC_{last}: (area under the concentration vs time curve from 0 to T_{last}; AUC_{INF}: area under the concentration vs time curve from 0 to infinity; $T_{1/2}$: terminal half-life; CL/F: apparent systemic clearance; Vz/F: apparent terminal volume of distribution; *: mean ± SEM.

at the last blood sampling time (6 h). ST7464AA1 was cleared from plasma with a $T_{1/2}$ of 3.8 h. ST7464AA1 pharmacokinetics parameters are summarized in Table 3. The drug showed a high CL/F; furthermore, its large Vz/F indicated a good propensity to distribute outside the systemic circulation.

DISCUSSION

Recently, a systematic study of medicinal chemistry aimed at identifying a new generation of HDAC inhibitors led us to select a new class of thiol-based potent pan-HDACis [19]. *In vivo* pharmacodynamic analysis of several preselected analogues resulted in the identification of ST7612AA1, (property of Sigma-Tau), a thioacetate-ω (γ-lactam amide) derivative, first synthetic thiol derivative, as potent oral pan-histone deacetylase inhibitor (HDACi), in preclinical phase. This a prodrug of ST7464AA1, which has exquisite potency toward all class I HDACs (IC_{50} values of 12.7 and 77.7 nM for HDAC1 and HDAC2, respectively) and toward HDAC isoforms encompassed within the class IIb HDACs (IC_{50} value of 3.18 nM for HDAC6). In agreement with the powerful inhibition of class I HDACs, here, we show that ST7612AA1 had a broad spectrum antiproliferative activity on cell lines derived from ovarian cancer, breast cancer, NSCLC, colon cancer and haematological tumors, including acute monocytic leukaemia, chronic myeloid leukaemia and lymphoma, at concentrations that are significantly below those achieved in plasma of mice (Cmax, 1577 ± 478 ng/mL, dosing ST7612AA1 po at 120 mg/kg). Importantly, the oral treatment with ST7612AA1, once daily, for 2

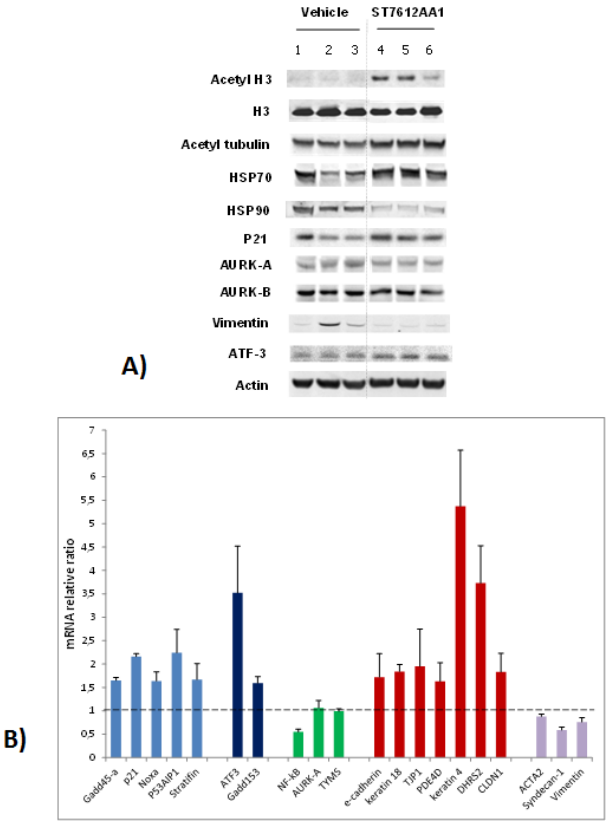

Figure 3: Effect of ST7612AA1 on key molecular targets in colon cancer. A) Western Blot analysis for assessing the degree of acetylation of histone H3 and tubulin, and for evaluating the expression levels of various target proteins in HCT-116 tumor xenografts collected 24 hours after the last treatment with 80 mg/10 mL/kg ST7612AA1 (lanes 4-6) once daily, according to the schedule qdx5/wx3w, with respect to vehicle-treated animals (lanes 1-3). Actin is shown as a control for protein loading. Representative blots of tumor samples from 3 animals/group are shown. B) Real-time qPCR analysis of ST7612-induced gene changes in HCT-116 tumor xenografts collected as above described. Data are normalized to cyclophilin A and presented as fold change (average ± s.d.) over the vehicle-treated control mice (n=3 animals/group). Sybr Green-based q-PCR analysis was performed using the primer set shown in Suppl. Table 3.

or 3 weeks, strongly inhibited tumor growth in several preclinical *in vivo* models derived from both solid tumors and haematological cancers. In particular, ST7612AA1 was able to significantly inhibit tumor growth of the Ras-mutant HCT116 colon carcinoma xenografts, thus suggesting a putative therapeutic approach towards this subset of strongly proliferating dedifferentiated colorectal carcinoma, characterized by overexpression of class I HDAC family members and associated with reduced patient survival [22].

In addition, our data indicate that ST7612AA1 can significantly inhibit *in vitro* the proliferation of NSCLC cell lines bearing wild type EGFR (and mutant KRAS), such as NCI-H460, as well as a secondary (T790M) EGFR mutation, which is known to confer resistance to tyrosine kinase inhibitors [23], such as NCI-H1975. Interestingly, ST7612AA1 showed also a significant *in vivo* antitumor effect against the latter tumor xenograft model.

Since class I HDAC isoforms are expressed at significantly higher levels in ovarian cancer compared to normal ovarian tissue [24], and various HDAC inhibitors can prevent both *in vitro* and *in vivo* growth of ovarian cancer cells [25, 26], we investigated the *in vivo* efficacy of ST7612AA1 also in two ovarian carcinoma models. Our data clearly showed a strong antitumor effect of ST7612AA1 against both the SKOV-3 model, characterized by low levels of PTEN and overexpression of EGFR and ErbB2 [27], and even more the A2780 xenograft, characterized by the absence of PTEN [19].

Triple-negative breast cancer (TNBC) represents a heterogeneous subset of neoplasms defined by the absence of estrogen receptor (ER), progesterone receptor (PR) and Her2/neu, which accounts for approximately 15% of globally diagnosed breast cancers and which does not respond to hormonal therapy (such as tamoxifen or aromatase inhibitors) or therapies that target HER2 receptors [28-31]. Anyhow, recent papers have suggested a putative therapeutic approach also with HDAC inhibitors [32, 33]. ST7612AA1 evidenced a strong antiproliferative activity *in vitro* against two TNBC cell lines (MDA-MB231 and MDA-MB436). Moreover, when tested *in vivo* against the BRCA1-defective MDA-MB436 tumor xenograft ortotopically implanted in mammary fat pad, ST7612AA1 caused a significant reduction of tumor growth associated to minimal animal toxicity, thus providing promising preclinical data that would suggest a putative therapeutic approach against this subset of breast cancer.

The ST7612AA1 treatment resulted also in a significant tumor growth inhibition of the AML model MV4;11, subcutaneously implanted in athymic nude mice. MV4;11 tumor is known to be driven by the tyrosine kinase receptor Flt3-ITD mutation. The activating internal tandem duplications (ITD) in the juxtamembrane domain of FLT3 have been identified in 35% AML patients [34]. MV4;11 has been shown to be dependent on FLT3-ITD by its sensitivity to selective FLT3 kinase inhibitors [35]. The best approach to the treatment of FLT3-ITD AML is currently undefined, and multiple clinical trials are investigating FLT3 kinase inhibitors [36] but, unfortunately, their action is very often transient, possibly due to inadequate dosing or insufficient selectivity of these

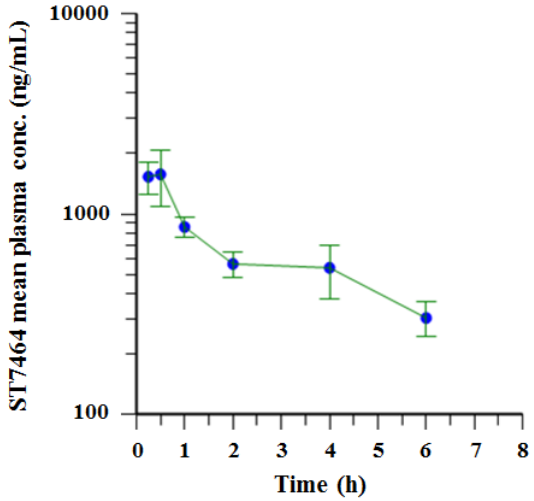

Figure 4: Plasma concentration-time profile of ST7464AA1 following oral (PO) administration of ST7612AA1 to mice. The pharmacokinetic parameters of ST7464AA1 are shown in Table 3. Mean (± SEM) plasma concentration versus time of ST7464AA1 after a single oral dose of 120 mg/kg of ST7612AA1 in CD1 male mice (lin-log scale) (n=5).

drugs. For these reasons, treatment with our HDACi might represent a promising therapeutic option also for patients with this kind of tumor.

Deregulation of proteins involved in chromatin remodelling is very frequent in lymphomas, which represent an interesting target for HDACi [12, 13, 37]. Here, ST7612AA1 presented a wide *in vitro* anti-proliferative activity on various models of lymphomas, induced apoptosis in TP53 wild type lymphoma cells, affected relevant pathogenetic pathways in DLBCL cell lines, and also reduced the growth of DLBCL xenografts. In particular, ST7612AA1 affected the NF-κB signaling, and this is of particular interest for the important role played by this pathway in the pathogenesis of certain lymphoma subtypes, such as the ABC-DLBCL, MCL and marginal zone lymphomas [38, 39]. Moreover, the compound was also able to down-regulate MYC target genes, and this might be clinically relevant for DLBCL, in which MYC confers a very poor clinical outcome when co-expressed with the BCL2 protein or when co-translocated with the *BCL2* gene [39, 40]. Importantly, the *in vivo* antitumor activity of ST7612AA1 was indeed observed against a cell line characterized by both MYC and BCL2 gene translocations. Thus, the compound appears worth of further investigation in the lymphoma context. Furthermore, present molecular and biochemical data suggest that, once hydrolyzed, ST7612AA1 acts both in nucleus and cytoplasm of the target tumor cell, through HDAC6 inhibition, as observed for other HDACi of the hydroxamate class [41]. In fact, beside restoring the balance of the histone acetylation that, in turn, results in a more relaxed chromatin structure, with areas of loosely compacted, and hencemore transcriptionally active chromatin that is more prone to DNA double strand breaks [42], ST7612AA1 is also able to target non-histone HDAC substrates involved, for example in the regulation of multiple cellular functions, such as P53, *alpha*-tubulin or the heat shock protein 90 (HSP90), through inhibition of HDAC6, which has been implicated in DNA damage signaling, transcription factor binding, and DNA repair processes [43]. Interestingly, at least when tested *in vivo* against colon carcinoma xenografts, ST7612AA1 induced increased transcription of e-cadherin, keratins and other typical epithelial markers and, concomitantly, induced down-regulation of vimentin and other genes associated to the mesenchymal phenotype, thus suggesting that treatment with ST7612AA1 might also cause a "cadherin switch" and reversion of the EMT process. Other HDAC inhibitors such as SAHA, TSA and panobinostat were shown to induce EMT phenotype, which was associated with increased expression of mesenchymal markers such as vimentin, N-cadherin and fibronectin [44, 45]. The ability of cells to transdifferentiate and dedifferentiate plays a key role in invasion and metastasis by the process of epithelial-mesenchymal-transition (EMT) [46], and differentiation patterning may be used as an additional prognostic and predictive indicator for therapeutic effectiveness.

Histone deacetylase inhibitors (HDACi) were primarily developed as anti-tumor agents for cancer, but many are now being explored for treating neurodegenerative, immunologic, metabolic, inflammatory and cardiovascular disorders [47].

ST7612AA1 was able to determine expression changes of transcripts involved in immune response and in key pathogenetic pathways, such as the NF-κB pathway and cell cycle alteration, thus suggesting a relevant putative involvement not only in cancer therapy but also in the inflammatory diseases [48]. Lysine acetylation is a key regulator of the NF-κB pathway, which works in concert with other PTMs *via* complex crosstalk mechanisms to determine the signaling output. Importantly, small molecule modulators of its writers (HATs) or erasers (HDACs) have been demonstrated to regulate NF-κB signaling, suggesting that these are potential drugs for inflammatory diseases.

These data combined with the excellent *in vivo* tolerability and the oral delivery may represent a therapeutic advantage for this novel HDAC inhibitor.

In conclusion, based upon the obtained data, ST7612AA1 appears as a candidate for clinical development to evaluate its therapeutic activity towards a broad spectrum of human solid and haematologic malignancies.

MATERIALS AND METHODS

Ethics Statement

All animal experiments were conducted according to relevant national and international guidelines. Experimental protocols were approved by the Ethic Committee for Animal Experimentation of Sigma Tau according to the United Kingdom Coordinating Committee on Cancer Research Guidelines. When tumor volume exceeded 2 cm^3, mice were euthanized by cervical dislocation.

Drugs

For *in vitro* experiments, stock solutions of ST7612AA1 (property of Sigma-Tau) were prepared in 100% dimethyl sulfoxide at 10 mM and stored at -20°C. For oral administration, ST7612AA1 was dissolved in solutol HS15 + water (1:20) and delivered in a volume of 10 mL/kg.

Cell lines and cell culture

Supplementary Table 1 lists all the cell lines used with their growth conditions and their origin. All cells were maintained in a humidified atmosphere with 5% CO_2 at 37°C. All experiments were always performed starting from frozen cell stocks of each cell line. Upon thawing, such cells were characterized in house, by assessing cell morphology, cell growth kinetics curve and absence of mycoplasma. The human cell lines purchased from accredited biological resource centers (i.e. ATCC, ECACC, DSMZ) have been originally authenticated and characterized directly by the providers (STR profiling). Lymphoma cell lines were validated by the Authors using DNA profiling within the last six months from the beginning of the study. All the experiments have been then performed using cells within 6-8 passages since thawing from an internal cell bank.

In vitro proliferation assay

Anti-proliferative activity was first assessed on a panel of cell lines derived from solid tumors and hematological cancers and then on a large panel of cell lines derived from mature B-cell lymphomas. In the first panel, cells were seeded in 96-wells tissue culture plates in complete medium and, 24 h after seeding, were exposed to increasing concentrations of ST7612AA1 for 72 h; the inhibition of proliferation was assessed by the sulphorodamine B assay. Lymphoma cells were seeded in 96-wells tissue culture plates in complete medium and were exposed to increasing concentrations of ST7612AA1 for 48 or 72 h; the anti-proliferative activity was assessed using 3-(4,5-dimethylthiazol-2-yl)-2,5-diphenyltetrazolium bromide (MTT). The drug potency was evaluated by means of the "ALLFIT" computer program and defined as IC_{50} (drug concentration required for 50% inhibition of cell survival).

Detection of apoptotic cells

Apoptosis was assessed, on cells treated with DMSO or different doses of ST7612AA1, by Annexin V-FITC apoptosis detection kit (BD Biosciences), according to the manufacturer's recommendations, on a FACScan flow cytometer (BD Biosciences).

Western Blotting Analysis

For assessing the *in vitro* effect of ST7612AA1 on acetylation of α-tubulin and histones, NSCLC cells were treated with the test compound at various concentrations (dose-response curve). SAHA 5 μM was used as reference inhibitor. Protein extraction, separation and immunoblotting were performed as previously described [19]. Immunoreactive bands were finally subjected to densitometry analysis by a phosphoimaging system (STORM, Molecular Dynamics), and then the IC_{50} values were calculated by the "ALLFIT" computer program. The antibodies used are listed in Supplementary Table 2.

In vivo xenograft models

Experiments on solid tumor and acute leukemia *in vivo* models were carried out at Sigma-Tau (Rome, Italy) using female athymic nude mice, 5-6 weeks-old (Harlan Laboratories, Udine, IT). Mice were maintained in laminar flow rooms with constant temperature and humidity in according to the NIH guidelines. The following human tumor xenograft models were used for antitumor activity studies: HCT116 derived from colon carcinoma), MV4;11 from acute myeloid leukaemia (AML), SKOV-3 from ovarian carcinoma, and NCI-H1975 from non-small cell lung cancer (NSCLC). Exponentially growing tumor cells were s.c. inoculated ($5x10^6$/mouse) in the right flank of nude mice. Groups of eight mice/group were employed to assess antitumor activity. MDA-MB436 breast carcinoma ($3x10^6$ cells/0.1 mL of M199/Matrigel GFR 50:50, vol/vol solution) was inoculated in mammary fat pad (mfp). Drug treatments were started from 3 to 11 days after tumor injection, depending on the tumor growth of the xenografted cancer model. ST7612AA1 was given daily for five days per week (qdx5/w). Tumor growth was followed by measurements of tumor diameters with a Vernier caliper. Tumor volume (TV) was calculated using the formula: TV (mm^3) = [d^2 x D]/2, where d and D are the shortest and the longest diameter, respectively. The efficacy of the drug treatment was assessed as: TV inhibition percentage (TVI%) in treated versus control mice, calculated as: TVI%=100-(mean TV treated/mean TV control x100). When tumors reached a volume of 500-1000 mm^3, mice were sacrificed by cervical dislocation. To examine the possible toxicity of treatment, body weight was recorded throughout the study. BWL% (body weight loss) was calculated as 100 – (mean BW_{dayx}/mean BW_{day1}x100), where day 1 is the first day of treatment and day x is any day after (maximum BWL%). DT as doubling time of control tumors was also evaluated.

In order to assess the *in vivo* effect of ST7612AA1 on the acetylation degree of α-tubulin and histones, and on the expression of other key proteins, HCT116 tumor xenografts (3 samples/group) were excised at different times after the last treatment, and then total protein lysates were prepared through the homogenization of tumor samples in lysis buffer containing 0.5% NP-40, supplemented with 10 μg/mL of protease inhibitor cocktail (Sigma Chemical Co., St. Louis, MO, USA). Determination of the protein concentration and Western Blotting analysis were finally performed as above described for the *in vitro* experiments. The antibodies used

are listed in Supplementary Table 2.

The *in vivo* experiment with lymphoma model was performed in the IOR laboratory according to study protocols approved by the local Cantonal Veterinary Authority (No. 5/2011). At day 1, tumors were established by injecting DOHH2 lymphoma cells (200 µL of PBS, $8x10^6$ cells/mouse) into the left flanks of 5-weeks old female NOD-SCID mice (Harlan Laboratories). Tumor size was measured on regular basis and until tumors reached around 0.5 mm in diameter (day 12). Then, treatments were conducted at day 12, 13, 15, 16, 18, 19. Tumors were measured at 12, 14, 17, 21, 25 days. Tumor volumes were calculated as described above. Mice were sacrificed when physical conditions became critical or when tumors reached a weight of about 0.5 gr. For comparison between a control and a treatment group, an unpaired Mann-Whitney's test was used. A *P*-value <0.05 was considered significant.

Quantitative Real-Time RT-PCR

Total RNA was extracted from tumour xenografts and then retrotranscribed using the Trizol reagent and the ThermoScript RT-PCR System (Invitrogen, Paisley, UK), respectively, according to the manufacturer's instructions. SYBR Green-based qPCR analyses were performed in 96-well plates by using the 7900HT Sequence Detection System instrument and software (Applied Biosystems). Amplification mixes (20 µL) contained 1x QuantiTect SYBR PCR kit (QIAGEN, Hilden, Germany), and 0.2-0.3 µM of each specific primer. In addition, the mRNA levels of *cyclophilin A* were quantitatively measured in each sample to control for sample-to-sample differences in RNA concentration. The cycling conditions comprised a 600 s denaturation step at at 95°C, followed by 40 cycles of denaturation at 95°C for 15 s, annealing at 60°C for 20 s, and extension at 72°C for 10 s. The oligonucleotides used as specific primers for each target gene were designed, using the manufacturer's software and the sequences available in GenBank, to overlap a splice junction thereby avoiding a potential amplification of contaminating genomic DNA, and are described in Supplementary Table 3. A six-point serial standard curve was generated for each target gene. All expression levels were finally normalized to *cyclophilin A* in each well.

PK sampling and analysis

CD1 nude mice were used. Male mice were treated with a single dose of ST7612AA1 at 120 mg/10 mL/kg p.o., using 5% Solutol HS 15 in water for injection as vehicle. Blood samples were collected at 0.25, 0.5, 1, 2, 4 and 6 h post treatment from 5 animals per time point. Levels of ST7612AA1 and ST7464AA1 were determined in plasma by quantitative LC-MS/MS having a limit of quantification of 25 ng/mL. The PK parameters C_{max} (maximum plasma concentration), T_{max} (time of maximum plasma concentration), C_{last} (last quantifiable concentration), T_{last} (time of last quantifiable plasma concentration), AUC_{last} (area under the concentration *vs* time curve from 0 to T_{last}), AUC_{INF} (area under the concentration *vs* time curve from 0 to infinity), $T_{1/2}$ (terminal half-life), CL/F (apparent systemic clearance) and Vz/F (apparent terminal volume of distribution) were derived from the analyte plasma concentration vs time data according to a model independent approach for sparse data sampling by using Phoenix WinNonlin® ver. 6.3 software (Pharsight, Cetara).

Gene expression profiling

Gene Expression Profiling (GEP) was done using the HumanHT-12 v4 Expression BeadChip (Illumina, San Diego, CA, USA), as previously described [49]. Three replicates were done for each condition. Data were quantile normalized and differential expression analysis was performed using LIMMA [50]. Quantitative Real-time Polymerase chain reaction (qRT-PCR) was performed as previously described [49] (primer sequences available upon request). Gene-sets differentially affected by exposure to ST7612AA1 were identified with the Gene Set Enrichment Analysis (GSEA) tool using the GSEA C2, C3.tft, C6 collections [51] and the Signature DB collection [52]. Raw data are available at the National Center for Biotechnology Information (NCBI) Gene Expression Omnibus (GEO) (http://www.ncbi.nlm.nih.gov/geo) database (series record: GSE62460).

Statistical analysis

Data are expressed as the mean ± S.E.M. Statistical analysis was performed using Mann-Whitney's test. A *P*-value of <0.05 was considered statistically significant.

ACKNOWLEDGEMENTS

The authors wish to thank Dr. MB Guglielmi, Dr. M Barbarino, Mrs P. Tobia, Mr. A. Marconi and Mr. M. De Santis for their excellent technical assistance. Work partially supported with research funds from the Nelia et Amadeo Barletta Foundation (to F.B.).

Disclosure of Potential Conflicts of Interest

L.V., F.M.M., R.D.S., S.P., G.G. are Sigma-Tau employees. F.B. has received research funds from Sigma-Tau. The remaining authors disclosed no conflicts of interest.

Authors's Contributions

L.V. supervisioned, designed experiments, interpreted data and co-wrote the manuscript; F.M.M. designed experiments, interpreted data and co-wrote the manuscript; E.B. performed experiments, interpreted data; R.D.S. revised the manuscript; E.G. performed experiments; I.K. performed data mining; A.R. performed gene expression profiling; S.P. designed and interpreted PK experiments; V.C. performed experiments; G.G. designed the drug candidate ST7612AA1 and reviewed the manuscript; F.B. designed experiments, performed data mining, interpreted data, co-wrote the manuscript. L.V. and E.B. equally contributed. All authors have approved the final manuscript.

REFERENCES

1. Lakshmaiah KC, Jacob LA, Aparna S, Lokanatha D, Saldanha SC. Epigenetic therapy of cancer with histone deacetylase inhibitors. J Cancer Res Therap. 2014; 10-469-78.
2. Lane AA, Chabner BA. Histone deacetylase inhibitors in cancer therapy. J Clin Oncol. 2009; 27: 5459-68
3. Drummond DC, Noble CO, Kirpotin DB, Guo Z, Scott GK, Benz CC. Clinical development of histone deacetylase inhibitors as anticancer agents. Annu Rev Pharmacol Toxicol. 2005; 45: 495-528.
4. Liu T, Kuljaca S, Tee A, Marshall GM. Histone deacetylase inhibitors: multifunctional anticancer agents. Cancer Treat Rev. 2006; 32: 157-165.
5. Lin HY, Chen CS, Lin SP, Weng JR, Chen CS. Targeting histone deacetylase in cancer therapy. Med Res Rev. 2006; 26: 397-413.
6. Kouzarides T. SnapShot: histone modifyng enzymes. Cell. 2007; 131: 822.
7. Konstantinopoulos PA, Karamouzis MV, Papavassiliou AG. Focus on acetylation: the role of histone deacetylase inhibitors in cancer therapy and beyond. Expert Opin Investig Drugs. 2007; 16: 569-71.
8. Xu WS, Parmigiani RB, Marks PA. Histone deacetylase inhibitors: molecular mechanisms of action. Oncogene. 2007; 26: 5541-52.
9. Nalabothula N and Carrier F. Cancer cells' epigenetic composition and predisposition to histone deacetylase inhibitor sensitization. Epigenomics. 2011; 3:144-5510.
10. Lee JH, Choy ML, Ngo L, Foster SS and Marks PA. Histone deacetylase inhibitor induces DNA damage, which normal but not transformed cells can repair. Proc Natl Acad Sci USA. 2010; 207: 14639-44.
11. Witt O, Deubzer HE, Milde T and Oehme I. HDAC family: what are the cancer relevant targets? Cancer Lett. 2009; 277: 8-21.
12. Marks PA, Breslow R. Dimethyl sulfoxide to vorinostat: development of this histone deacetylase inhibitor as an anticancer drug. Nat Biotechnol. 2007; 25: 84-90.
13. Campas-Moya C. Romidepsin for the treatment of cutaneous T-cell lymphoma. Drugs Today. 2009; 45: 787-9514.
14. Bodiford A, Bodge M, Talbott MS, Reddy NM. Profile of belinostat for the treatment of relapsed or refractory peripheral T-cell lymphoma. Oncotargets and Therapy. 2014; 7: 1971-77.
15. Prince HM, Bishton MJ, Harrison SJ. Clinical studies of histone deacetylase inhibitors. Clin Cancer Res. 2009; 15: 3958-69.
16. Oheme I, Deubzer HE, Wegener D, Pickert D, Linke JP, Hero B, Kopp-Schneider A, Wetermann F, Ulrich SM, von Deimling A., Fischer M and Witt O. Histone deacetylase 8 in neuroblastoma tumorigenesis. Clin Cancer Res. 2009; 15: 91-99.
17. Marks PA. The clinical development of histone deacetylase inhibitors as targeted anticancer drugs. Expert Opin Investig Drugs. 2010; 19: 1049-66.
18. Schneider-Stock R, Ocker M. Epigenetic therapy in cancer: molecular background and clinical development of histone deacetylase and DNA methyltransferase inhibitors. IDrugs. 2007; 10: 557-61.
19. Giannini G, Vesci L, Battistuzzi G, Vignola D, Milazzo FM, Guglielmi MB, Barbarino M, Santaniello M, Fantò N, Mor M, Rivara S, Pala D, Taddei M et al. ST7612AA1, a Thioacetate-ω(γ-lactam carboxamide) derivative selected from a novel generation of oral HDAC inhibitors. J.Med. Chem. 2014, 57, 8358−8377.
20. Bruzzese F, Leone A, Rocco M, Carbone C, Piro G, Caraglia M, Di Gennaro E, Budillon A. HDAC inhibitor vorinostat enhances the antitumor effect of gefitinib in squamous cell carcinoma of head and neck by modulating ErbB receptor expression and reverting EMT. J Cell Physiol. 2011; 226: 2378-2390.
21. Kiesslich T, Pichler M, Neureiter D. Epigenetic control of epithelial-mesenchymal-transition in human cancer. Mol Clin Oncol. 2013; 1: 3-11.
22. Weichert W, Roske A, Niesporek S, Noske A, Buckendahl AC, Dietel M, Gekeler V, Boehm M, Beckers T, Denkert C. Class I histone deacetylase expression has independent prognostic impact in human colorectal cancer: specific role of class I histone deacetylases *in vitro* and *in vivo*. Clin Cancer Res. 2008; 14: 1669-77.
23. Pao W, Miller VA, Politi KA, Riely GJ, Somwar R, Zakowski MF, Kris MG, Varmus H. Acquired resistance of lung adenocarcinomas to gefitinib or erlotinib is associated with a second mutation in the EGFR kinase domain. PLoS Med. 2005; 2:e73.
24. Khabele D, Son DS, Parl AK, Goldberg GL, Augenlicht LH, Mariadason JM, Rice VM. Drug-induced inactivation or gene silencing of class I histone deacetylases suppresses

ovarian cancer cell growth: implications for therapy. Cancer Biol Ther. 2007; 6:795-801.

25. Dietrich CS, Greenberg VL, DeSimone CP, Modesitt SC, Van Nagell JL, Craven R, Zimmer SG. Suberoylanilide hydroxamic acid (SAHA) potentiates paclitaxel-induced apoptosis in ovarian cancer cell lines. Gynecol Oncol. 2010; 116: 126-30.
26. Modesitt SC, Sill M, Hoffman JS, Bender DP. A phase II study of vorinostat in the treatment of persistent or recurrent epithelial ovarian or primary peritoneal carcinoma: a Gynecologic Oncology Group Study. Gynecol Oncol. 2008; 109: 182-6.
27. Longva KE, Pedersen NM, Haslekas C, Stang E, Madshus IH. Herceptin-induced inhibition of Erbb2 signaling involves reduced phorophylation of Akt but not endocytic down-regulation of Erbb2. Int J Cancer. 2005; 116: 359-67.
28. Elias AD. Triple-negative breast cancer: a short review. Am J Clin Oncol 2010; 33: 637-45.
29. Jernal A, Bray F, Center MM, Ferlay J, Ward E, Forman D. Global cancer statistics. Cancer J Clin. 2011; 61: 69-90.
30. Anders CK, Carey LA. Biology metastatic patterns, and treatment of patients with triple-negative breast cancer. Clin Breast Cancer. 2009; 9: S73-81.
31. Hudis CA, Gianni L. Triple-negative breast cancer: an unmet medical need. Oncologist. 2011; 16: 1-11.
32. Tate CR, Rhodes LV, Segar HC, Driver JL, Pounder FN, Burow ME, Collins-Burow BM. Targeting triple-negative breast cancer cells with the histone deacetylase inhibitor panobinostat. Breast Cancer Research. 2012; 14:R79.
33. Ha K, Fiskus W, Choi DS, Bhaskara S, Cerchietti L, Devaraj SG, Shah B, Sharma S, Chang JC, Melnick AM, Hiebert S, Bhalla KN. Histone deacetylase inhibitor treatment induces 'BRCAness' and synergistic lethality with PARP inhibitor and cisplatin against human triple negative breast cancer cells. Oncotarget. 2014; 5: 5637-5650.
34. Gilliland DG, Griffin JD. Role of FLT3 in leukemia. Curr Opin Hematol. 2002; 9: 274-81.
35. Lopes de Menezes DE, Peng J, Garrett EN, Louie SG, Lee SH, Wiesmann M, Tang Y, Shephard L, Goldbeck C, Oei Y, Ye H, Aukerman SL, Heise C. CHIR-258: a potent inhibitor of FLT3 kinase in experimental tumor xenograft model of human acute myelogenous leukemia. Clin Cancer Res. 2005; 11: 5281-91.
36. Fathi AT, Chabner BA. FLT3 inhibition as therapy in acute myeloid leukemia: a record of trials and tribulations. Oncologist. 2011; 16: 1162-74.
37. Cerchietti L, Leonard JP. Targeting the epigenome and other new strategies in diffuse large B-cell lymphoma: beyond R-CHOP. Hematology Am Soc Hematol Educ Program. 2013; 2013:591-95.
38. Staudt LM. II Therapy of DLBCL based on genomics. Hematol Oncol. 2013; 31: S1 (26-28).
39. Bertoni F. Pathologic diagnosis: molecular genetics. In: Carbone A, Younes A. eds. Non-Hodgkin Lymphomas: Advanced Diagnostics and Personalized Therapies. London, UK: Future Medicine Ltd; 2013: 56-81.
40. Aukema SM, Siebert R, Schuuring E, Van Imhoff GW, Kluin-Nelemans HC, Boerma EJ, Kluin PM. Double-hit B cell lymphomas. Blood. 2011; 117: 2319-31.
41. Minucci S, Pelicci PG. Histone deacetylase inhibitors and the promise of epigenetic (and more) treatments for cancer. Nat Rev Cancer. 2006; 6: 38-51.
42. Kim MS, Blake M, Baek JK, Kohlhagen G, Pommier Y, Carrier F. Inhibition of histone deacetylase increases cytotoxicity to anticancer drugs targeting DNA. Cancer Res. 2003; 63: 7291-300.
43. Namdar M, Perez G, Ngo L, Marks PA. Selective inhibition of histone deacetylase 6 (HDAC6) induces DNA damage and sensitizes transformed cells to anticancer agents. Proc Natl Acad Sci. 2010; 107: 20003-8.
44. Kong D, Ahmad A, Bao B, Li Y, Banerjie S, Sarkar S, Sarkar FH. Histone deacetylase inhibitors induce epithelial-to-mesenchymal transition in prostate cancer cells. Plos One. 2012; 7: e45045.
45. Di Fazio P, Montalbano R, Quint K, Alinger B, Kemmerling E, Kiesslich T, Ocker M, Neureiter D. The pan-deacetylase inhibitor panobinostat modulates the expression of epithelial-mesenchymal transition markers in hepatocellular carcinoma models. Oncol Lett. 2013; 5: 127–134.
46. Gavert N, Ben-Ze'ev A. Epithelial-mesenchymal transition and the invasive potential of tumors. Trends Mol Med. 2008; 14: 199-209.
47. Dinarello CA, Fossati G, Mascagni P. Histone deacetylase inhibitors for treating a spectrum of diseases not related to cancer. Mol Med. 2010; 17: 333-52.
48. Dekker FJ, Van den Bosch T, Martin NI. Small molecule inhibitors of histone acetyltransferases and deacetylases are potential drugs for inflammatory diseases. Drug Discovery Today. 2014; 19:654-60.
49. Bonetti P, Testoni M, Scandurra M, Ponzoni M, Piva R, Mensah AA, Rinaldi A, Kwee I, Tibiletti MG, Igbal J, Greiner TC, Chan WC, Gaidano G et al. Deregulation of ETS1 and FLI1 contributes to the pathogenesis of diffuse large B-cell lymphoma. Blood. 2013; 122: 2233-41.
50. Smyth GK. Linear models and empirical Bayes methods for assessing differential expression in microarray experiments. Stat Appl Genet Mol Biol. 2004; 3: 3.
51. Subramanian A, Tamayo P, Mootha VK, Mukherjiee S, Ebert BL, Gillette MA, Paulovich A, Pomeroy SL, Golub TR, Lander ES, Mesirov JP. Gene set enrichment analysis: A knowledge-based approach for interpreting genome-wide expression profiles. PNAS. 2005; 102: 15545-50.
52. Shaffer AL, Wright G, Yang L, Powell J, Ngo V, Lamy L, Lam LT, Davis RE, Staudt LM. A library of gene expression signatures to illuminate normal and pathological lymphoid biology. Immunol Rev. 2006; 210:67-85.

ARTICLE 2

Published OnlineFirst January 26, 2015; DOI: 10.1158/1078-0432.CCR-14-1561

Cancer Therapy: Preclinical

Clinical Cancer Research

The BET Bromodomain Inhibitor OTX015 Affects Pathogenetic Pathways in Preclinical B-cell Tumor Models and Synergizes with Targeted Drugs

Michela Boi[1], Eugenio Gaudio[1], Paola Bonetti[1], Ivo Kwee[1,2,3], Elena Bernasconi[1], Chiara Tarantelli[1], Andrea Rinaldi[1], Monica Testoni[1], Luciano Cascione[1,4], Maurilio Ponzoni[5], Afua Adjeiwaa Mensah[1], Anastasios Stathis[4], Georg Stussi[4], María Eugenia Riveiro[6], Patrice Herait[7], Giorgio Inghirami[8,9,10], Esteban Cvitkovic[6,7], Emanuele Zucca[4], and Francesco Bertoni[1,4]

Abstract

Purpose: In cancer cells, the epigenome is often deregulated, and inhibition of the bromodomain and extra-terminal (BET) family of bromodomain-containing proteins is a novel epigenetic therapeutic approach. Preliminary results of an ongoing phase I trial have reported promising activity and tolerability with the new BET bromodomain inhibitor OTX015.

Experimental Design: We assessed the preclinical activity of OTX015 as single agent and in combination in mature B-cell lymphoma models and performed *in vitro* and *in vivo* experiments to identify the mechanism of action and the genetic features associated with sensitivity to the compound.

Results: OTX015 showed antiproliferative activity in a large panel of cell lines derived from mature B-cell lymphoid tumors with median IC_{50} of 240 nmol/L, without significant differences among the different histotypes. *In vitro* and *in vivo* experiments showed that OTX015 targeted NFKB/TLR/JAK/STAT signaling pathways, MYC- and E2F1-regulated genes, cell-cycle regulation, and chromatin structure. OTX015 presented *in vitro* synergism with several anticancer agents, especially with mTOR and BTK inhibitors. Gene expression signatures associated with different degrees of sensitivity to OTX015 were identified. Although OTX015 was mostly cytostatic, the compound induced apoptosis in a genetically defined subgroup of cells, derived from activated B-cell–like diffuse large B-cell lymphoma, bearing wt*TP53*, mutations in *MYD88*, and *CD79B* or *CARD11*.

Conclusions: Together with the data coming from the ongoing phase I study, the *in vitro* and *in vivo* data presented here provide the basis for further clinical investigation of OTX015 as single agent and in combination therapies. *Clin Cancer Res; 21(7); 1–11.* ©2015 AACR.

Introduction

The epigenome is in a highly dynamic condition due to precise temporal and spatial chromatin modifications, and proper chromatin regulation is fundamental in controlling gene expression and critical for fundamental cellular processes, including self-renewal, differentiation, and proliferation (1, 2). In cancer cells, the epigenome is very often deregulated due to aberrant changes in histone modifications, DNA methylation, and noncoding RNA expression levels (1). The contribution to the assembly and the positioning of the transcriptional machinery represents one of the most important functions of chromatin remodeling that is largely mediated by a variety of histone-modifying enzymes that write and read the "histone code" (1, 2). Epigenetic writers are enzymes that chemically modify DNA or histones, erasers remove such chemical modifications, and, finally, readers recognize specific histone acetylated lysine residues and facilitate transcriptional activation by recruiting transcription factors and other elements of the transcription machinery. Importantly, chromatin modifications can be manipulated and reversed (3), providing the rational to pharmacologically target the epigenome. In the lymphoma field, the epigenetic erasers histone deacetylases (HDAC) represent the currently most explored therapeutic targets (3), with HDAC inhibitors (HDACI), vorinostat and romidepsin, approved by the FDA for cutaneous T-cell lymphomas.

[1]Lymphoma and Genomics Research Program, IOR Institute of Oncology Research, Bellinzona, Switzerland. [2]Dalle Molle Institute for Artificial Intelligence (IDSIA), Manno, Switzerland. [3]Swiss Institute of Bioinformatics (SIB), Lausanne, Switzerland. [4]IOSI Oncology Institute of Southern Switzerland, Bellinzona, Switzerland. [5]Unit of Lymphoid Malignancies, Department of Onco-Haematology, San Raffaele Scientific Institute, Milan, Italy. [6]OTD Oncology Therapeutic Development, Clichy, France. [7]Oncoethix, Lausanne, Switzerland. [8]Department of Pathology and Center for Experimental Research and Medical Studies (CeRMS), University of Turin, Turin, Italy. [9]Department of Pathology and Laboratory Medicine, Weill Cornell Medical College, New York, New York. [10]Department of Pathology and NYU Cancer Center, New York University School of Medicine, New York, New York.

Note: Supplementary data for this article are available at Clinical Cancer Research Online (http://clincancerres.aacrjournals.org/).

M. Boi, E. Gaudio, and P. Bonetti contributed equally to this article.

Current address for M. Boi: Weill Cornell Medical College, New York, New York; current address for G. Inghirami, Weill Cornell Medical College, New York, New York; current address for P. Bonetti, Italian Institute of Technology, Center for Genomic Sciences, Milan, Italy.

Corresponding Author: Francesco Bertoni, Lymphoma and Genomics Research Program, IOR Institute of Oncology Research, via Vincenzo Vela 6, 6500 Bellinzona, Switzerland. Phone: 419-1820-0367; Fax: 419-1820-0305; E-mail: frbertoni@mac.com

doi: 10.1158/1078-0432.CCR-14-1561

Published OnlineFirst January 26, 2015; DOI: 10.1158/1078-0432.CCR-14-1561

Translational Relevance

In cancer cells, the epigenome is often deregulated, and inhibition of the bromodomain and extra-terminal (BET) family of bromodomain-containing proteins is a novel epigenetic therapeutic approach. OTX015, a new oral BET bromodomain inhibitor that is now in its early clinical development, shows a wide preclinical activity in lymphoma models and it affects important biologic pathways, such as MYC, NFKB, TLR, and JAK/STAT pathways. The observed synergism with different compounds provides the basis for the future clinical development of OTX015 in combination.

Inhibition of the bromodomain and extra-terminal (BET) family of bromodomain-containing proteins (BRD2, BRD3, BRD4, and the testis-specific BRDT) is a novel and promising epigenetic therapeutic approach (4, 5). The BET bromodomain proteins mainly act as epigenetic readers (2, 6), and their important role in transcription regulation is demonstrated by their enrichment in superenhancers, clusters of enhancers incorporating high amounts of transcription factors and coactivators that modulate the expression of key genes controlling cell identity in normal cells and of oncogenes (6, 7). Different evidence supports the direct involvement of BET bromodomain proteins in cancer (2), including the observation that *Eμ-BRD2* transgenic mice, overexpressing BRD2 in the B-cell compartment, develop aggressive B-cell leukemias, and lymphomas resembling diffuse large B-cell lymphomas (DLBCL; ref. 8). Furthermore, BET bromodomain inhibitors have shown antitumor activity in different preclinical models derived from hematologic or solid tumors (4, 5, 9–20). The compounds induce cell-cycle arrest in G_1 and, depending on the type of tumor model, apoptosis or cell differentiation (4, 5, 9, 11, 21). BET bromodomain inhibitors highly downregulate the transcription of genes regulated by superenhancers, such as MYC and other genes fundamental for neoplastic cells (4–6, 10, 14, 15). At least four BET bromodomain inhibitors are in ongoing oncology/hematology phase I clinical studies (CPI-0610, NCT01949883; GSK525762, NCT01587703; OTX015, NCT01713582; TEN-010, NCT01987362). The first results from the phase I with the orally available BET bromodomain inhibitor OTX015 (17) have been reported with clinical responses in both leukemia and lymphoma patients in the absence of major toxicities (22). Here, we show the preclinical activity of OTX015, as a single agent and in combination, in mature B-cell lymphomas, and we report data on the possible mechanism of action and on genetic features associated with sensitivity to the compound.

Materials and Methods

Cell lines and molecules

Established human cell lines derived from DLBCL, mantle cell lymphomas (MCL), multiple myeloma (MM), splenic marginal zone lymphoma (splenic MZL), and prolymphocytic leukemia (PLL) were cultured in the culture media listed in Supplementary Table S1. The cell lines were not authenticated independently. OTX015 was provided by Oncoethix SA. Other compounds used were everolimus, doxorubicin, ibrutinib, lenalidomide, bendamustine, decitabine, idelalisib, vorinostat, romidepsin (Selleckchem), and rituximab (Roche).

Cell proliferation, cell death, cell cycle

The effect on cell proliferation, cell growth, apoptosis, and cell cycle were assessed as previously described (23, 24).

Senescence

Cells were treated with DMSO or different doses of OTX015 and stained using a β-Galactosidase Staining Kit (Calbiochem). Cells were fixed with 4% formalin and the nuclei stained with fast-red dye. Images were acquired using a Zeiss light microscope. Senescence-associated β-galactosidase (SA-βgal) activity was also assessed by a fluorescence-based assay using flow cytometry. Cells were seeded and treated with OTX015 or the equivalent amount of DMSO and, after the treatment, were incubated with 100 nmol/L Bafilomycin A1 (Sigma-Aldrich) for 1 hour to alkalize the lysosomes. Cells were then incubated for 2 hours with 33 μL of 2 mmol/L 5-dodecanoylaminofluorescein-di-β-D-galactopyranoside (C12FDG; Invitrogen), washed thoroughly and analyzed with a FACSCan flow cytometer (Becton Dickinson AG). Data were analyzed with FlowJo 7.6.3 software (Tree Star).

Western blotting analysis

Protein extraction, separation, and immunoblotting were performed as previously described (23). The following antibodies were used: anti-BRD2 (ab37633), anti-BRD3 (ab56342), anti-BRD4 (ab75898, AbCam), anti-MYC (9E10, Becton Dickinson AG or Cell Signaling Technology), anti-α-GAPDH (MAB374, Millipore), anti-STAT3 (9139), anti-phospho-STAT3 (Ser727; 9134), and anti-phospho-STAT3 (Tyr705; 9131; Cell Signaling Technology).

Immunohistochemistry

Monoclonal antibodies against phospho-STAT, p50 (Cell Signaling Technology) were applied. In all instances, antigen retrieval was performed with Tris-EDTA at pH 9, 30 minutes at 98°C. Reactions were developed with Ultravision Quanto Detection System (TL-125-QHL; Thermo Scientific).

Real-time PCR

RNA was extracted using the RNeasy Kit (Qiagen AG). Real-time PCR was performed as previously described (ref. 23; sequences available upon request).

Gene expression profiling

Gene expression profiling (GEP) was done using the HumanHT-12-v4 Expression BeadChip (Illumina). Data processing and statistical analysis was performed using R/Bioconductor (25). Transcript mapping was based on HG19 using manufacturer supplied annotation. Data were quantile normalized and subsequently batch corrected using ComBat (26). Differential expression analysis was performed using LIMMA (27). Functional annotation was performed using the Gene set enrichment analysis (28) and Metacore (Thomson Reuters) tools. The top significantly differentially expressed genes between treated and untreated cells were analyzed in MetaCore by building a network consisting of the shortest paths (that is, having the smallest possible number of directed one-step interactions) between pairs of the transcripts in each direction, using standard Dijkstra shortest paths algorithm, maximum path

Published OnlineFirst January 26, 2015; DOI: 10.1158/1078-0432.CCR-14-1561

length of two, and filtering by limiting the interactions type to transcription regulation, influence on expression, and miRNA binding. Raw data will be available at the National Center for Biotechnology Information Gene Expression Omnibus (http://www.ncbi.nlm.nih.gov/geo) database.

Evaluation of interleukins production

Cells treated with OTX015 or DMSO were harvested, washed, and resuspended in fix-perm buffer (Becton Dickinson AG) and left for 30 minutes at 4°C. After a wash with perm buffer (Becton Dickinson AG), cells were resuspended in perm buffer and the antibodies anti-IL4-PE and anti-IL10-PE (eBioscience). Samples were left for 30 minutes in the dark. After the incubation, cells were washed in PBS, resuspended in PBS, analyzed using the FACScan flow cytometer. Data were analyzed with FlowJo 7.6.3 software.

Chromatin immunoprecipitation followed by high-throughput DNA sequencing

We analyzed the publicly available chromatin immunoprecipitation followed by high-throughput DNA sequencing (ChIP-Seq) dataset from the Short Read Archive under accession number SRP043524 (20). The 36-bp sequence reads were aligned to human reference genome build GRCh37 (hg19) using Bowtie (29). Redundant reads were removed and reads uniquely mapping to reference genome were used for further analysis. A maximum of one mismatch was allowed for each read. The detection of genomic regions enriched by chromatin immunoprecipitation (ChIP) versus the negative control immunoprecipitation (IP) experiment done with an anti-Flag antibody was carried out using HOMER v2.6 (30). Specific peaks were defined as having at least a 4-fold difference in enrichment within a 200-bp region between the two SRP043524 experimental conditions (DMSO vs. JQ1) and applying the HOMER default thresholds for statistical significance (FDR = 0.001 and Poisson *P* cutoff = 1e−04). All discovered putative peaks were ranked by their normalized tag counts (number of tags found at the peak, normalized to 10 million total mapped tags) and annotated with annotatePeaks.pl using the GCRh37 (hg19) dataset.

Chromatin immunoprecipitation

Cells were cross-linked with 1% formaldehyde. Cross-linking was quenched with 125 mmol/L glycine. Cells were washed with ice-cold PBS containing 1× HALT protease inhibitor (Thermo Scientific) and resuspended in SDS lysis buffer (ChIP Assay Kit, Millipore) before sonication. For each immunoprecipitation reaction, 1×10^6 chromatin cell equivalents were incubated overnight with 5 μg anti-BRD4 antibody (catalog no. A301-985A; Bethyl Laboratories) or 3 μg of the negative control antibody, anti-IgG (Millipore). Immune complexes were collected by incubation with 20 μL magnetic protein G beads (4°C, 1.5 hours). Protein G-bound complexes were sequentially washed with low salt wash buffer, high salt wash buffer, LiCl wash buffer, and twice with TE Buffer (ChIP Assay Kit; Millipore). Elution of protein/DNA complexes was performed using 1% SDS and 0.1 mol/L $NaHCO_3$. Following reversal of cross-links (65°C for 4 hours), samples were treated with RNAse A and then Proteinase K. DNA samples purification was performed with QIAquick PCR Purification Kit (Qiagen). Chromatin samples to which no antibody had been added were processed in parallel as input references. Quantitative real-time PCR of ChIP-DNA was performed using primers specific for a locus of BRD4 binding in the upstream regulatory region of *MYD88* (chr3:38179682-38179840) as determined by analyzing the ChIP-Seq dataset SRP043524 (20); primers specific for human alpha-satellite were used as a negative control (sequences available upon request).

***In vivo* experiments**

At day 1, tumors were established by injecting SU-DHL-2 lymphoma cells (200 μL of PBS, 15×10^6 cells/mouse) into the left flanks of female NOD-SCID mice (approximately 20 g of body weight; The Harlan Laboratory, S. Pietro al Natisone, Udine, Italy). Tumor size was measured on regular basis. Treatments were conducted daily, twice a day. Mice maintenance and animal experiments were performed with study protocols approved by the local Cantonal Veterinary Authority (No. 5/2011). Differences in tumor volumes were calculated using the Wilcoxon rank-sum test (Stata/SE 12.1 for Mac, Stata Corporation). The *P* value for significance was <0.05.

Drug combinations and evaluation of synergism

Cells were seeded in 96-well plates at 10^4 cells per well. Molecules were serially diluted in tissue culture media and added to cells (in five replicates) and incubated for 72 hours at 37°C, 5% CO_2. MTT assay was then performed as described (31). The combinations were evaluated using the Chou–Talalay Combination Index (CI), calculated with the Synergy R package (32). The effect of the combinations was defined synergistic (CI < 0.9), additive (CI, 0–9–1.1) or antagonist (CI > 1.1).

Results

OTX015 has antiproliferative activity in *in vitro* models of B-cell lymphomas

We first evaluated the antiproliferative activity of the BET bromodomain inhibitor OTX015 in a panel of 33 cell lines derived from mature B-cell lymphoid tumors. As assessed by MTT assays performed after 72 hours of drug exposure, OTX015 was active in a dose-dependent manner in almost all the cell lines (Fig. 1A), at concentrations achievable in the clinical setting (33). The median IC_{50} value for the whole series was 240 nmol/L (range, 70 nmol/L–15 μmol/L). The median values for the individual lymphoma entities were 195 nmol/L (70 nmol/L–1.5 μmol/L) in DLBCL, 470 nmol/L (340 nmol/L–15 μmol/L) in MCL, 170 nmol/L (105–240 nmol/L) in splenic MZL, 450 nmol/L (60–700 nmol/L) in MM, and 90 nmol/L in the PLL cell line. The antiproliferative effect of OTX015 did not significantly differ among the different the histotypes, or between germinal-center type (GCB) DLBCL (190 nmol/L; 80 nmol/L–1.5 μmol/L) and activated B-cell–like (ABC) DLBCL (200 nmol/L; 70 nmol/L–2.28 μmol/L).

In accordance with the observed antiproliferative activity, OTX015 treatment of DLBCL cells inhibited cell growth and induced cell-cycle arrest with G_1 accumulation and decreased S-phase (Fig. 1B and Supplementary Fig. S1). OTX015 also induced a time-dependent increase of β-Gal–positive cells (Fig. 1C).

OTX015 induces apoptosis in a genetically defined subgroup of DLBCL

We then assessed the induction of apoptosis after OTX015 exposure in DLBCL cells. Dose- and time-dependent apoptosis was observed in 3 of 22 (14%) cell lines treated for 72 hours with a

Published OnlineFirst January 26, 2015; DOI: 10.1158/1078-0432.CCR-14-1561

Boi et al.

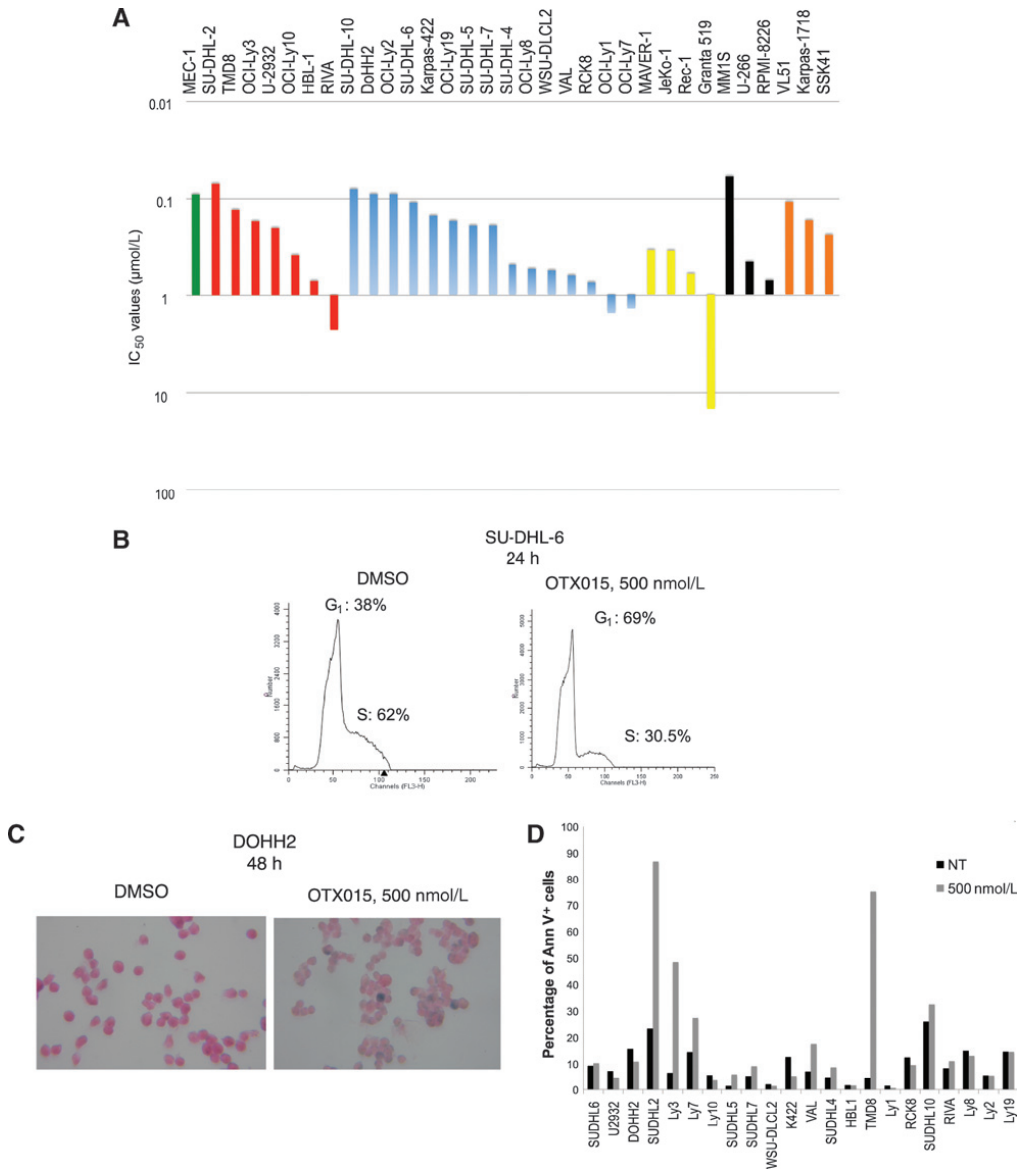

Figure 1.
OTX015 has antiproliferative activity in *in vitro* models of B-cell lymphomas. A, IC_{50} values calculated through MTT assay in 33 mature B-cell lymphoid tumor cell lines after 72 hours of drug exposure (experiments done in triplicate). Green, PLL; red, ABC-DLBCL; blue, GCB-DLBCL; yellow, MCL; black, MM; orange, splenic MZL. B, representative flow cytometry profiles showing cell-cycle alterations induced by OTX015 (500 nmol/L) in the SU-DHL-6 cell line. C, representative image showing the appearance of β-Gal–positive cells after exposure of the DoHH2 cell line to OTX015. D, percentage of apoptotic cells before and after 72 hours of OTX015 (500 nmol/L) or DMSO (NT).

Published OnlineFirst January 26, 2015; DOI: 10.1158/1078-0432.CCR-14-1561

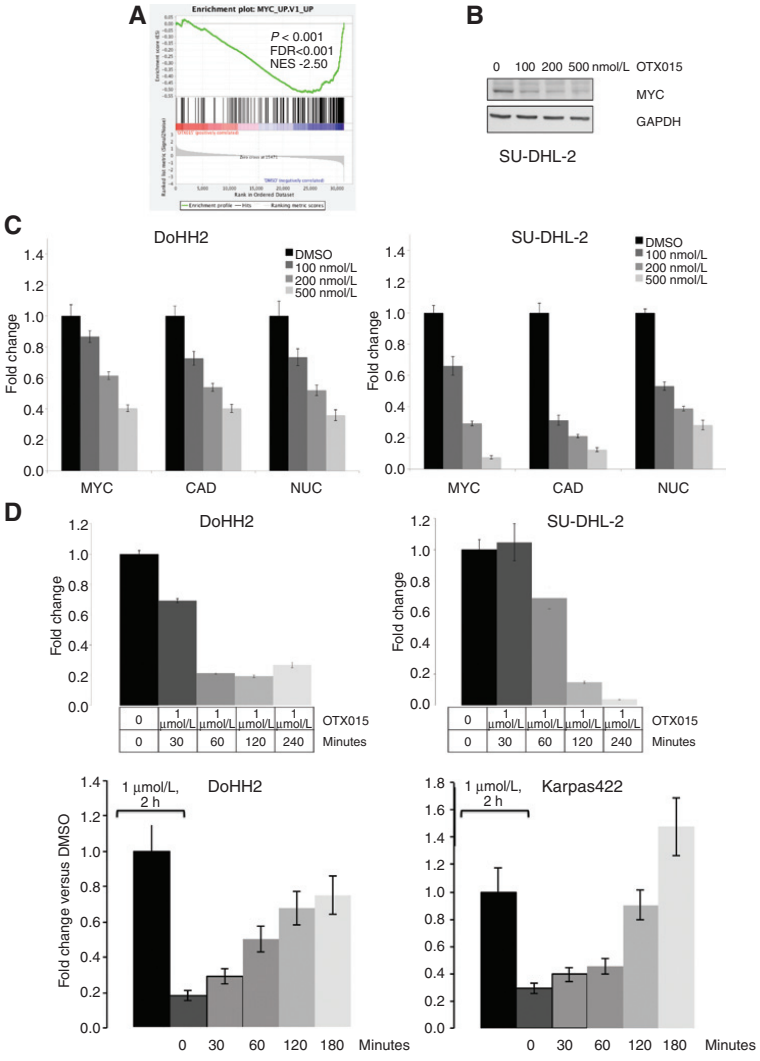

Figure 2.
OTX015 induces MYC downregulation in B-cell lymphomas. A, GSEA plot illustrating the enrichment of the GSEA M2711 MYC oncogenic signature in SU-DHL-2 and SU-DHL-6 cells treated with OTX015 (500 nmol/L). FDR, false discovery rate; NES, normalized enrichment score. B, MYC protein levels are downregulated after OTX015 treatment. C, MYC and MYC targets CAD and NUC mRNA are downregulated after OTX015 treatment for 8 hours in a dose-dependent manner. *Y* axis, fold change versus GAPDH and DMSO-treated cells. D, MYC mRNA levels are downregulated in a time-dependent manner by OTX015 and restored after removal of the compound from the media after 2 hours of treatment. *Y* axis, fold change versus GAPDH and DMSO-treated cells.

dose of 500 nmol/L (Fig. 1D and Supplementary Fig. S2). A massive apoptotic induction was obtained in SU-DHL-2 and TMD8, whereas OCI-Ly3 had a lower, although significant, induction of apoptosis. All these three cell lines presented common genetic and biologic features: derivation from ABC-DLBCL, mutated *MYD88* gene, wild-type *TP53*, mutations in *CD79B* (SU-DHL-2, TMD8), or in *CARD11* (OCI-Ly3). The presence of mutations in genes coding for MYD88 and for components of the BCR signaling was significantly associated with apoptosis induction ($P = 0.027$).

Transcriptional signature of OTX015 in DLBCL cell lines

To obtain a global view of the transcriptional changes after OTX015 treatment, we performed GEP on two sensitive cell lines, one derived from GCB-DLBCL (SU-DHL-6) and one from ABC-DLBCL (SU-DHL-2), treated with DMSO or with OTX015 (500 nmol/L) for 1, 2, 4, 8, and 12 hours. OTX015 affected, in a time-dependent manner, important biologic processes: NF-κB, Toll-like receptor (TLR), Janus kinase (JAK)/STAT signaling pathways, MYC- and E2F1-regulated genes, cell-cycle regulation, and chromatin structure (Fig. 2 and Supplementary Figs. S3 and S4;

Published OnlineFirst January 26, 2015; DOI: 10.1158/1078-0432.CCR-14-1561

Supplementary Table S2). The upregulated genes were mainly represented by transcripts coding for histones, overlapping with those upregulated by HDACi, while the downregulated transcripts comprised *MYC* and *E2F1* targets or genes involved in NFKB/TLR/JAK/STAT pathways. Supplementary Table S3 lists the top most differentially expressed probes (adjusted $P < 0.01$ and absolute fold change >1.5), with MYC as the most downregulated transcript. The OTX015 GEP signature appeared similar to that reported following exposure to another BET bromodomain inhibitor, JQ1, in different tumor models (4, 5, 14, 15, 21) (Supplementary Fig. S5). OTX015 appeared similar to JQ1 also in terms of activity on cell viability and induction of apoptosis in SU-DHL-2 and DOHH2 DLBCL cell lines (data not shown), as also recently reported by Chapuy and colleagues (10).

OTX015 induces MYC downregulation in DLBCL

Similar to that reported for other BET bromodomain inhibitors (4, 5, 21), treatment with OTX015 led to an important negative regulation of MYC and its target genes. MYC was the central hub connecting almost all the most significantly OTX015-regulated genes (Supplementary Fig. S4), and MYC target genes were significantly enriched among OTX015-regulated transcripts (Fig. 2A). MYC changes were validated at RNA and protein level (Fig. 2B and C). The effect of OTX015 on *MYC* and its target genes was both time and dose dependent (Fig. 2C and D). The effect on MYC appeared reversible, as the mRNA levels started to be restored in a time-dependent manner, albeit with different kinetics among the individual DLBCL cell lines, after replacing drug-containing medium with fresh medium (Fig. 2D). The level and the kinetics of *MYC* downregulation after drug exposure did not appear associated with the sensitivity to OTX015 (data not shown).

OTX015 affects the NFKB, TLR, and JAK/STAT signaling pathways in DLBCL cells

OTX015 negatively regulated transcripts encoding members of the NF-κB, TLR, and JAK/STAT signaling pathways, such as *MYD88*, *IRAK1*, *TLR6*, *TNFRSF17*, *IL6*, and *IRF4*, in both GCB- and ABC-DLBCL cells (Fig. 3). The inhibitory effect of OTX015 on the pathways was further confirmed at protein level. Both immunoblotting and immunohistochemistry showed a reduction of the transcriptionally active phospho-STAT3 in SU-DHL-2 and TMD8, two ABC-DLBCL cell lines, as well a reduction of the nuclear localization of p50 (NFKB1), indicating a clear inhibitory effect of OTX015 on the canonical NF-κB pathway (Fig. 3B–D). In ABC-DLBCL cell lines, we observed a reduced production of IL10 and IL4 after 24 hours of OTX015 treatment (Supplementary Fig. S6) and a dose-dependent downregulation of additional transcripts suggestive of NF-κB activation (*BIRC3*, *TNFAIP3*; data not shown).

On the basis of the hypothesis that MYD88 may play a central role in the mechanism of action of OTX015, we sought to understand whether BET bromodomain inhibitors had a direct effect on the gene regulation. We first analyzed the publicly available ChIP-Seq data obtained for HBL1 ABC-DLBCL cells treated with the BET bromodomain inhibitor JQ1 (20). Treatment with JQ1 (500 nmol/L) for 3 hours reduced the binding of BRD4 to the upstream regulatory region of *MYD88* (FDR < 0.001; Supplementary Fig. S7A). We then performed a ChIP experiment in SU-DHL-2 ABC-DLBCL cells exposed to DMSO or to OTX015 (500 nmol/L) for 3 hours. The drug appeared to reduce the binding of BRD4 to the upstream regulatory regions of the *MYD88* gene (Supplementary Fig. S7B). These data suggest that BET bromodomain inhibitors dislocate BRD4 from MYD88 regulatory regions.

OTX015 has biologic activity in a DLBCL *in vivo* model

We then assessed the ability of OTX015 to downregulate MYC, the NF-κB, TLR, and JAK/STAT pathway also in an *in vivo* model. We treated SU-DHL-2 xenografts grown subcutaneously in NOD-SCID mice with OTX015 (50 mg/kg, orally, twice a day; $n = 4$ mice) or with control (vehicle orally, twice a day; $n = 4$ mice) for three days, starting when the tumors had reached the volume of 500 mm^3. No body weight losses were registered during the three days of treatment. Real-time PCR showed that there was a significant downregulation of *MYC*, *IL6*, *TLR6*, *TNFSRF17* and, although not reaching the statistical significance, of *IRAK1*, *IRF4*, and *STAT3* (Fig. 4A).

We then assessed the *in vivo* antilymphoma activity of OTX015. NOD-SCID mice were treated with control vehicle (*per os*, twice a day; $n = 7$ mice) or with OTX015 (25 mg/kg, orally, twice a day; $n = 8$ mice), starting 5 days after the subcutaneous injection of SU-DHL-2 cells and then each day for 25 days. No loss in body weight was observed. OTX015 induced a reduced growth of the lymphoma xenografts at each analyzed time point (days 7, 10, 14, 17, 21, and 25; Fig. 4B). At the end of the experiment (day 25), the median tumor volumes for the control and for the experimental arm were 600 mm^3 (95% CI, 550–684) and 239 mm^3 (95% CI, 0–582), respectively ($P = 0.001$).

OTX015 shows *in vitro* synergism with several anticancer agents

We evaluated the combination of OTX015 with a series of conventional and targeted antilymphoma agents in a panel of five DLBCL cell lines (Fig. 5). Strong synergism was observed, in all the cell lines, when OTX015 was combined with the mTOR inhibitor everolimus (median CI, 0.11; range, 0.1–0.17) and, in ABC-cells, with the BTK inhibitor ibrutinib (CI, 0.04; 0.02–0.1). Synergism was also observed with OTX015 plus the PI3K-delta inhibitor idelalisib (CI, 0.5; 0.04–2.4), the class I and II HDACi vorinostat (CI, 0.5; 0.3–0.6), anti-CD20 mAb rituximab (CI, 0.5; 0.4–0.5), the hypomethylating agent decitabine (CI, 0.6; 0.6–0.7), the immunomodulant lenalidomide (CI, 0.7; 0.6–0.7). OTX015 combinations with the class I HDACi romidepsin (CI, 1.08; 1–1.22) and with the chemotherapy agents bendamustine (CI, 0.63; 0.1–3.97) and doxorubicin (CI, 0.83; 0.71–0.96) presented a moderate additive effect. GCB- and ABC-DLBCL cells showed a different sensitivity to the combinations: a stronger synergism was observed in ABC than in GCB DLBCL cells for ibrutinib ($P < 0.0001$), for idelalisib ($P < 0.0001$), lenalidomide ($P = 0.0001$), and rituximab ($P = 0.007$).

Baseline gene expression profile is associated with response to OTX015

To identify genes and pathways that might predict sensitivity to OTX015 in DLBCL we integrated the sensitivity data with the baseline gene expression profile in 14 cell lines with an IC_{50} lower than 500 nmol/L and eight with a higher IC_{50}.

Transcripts positively associated with OTX015 sensitivity were significantly enriched of genes involved in IFN, IL6 and IL10 signaling genes, TLR and JAK/STAT signaling, STAT3 targets, genes involved in glucose metabolism, and hypoxia-regulated genes (Fig. 6A and Supplementary Table S4A). The leading edge genes (the top differentially ranked transcripts based on sensitivity to

Published OnlineFirst January 26, 2015; DOI: 10.1158/1078-0432.CCR-14-1561

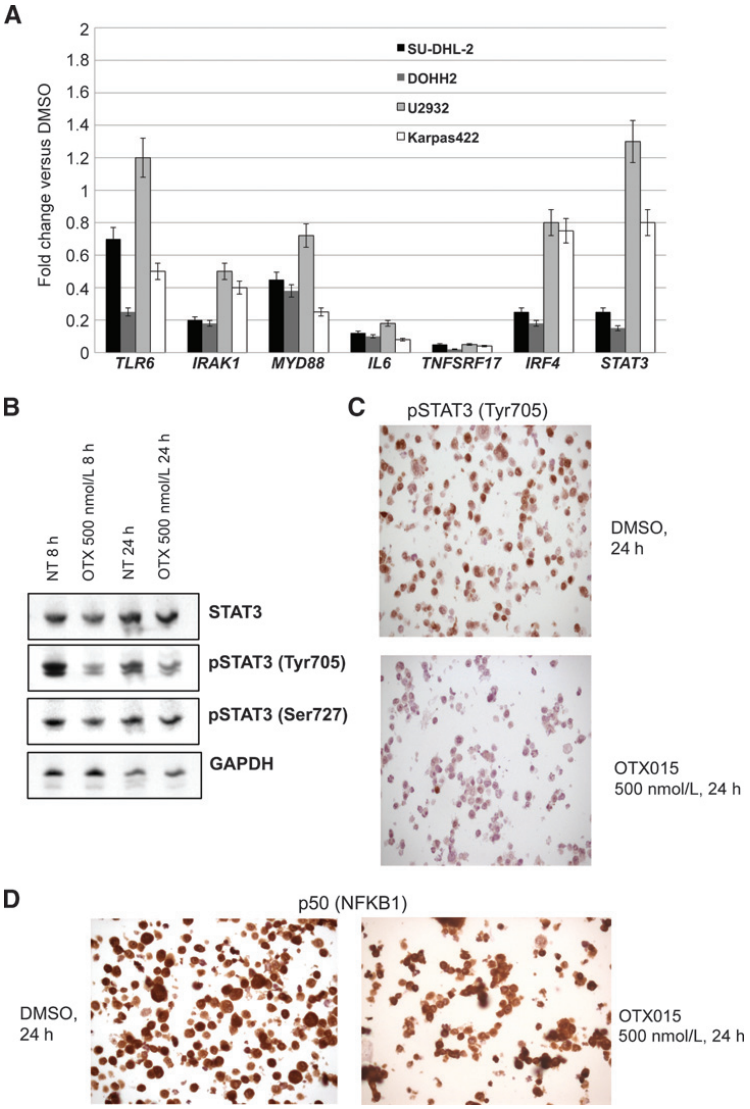

Figure 3.
OTX015 downregulates NFKB/TLR/JAK/STAT pathways in DLBCL *in vitro* models. A, expression changes of *TLR6*, *IRAK1*, *MYD88*, *IL6*, *TNFRSF17*, *IRF4*, and *STAT3* in four DLBCL cell lines exposed to OTX015 (500 nmol/L) for 24 hours. *Y* axis, fold change versus GAPDH and DMSO-treated cells. B, protein levels of total STAT3 and phosphorylated STAT3 in SU-DHL-2 cell line treated with DMSO or OTX015 (500 nmol/L) for 8 or 24 hours, GAPDH was used as a loading control. C, immunohistochemistry for phosphorylated STAT3 in the SU-DHL-2 cell line treated with DMSO or OTX015 (500 nmol/L) for 24 hours. D, immunohistochemistry for p50 (NFKB1) in the SU-DHL-2 cell line treated with DMSO or OTX015 (500 nmol/L) for 24 hours.

OTX015) comprised *STAT1*, *STAT3*, *STAT4*, *STAT6*, *IL6*, *JAK1*, *JAK2*, *TNF*, *IRAK1*, *TLR9*, *MYD88*, *TLR8*, *TRAF3*, and *AKT1*.

Transcripts associated with lower sensitivity to OTX015 were significantly enriched of E2F target genes, genes involved in cell-cycle regulation, DNA repair, P53 signaling, chromatin structure, and apoptosis (Fig. 6B; Supplementary Table S4B). *BCL2L1*, *HDAC1*, *HDAC2*, *HDAC5*, *HDAC8*, *CHEK1*, *CHEK2*, *TP53*, *ATM*, *BRCA1*, *CDKN1A*, *CDKN2A*, *BIRC5*, *MGMT* were among the leading edge genes. *MYC* or MYC targets did not appear associated with sensitivity to OTX015.

Discussion

We have evaluated the activity and the mechanism of action of a new BET bromodomain inhibitor, OTX015, in preclinical models of mature B-cell lymphoid tumors. We have shown that: (i) OTX015 has *in vitro* and *in vivo* antiproliferative activity; (ii) OTX015 effect is largely cytostatic, with induction of apoptosis in only a genetically defined subset of cell lines; (iii) OTX015 inhibits MYC, NF-κB, TLR, and JAK/STAT pathways; (iv) OTX015 shows synergistic or additive effects when combined with several

Published OnlineFirst January 26, 2015; DOI: 10.1158/1078-0432.CCR-14-1561

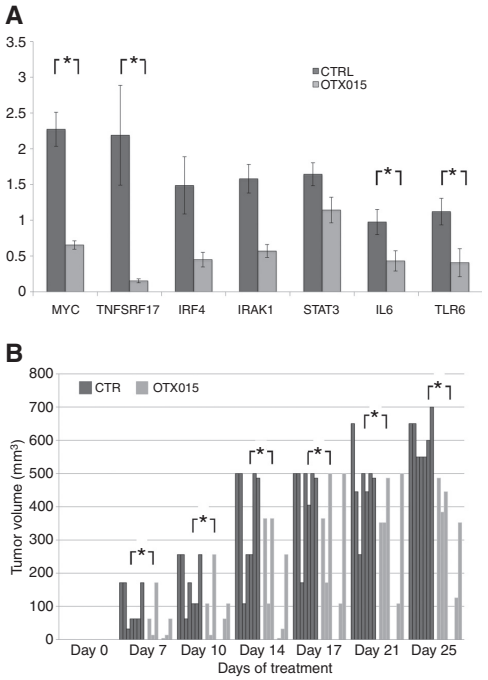

Figure 4.
OTX015 has biologic activity in DLBCL *in vivo* models. A, OTX015 downregulates MYC and NFKB/TLR/JAK/STAT pathways in an ABC-DLBCL *in vivo* model. Average of expression levels of MYC, TNFRSF17, IRF4, IRAK1, STAT3, IL6, and TLR6, in SU-DHL-2 xenografts from four untreated mice (CTR) and in four SU-DHL-2 xenografts from four mice treated with OTX015 for three days. *Y* axis, average expression levels normalized to GAPDH and to one CTR sample. *, $P < 0.05$. B, OTX015 reduces the growth of an ABC-DLBCL *in vivo* model. NOD-SCID mice were treated with oral control vehicle (twice a day; $n = 7$ mice) or with oral OTX015 (25 mg/kg, twice a day; $n = 8$ mice), starting 5 days after the subcutaneous injection of SU-DHL-2 cells and then each day for 25 days. *, $P < 0.05$. *Y* axis, tumor volume in mm^3. *X* axis, days of treatment. Each column represents one individual animal.

antilymphoma agents; (v) specific baseline gene expression features are associated with a different sensitivity to OTX015.

At clinically achievable concentrations (33), OTX015 had an antiproliferative activity in the most of the lymphoma cell lines tested, with no differences in sensitivity among the histologic subtypes. The effect was largely cytostatic, with apoptosis limited to a few cell lines. OTX015 appeared to induce a senescence-like phenotype, possibly compatible with the recently described "senescence with incomplete growth arrest," also observed after treatment of DLBCL cells with demethylating agents (34). The antitumor activity of OTX015 was validated in an *in vivo* model of ABC-DLBCL with demonstration of a reduced tumor growth.

Similarly to other BRD inhibitors (4, 5, 10, 21, 35), OTX015 determined a downregulation of MYC and of MYC target genes in DLBCL cell lines carrying a wild-type MYC and in cells in which the oncogene is translocated or amplified. This is a remarkable achievement since MYC is a difficult therapeutic target and it plays a major role in the pathogenesis and progression of lymphomas, as exemplified by the very poor outcome of DLBCL cases overexpressing both MYC and BCL2 proteins and of "double hit" lymphomas usually bearing concomitant translocations of *MYC* and *BCL2* oncogenes (36).

An important biologic effect we observed with OTX015, both in the *in vitro* and *in vivo* setting, was the downregulation of the NF-κB, TLR, and JAK/STAT3 signaling pathways, important in both the pathogenesis and the chemoresistance of lymphomas, and particularly of ABC-DLBCL. This observation is in accordance with the strong suppression of the TLR signaling-mediated lipopolysaccharide-induced inflammatory response, reported with BET bromodomain inhibitors (37). A similar effect has been reported for JQ1 in different DLBCL cell lines (10). Additional observations indicated that the downregulation of the TLR and JAK/STAT3 signaling pathways is a relevant mechanism of action of OTX015 in DLBCL. First, high expression of genes involved in interferon, TLR and JAK/STAT signaling and STAT3 targets were highly associated with the sensitivity to the compound. Second, OTX015-induced apoptosis was limited to cell lines, bearing a functional TP53, derived from ABC-DLBCL with somatic mutations activating both BCR signaling and MYD88. Mutations activating the BCR and TLR/MYD88 signaling are common in ABC-DLBCL, in which they represent driver events (38), and their prevalence is especially high in two aggressive extranodal forms of DLBCL, primary central nervous system lymphoma and primary testis DLBCL (39, 40). CD79A and CD79B are upstream of BTK. BTK binds to MYD88, especially if the latter is encoded by the L265P somatic variant (41). OTX015 downregulated the expression of MYD88 and of additional members of the TLR pathway, and both OTX015 and JQ1 reduced the BRD4 binding to *MYD88* upstream regulatory region. These events could inhibit both BCR and TLR signaling, particularly affecting cells dependent on these pathways. Similarly, the BTK inhibitor ibrutinib is more active in ABC-DLBCL cases with both *CD79B*/*CD79A* and *MYD88* mutated genes (38, 42). Importantly, the combination of OTX015 and ibrutinib was strongly synergistic in ABC-DLBCL cells. The downregulation of IRF4 might contribute to the synergism, as reported for the combination of ibrutinib and lenalidomide (43). Notably, OTX015 was active also in ABC-DLBCL cells carrying somatic mutations of *CARD11*, coding for a protein downstream of BTK, and, accordingly, representing a marker of resistance to ibrutinib (38, 42).

Besides ibrutinib, additional antilymphoma agents presented an increased activity when combined with OTX015. The strongest synergism was obtained with the combination with the mTOR inhibitor everolimus at doses that can be reached in patients (44). The mTOR is central to a signaling cascade leading to cell growth and proliferation, and mTOR inhibitors are approved for treatment of relapsed MCL (45). OTX015 was also synergistic with the PI3K-delta inhibitor idelalisib, which has shown promising clinical responses in B-cell lymphomas (46), and with the lenalidomide, as also recently reported for another BET bromodomain inhibitor in MCL (47).

The synergism observed for OTX015 combined with clinically achievable doses of rituximab is reinforced by recent reports with another BET bromodomain inhibitor (13). The downregulation of *CCDC86*, coding for the nuclear factor cyclon, by both JQ1 (13) and OTX015, might represent the mechanism of action of the synergism. The combination appeared more active in ABC-DLBCL cell lines, maybe due the common targeting of the IL10 and STAT3 pathway by both OTX015 and rituximab (48).

Published OnlineFirst January 26, 2015; DOI: 10.1158/1078-0432.CCR-14-1561

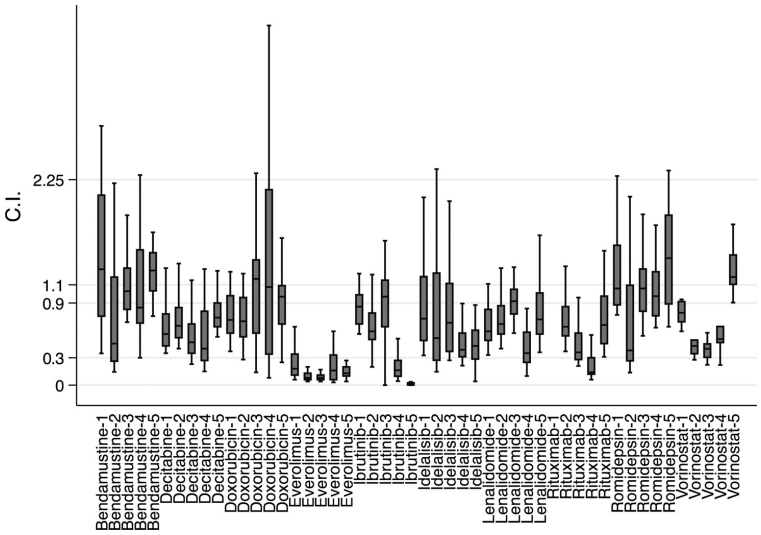

Figure 5.
OTX015 combination showing additive effect or synergism in most instances with different additional drugs. *Y* axis: CI < 0.3, strong synergism; 0.3–0.9, synergism; 0.9–1.1 additive effect. *X* axis, drugs combined with OTX015 in GCB (1 DOHH2; 2 Karpas422; 3 SUDHL6) and ABC-DLBCL (4 U2932; 5 TMD8). C.I. for OTX015/rituximab in DOHH2 is not plotted due to a median value > 3. In each box-plot, the line in the middle of the box represents the median and the box extends from the 25th to the 75th percentile (interquartile range, IQ); the whiskers extend to the upper and lower adjacent values (i.e., ±1.5 IQ).

OTX015 presented synergism with the demethylating agent decitabine and the HDACi vorinostat at concentrations pharmacologically achievable in clinical use (49, 50), in accordance with the similarities here observed at the level of gene expression signatures, and also with published data obtained with other BET bromodomain inhibitors (11). HDACs of both classes I and II were associated with a lower sensitivity to OTX015 as single agent and, indeed the synergism appeared stronger with the class I and IIa/b HDACi vorinostat than that seen with the class I HDACi romidepsin suggesting that the synergism might be class dependent.

The integration of baseline GEP and sensitivity in a large panel of DLBCL cell lines allowed the identification of functional pathways that might predict the response to the BET bromodomain inhibitor. The cells with the highest sensitivity to OTX015 had not only high expression levels of genes involved in the TLR/JAK/STAT pathway, but also of transcripts that code for proteins implicated in glucose metabolism and in hypoxia. Although the latter two features can be associated with an active MYC program, it is important to underline that we did not detect any association between expression of MYC or MYC targets and sensitivity to OTX015. On the basis of our data, it will be important to correlate the demonstration of an active TLR/JAK/STAT pathway (for example detecting pSTAT3) and/or the presence of somatic mutations of *MYD88*, *CD79A/B*, *CARD11*, and *TP53* with the response to BET bromodomain inhibitors in the ongoing clinical trials.

A strong E2F gene expression signature was associated with lower sensitivity to OTX015, although not with a clear resistance to the compound as all our cell lines were much more sensitive to the BET bromodomain inhibitor than other large series of cancer cell lines comprising solid tumors models (5, 14, 15). In accordance with the cell-cycle arrest observed at 24 to 48 hours, E2F1 target genes, but not E2F1 itself, are downregulated by both OTX015 and JQ1 (10), at a later time point than the effect on MYC or on TLR/JAK/STAT pathways. The high synergism reported in leukemia preclinical models with the combination of the BET bromodomain inhibitor PFI-1 with a pan-aurora kinase inhibitor (12) suggests that the combination of BET bromodomain inhibitors with drugs targeting the cell cycle might overcome the observed lower sensitivity.

The gene expression signatures associated with a lower sensitivity to OTX015 comprised transcripts (*BCL2L1*, *BIRC5*, *MGMT*, *CHEK1*, *CHEK2*), which represent potential molecules to be inhibited in combination with BET bromodomain inhibitors.

There are now different BET bromodomain inhibitors under development with some of them, including OTX015, already in phase I clinical studies. On the basis of our data of an OTX015 gene expression signature highly overlapping with that reported with JQ1, and on the literature (10, 12, 16, 51) all the molecules, so far all pan-BET bromodomain inhibitors, have similar preclinical activity data and mechanism of action. Alongside the different drug delivery modalities (for example, OTX015 and GSK525762 are given orally, TEN-010 subcutaneously), the toxicity and pharmacokinetics data that from the ongoing clinical studies will be most relevant for the further clinical development of this class of compounds.

In conclusion, the BET bromodomain inhibitor OTX015 appears as a promising new antilymphoma agent with antiproliferative activity in the vast majority of the examined preclinical models, capable of downregulating important signaling pathways and of synergizing with other anticancer molecules. Particular genetic lesions and gene expression signatures are associated with high sensitivity to OTX015 antitumor activity. Additional studies are needed to elucidate the mechanism of action of OTX015, particularly when combined with other targeted agents. Together with the early report of clinical responses in both leukemia and lymphoma patients treated with OTX015 in the absence of major toxicities (22), the data presented here provide the basis for further clinical investigation of OTX015 in combination therapies.

Published OnlineFirst January 26, 2015; DOI: 10.1158/1078-0432.CCR-14-1561

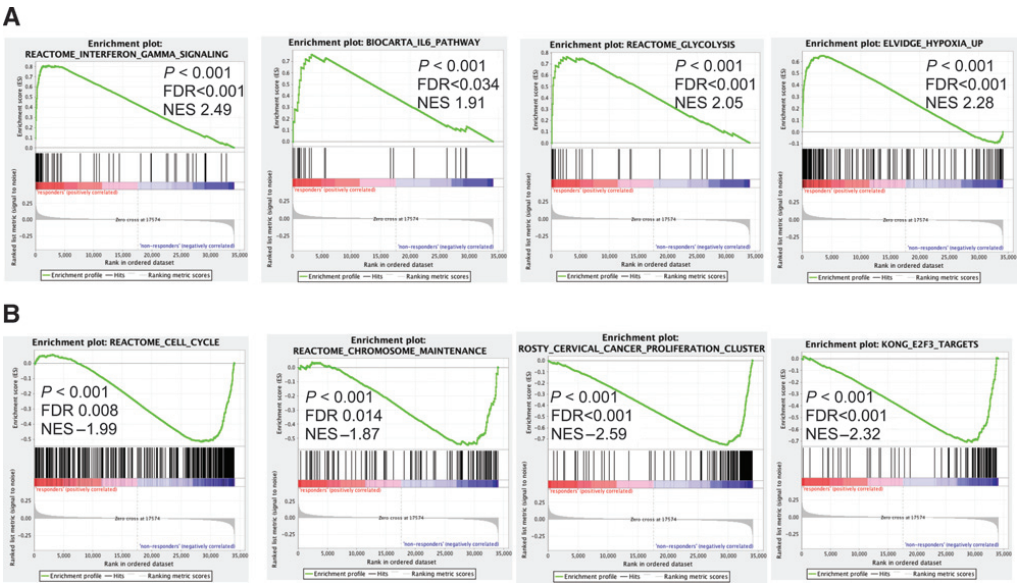

Figure 6.
Specific baseline gene expression signatures are associated with higher (A) or lower (B) sensitivity to OTX015. Representative GSEA plots illustrating: A, the enrichment of genes involved in IFN and IL6 signaling, in glucose metabolism, and in hypoxia among the transcripts associated with a higher OTX015 sensitivity; B, the enrichment of genes involved in cell-cycle regulation and chromatin structure and of E2F targets among the transcripts associated with a lower sensitivity to OTX015. FDR, false discovery rate; NES, normalized enrichment score.

Disclosure of Potential Conflicts of Interest

P. Herait has ownership interest (including patents) in Oncoethix. F. Bertoni reports receiving commercial research grants from Oncoethix and is a consultant/advisory board member for Celgene. No potential conflicts of interest were disclosed by the other authors.

Authors' Contributions

Conception and design: E. Gaudio, P. Bonetti, G. Inghirami, E. Zucca, F. Bertoni
Development of methodology: E. Gaudio, P. Bonetti, C. Tarantelli, G. Inghirami
Acquisition of data (provided animals, acquired and managed patients, provided facilities, etc.): A. Rinaldi, M. Ponzoni, G. Stussi, G. Inghirami
Analysis and interpretation of data (e.g., statistical analysis, biostatistics, computational analysis): M. Boi, P. Bonetti, I. Kwee, A. Rinaldi, L. Cascione, M. Ponzoni, G. Stussi, G. Inghirami, E. Zucca, F. Bertoni
Writing, review, and/or revision of the manuscript: M. Boi, E. Gaudio, P. Bonetti, M. Ponzoni, A. Stathis, G. Stussi, M.E. Riveiro, G. Inghirami, E. Cvitkovic, E. Zucca, F. Bertoni
Administrative, technical, or material support (i.e., reporting or organizing data, constructing databases): E. Bernasconi, M. Testoni, P. Herait, F. Bertoni
Study supervision: M.E. Riveiro, G. Inghirami, E. Cvitkovic, F. Bertoni
Other (performed experiments): A.A. Mensah

Acknowledgments

The authors thank Diletta Di Mitri for her help in the evaluation of interleukins production.

Grant Support

This work was supported by research funds from Oncoethix (to F. Bertoni), Nelia et Amadeo Barletta Foundation (to F. Bertoni), and AIRC 5x1000 No. 10007 (to G. Inghirami).

The costs of publication of this article were defrayed in part by the payment of page charges. This article must therefore be hereby marked *advertisement* in accordance with 18 U.S.C. Section 1734 solely to indicate this fact.

Received June 19, 2014; revised January 9, 2015; accepted January 19, 2015; published OnlineFirst January 26, 2015.

References

1. Jiang Y, Hatzi K, Shaknovich R. Mechanisms of epigenetic deregulation in lymphoid neoplasms. Blood 2013;121:4271–9.
2. Dawson MA, Kouzarides T, Huntly BJ. Targeting epigenetic readers in cancer. N Engl J Med 2012;367:647–57.
3. Geutjes EJ, Bajpe PK, Bernards R. Targeting the epigenome for treatment of cancer. Oncogene 2012;31:3827–44.
4. Delmore JE, Issa GC, Lemieux ME, Rahl PB, Shi J, Jacobs HM, et al. BET bromodomain inhibition as a therapeutic strategy to target c-Myc. Cell 2011;146:904–17.
5. Mertz JA, Conery AR, Bryant BM, Sandy P, Balasubramanian S, Mele DA, et al. Targeting MYC dependence in cancer by inhibiting BET bromodomains. Proc Natl Acad Sci U S A 2011;108:16669–74.
6. Loven J, Hoke HA, Lin CY, Lau A, Orlando DA, Vakoc CR, et al. Selective inhibition of tumor oncogenes by disruption of super-enhancers. Cell 2013;153:320–34.
7. Hnisz D, Abraham BJ, Lee TI, Lau A, Saint-Andre V, Sigova AA, et al. Super-enhancers in the control of cell identity and disease. Cell 2013;155:934–47.

Published OnlineFirst January 26, 2015; DOI: 10.1158/1078-0432.CCR-14-1561

8. Greenwald RJ, Tumang JR, Sinha A, Currier N, Cardiff RD, Rothstein TL, et al. E mu-BRD2 transgenic mice develop B-cell lymphoma and leukemia. Blood 2004;103:1475–84.
9. Dawson MA, Prinjha RK, Dittmann A, Giotopoulos G, Bantscheff M, Chan WI, et al. Inhibition of BET recruitment to chromatin as an effective treatment for MLL-fusion leukaemia. Nature 2011;478:529–33.
10. Chapuy B, McKeown MR, Lin CY, Monti S, Roemer MG, Qi J, et al. Discovery and characterization of super-enhancer-associated dependencies in diffuse large B cell lymphoma. Cancer Cell 2013;24:777–90.
11. Bhadury J, Nilsson LM, Muralidharan SV, Green LC, Li Z, Gesner EM, et al. BET and HDAC inhibitors induce similar genes and biological effects and synergize to kill in Myc-induced murine lymphoma. Proc Natl Acad Sci U S A 2014;111:E2721–30.
12. Picaud S, Da Costa D, Thanasopoulou A, Filippakopoulos P, Fish PV, Philpott M, et al. PFI-1, a highly selective protein interaction inhibitor, targeting BET Bromodomains. Cancer Res 2013;73:3336–46.
13. Emadali A, Rousseaux S, Bruder-Costa J, Rome C, Duley S, Hamaidia S, et al. Identification of a novel BET bromodomain inhibitor-sensitive, gene regulatory circuit that controls Rituximab response and tumour growth in aggressive lymphoid cancers. EMBO Mol Med 2013;5:1180–95.
14. Lockwood WW, Zejnullahu K, Bradner JE, Varmus H. Sensitivity of human lung adenocarcinoma cell lines to targeted inhibition of BET epigenetic signaling proteins. Proc Natl Acad Sci U S A 2012;109:19408–13.
15. Puissant A, Frumm SM, Alexe G, Bassil CF, Qi J, Chanthery YH, et al. Targeting MYCN in neuroblastoma by BET bromodomain inhibition. Cancer Discov 2013;3:308–23.
16. Cheng Z, Gong Y, Ma Y, Lu K, Lu X, Pierce LA, et al. Inhibition of BET bromodomain targets genetically diverse glioblastoma. Clin Cancer Res 2013;19:1748–59.
17. Noel JK, Iwata K, Ooike S, Sugahara K, Nakamura H, Daibata M. Abstract C244: Development of the BET bromodomain inhibitor OTX015. Molec Can Therapeut 2014;12:C244-C.
18. Bandopadhayay P, Bergthold G, Nguyen B, Schubert S, Gholamin S, Tang Y, et al. BET bromodomain inhibition of MYC-amplified medulloblastoma. Clin Cancer Res 2014;20:912–25.
19. Trabucco SE, Gerstein RM, Evens AM, Bradner JE, Shultz LD, Greiner DL, et al. Inhibition of bromodomain proteins for the treatment of human diffuse large B-cell lymphoma. Clin Cancer Res 2015;21:113–22.
20. Ceribelli M, Kelly PN, Shaffer AL, Wright GW, Xiao W, Yang Y, et al. Blockade of oncogenic IkappaB kinase activity in diffuse large B-cell lymphoma by bromodomain and extraterminal domain protein inhibitors. Proc Natl Acad Sci U S A 2014;111:11365–70.
21. Ott CJ, Kopp N, Bird L, Paranal RM, Qi J, Bowman T, et al. BET bromodomain inhibition targets both c-Myc and IL7R in high-risk acute lymphoblastic leukemia. Blood 2012;120:2843–52.
22. Stathis A, Quesnel B, Amorim S, Thieblemont C, Zucca E, Raffoux E, et al. 5LBA Results of a first-in-man phase I trial assessing OTX015, an orally available BET-bromodomain (BRD) inhibitor, in advanced hematologic malignancies. Eur J Cancer 2014;50:196.
23. Boi M, Rinaldi A, Kwee I, Bonetti P, Todaro M, Tabbo F, et al. PRDM1/BLIMP1 is commonly inactivated in anaplastic large T-cell lymphoma. Blood 2013;122:2683–93.
24. Mensah AA, Kwee I, Gaudio E, Rinaldi A, Ponzoni A, Cascione L, et al. Novel HDAC inhibitors exhibit pre-clinical efficacy in lymphoma models and point to the importance of CDKN1A expression levels in mediating their anti-tumor response. Oncotarget 2014 Dec 30. [Epub ahead of print].
25. Gentleman R, Carey V, Dudoit S, Irizarry R, Huber W, editors. Bioinformatics and computational biology solutions using R and Bioconductor; New York, NY: Springer; 2005.
26. Johnson WE, Li C, Rabinovic A. Adjusting batch effects in microarray expression data using empirical Bayes methods. Biostatistics 2007;8:118–27.
27. Smyth GK. Linear models and empirical Bayes methods for assessing differential expression in microarray experiments. Stat Appl Genet Mol Biol 2004;3:Article3.
28. Subramanian A, Tamayo P, Mootha VK, Mukherjee S, Ebert BL, Gillette MA, et al. Gene set enrichment analysis: a knowledge-based approach for interpreting genome-wide expression profiles. Proc Natl Acad Sci U S A 2005;102:15545–50.
29. Langmead B, Trapnell C, Pop M, Salzberg SL. Ultrafast and memory-efficient alignment of short DNA sequences to the human genome. Genome Biol 2009;10:R25.
30. Heinz S, Benner C, Spann N, Bertolino E, Lin YC, Laslo P, et al. Simple combinations of lineage-determining transcription factors prime cis-regulatory elements required for macrophage and B cell identities. Mol Cell 2010;38:576–89.
31. Lacrima K, Valentini A, Lambertini C, Taborelli M, Rinaldi A, Zucca E, et al. In vitro activity of cyclin-dependent kinase inhibitor CYC202 (Seliciclib, R-roscovitine) in mantle cell lymphomas. Ann Oncol 2005;16:1169–76.
32. Lee JJ, Kong M, Ayers GD, Lotan R. Interaction index and different methods for determining drug interaction in combination therapy. J Biopharm Stat 2007;17:461–80.
33. Odore E, Rezai K, Riveiro E, Bourdel F, Herait P, Cvitkovic E, et al. Abstract LB-231: a phase I pharmacokinetic study of OTX015 for the treatment of patients with hematologic malignancies. Cancer Res 2014;74:LB-231.
34. Clozel T, Yang S, Elstrom RL, Tam W, Martin P, Kormaksson M, et al. Mechanism-based epigenetic chemosensitization therapy of diffuse large B-cell lymphoma. Cancer Discov 2013;3:1002–19.
35. Zhao X, Lwin T, Zhang X, Huang A, Wang J, Marquez VE, et al. Disruption of the MYC-miRNA-EZH2 loop to suppress aggressive B-cell lymphoma survival and clonogenicity. Leukemia 2013;27:2341–50.
36. Thieblemont C, Briere J. MYC, BCL2, BCL6 in DLBCL: impact for clinics in the future? Blood 2013;121:2165–6.
37. Nicodeme E, Jeffrey KL, Schaefer U, Beinke S, Dewell S, Chung CW, et al. Suppression of inflammation by a synthetic histone mimic. Nature 2010;468:1119–23.
38. Staudt LM II. Therapy of DLBCL based on genomics. Hematol Oncol 2013;31 Suppl 1:26–8.
39. Gonzalez-Aguilar A, Idbaih A, Boisselier B, Habbita N, Rossetto M, Laurenge A, et al. Recurrent mutations of MYD88 and TBL1XR1 in primary central nervous system lymphomas. Clin Cancer Res 2012;18:5203–11.
40. Kraan W, Horlings HM, van Keimpema M, Schilder-Tol EJ, Oud ME, Scheepstra C, et al. High prevalence of oncogenic MYD88 and CD79B mutations in diffuse large B-cell lymphomas presenting at immune-privileged sites. Blood Cancer J 2013;3:e139.
41. Yang G, Zhou Y, Liu X, Xu L, Cao Y, Manning RJ, et al. A mutation in MYD88 (L265P) supports the survival of lymphoplasmacytic cells by activation of Bruton's tyrosine kinase in Waldenstrom's macroglobulinemia. Blood 2013;122:1222–32.
42. Honigberg LA, Smith AM, Sirisawad M, Verner E, Loury D, Chang B, et al. The Bruton tyrosine kinase inhibitor PCI-32765 blocks B-cell activation and is efficacious in models of autoimmune disease and B-cell malignancy. Proc Natl Acad Sci U S A 2010;107:13075–80.
43. Yang Y, Shaffer AL III, Emre NC, Ceribelli M, Zhang M, Wright G, et al. Exploiting synthetic lethality for the therapy of ABC diffuse large B cell lymphoma. Cancer Cell 2012;21:723–37.
44. Tabernero J, Rojo F, Calvo E, Burris H, Judson I, Hazell K, et al. Dose- and schedule-dependent inhibition of the mammalian target of rapamycin pathway with everolimus: a phase I tumor pharmacodynamic study in patients with advanced solid tumors. J Clin Oncol 2008;26:1603–10.
45. Reeder CB, Ansell SM. Novel therapeutic agents for B-cell lymphoma: developing rational combinations. Blood 2011;117:1453–62.
46. Gopal AK, Kahl BS, de Vos S, Wagner-Johnston ND, Schuster SJ, Jurczak WJ, et al. PI3Kdelta inhibition by idelalisib in patients with relapsed indolent lymphoma. N Engl J Med 2014;370:1008–18.
47. Moros A, Rodriguez V, Saborit-Villarroya I, Montraveta A, Balsas P, Sandy P, et al. Synergistic antitumor activity of lenalidomide with the BET bromodomain inhibitor CPI203 in bortezomib-resistant mantle cell lymphoma. Leukemia 2014;28:2049–59.
48. Jazirehi AR, Bonavida B. Cellular and molecular signal transduction pathways modulated by rituximab (rituxan, anti-CD20 mAb) in non-Hodgkin's lymphoma: implications in chemosensitization and therapeutic intervention. Oncogene 2005;24:2121–43.
49. Momparler RL. Pharmacology of 5-Aza-2′-deoxycytidine (decitabine). Semin Hematol 2005;42:S9–16.
50. Smith MA, Houghton P. A proposal regarding reporting of in vitro testing results. Clin Cancer Res 2013;19:2828–33.
51. Gupta SS, Maetzig T, Maertens GN, Sharif A, Rothe M, Weidner-Glunde M, et al. Bromo- and extraterminal domain chromatin regulators serve as cofactors for murine leukemia virus integration. J Virol 2013;87:12721–36.

ARTICLE 3

BAY 1238097, BAY-7575 and BAY-5627 are novel BET Bromodomain inhibitors with anti-lymphoma activity

Elena Bernasconi [1*], Eugenio Gaudio [1*], Pascale Lejeune [2], Chiara Tarantelli [1], Luciano Cascione [1,3], Ivo Kwee [1,4,5], Filippo Spriano [1], Andrea Rinaldi [1], Afua Adjeiwaa Mensah [1], Elaine Chung [1], Anastasios Stathis [3], Stephan Siegel [2], Norbert Schmees [2], Matthias Ocker [2], Emanuele Zucca [3], Bernard Haendler [2], and Francesco Bertoni [1,3]

[1] Lymphoma and Genomics Research Program, IOR Institute of Oncology Research, Bellinzona, Switzerland; [2] Drug Discovery, Bayer AG, Berlin, Germany; [3] IOSI Oncology Institute of Southern Switzerland, Bellinzona, Switzerland; [4] IDSIA Dalle Molle Institute for Artificial Intelligence, Manno, CH-6928 Switzerland; [5] SIB Swiss Institute of Bioinformatics, Lausanne, Switzerland.

*Equally contributed

Running Title: Novel inhibitors in lymphomas

Key words: Lymphoma, BET Bromodomain, Epigenetics, JQ1, MYC

Financial Support: Institutional funds from Bayer AG, and Gelu Foundation (to FB).

Corresponding author: Dr Francesco Bertoni, Lymphoma and Genomics Research Program, IOR Institute of Oncology Research, via Vincenzo Vela 6, 6500 Bellinzona, Switzerland. Phone: +41 91 8200 367; fax: +41 91 8200 305; e-mail: frbertoni@mac.com.

Disclosure of Potential Conflicts of Interest

FB has received institutional research funds from Bayer AG, Oncoethix SA and Oncology Therapeutic Development. PL, SS, NS, MO and BH are Bayer employees. The remaining authors have no conflict of interest.

Title: 13 characters

Text: 3307 words/5000

References: 49/75

Figures & Tables: 6/6 total figures and/or tables

ABSTRACT (197 words)

The epigenome is often deregulated in cancer and treatment with inhibitors of bromodomain and extra- terminal (BET) proteins, the readers of epigenetic acetylation marks, represents a novel therapeutic approach. Here, we have characterized the anti-tumor activity of three novel BET inhibitors in preclinical lymphoma models.

The novel BET inhibitors BAY 1238097, BAY-7575 and BAY-5627 showed anti-proliferative activity in a large panel of cell lines derived from lymphoma with median IC50 comprised between 70 and 208 nM. BAY 1238097 showed strong antitumor efficacy *in vivo* as single agent in two diffuse large B cell lymphoma models. Gene expression profiling showed BAY 1238097 targeted the NFKB/TLR/JAK/STAT signaling pathways, MYC and E2F1-regulated genes, cell cycle regulation and chromatin structure. The gene expression profiling signatures also highly overlapped with the signatures obtained with other BET Bromodomain inhibitors and partially overlapped with HDAC-i, mTOR-i and demethylating agents. Notably, BAY 1238097 presented *in vitro* synergism with EZH2, mTOR and BTK inhibitors.

In conclusion, the novel BET inhibitors presented promising anti-lymphoma preclinical activity *in vitro* and *in vivo* mediated by the interference with biologic processes driving the lymphoma cells. Our data also point to combination schemes targeting EZH2, mTOR and BTK alongside BET bromodomains.

Introduction

The members of the Bromodomain and extra-terminal (BET) family (BRD2, BRD3, BRD4 and BRDT) bind to acetylated proteins, including histones H3 and H4 (1), thereby acting as epigenetic readers especially at the so-called super-enhancers, the clusters of enhancers incorporating high amounts of transcription factors and co-activators and regulating the expression of key genes controlling cell identity in normal cells and of oncogenes in cancer cells (2,3). Targeting BET proteins has recently emerged as a novel and promising therapeutic approach to interfere with cancer cell transcription programs both in hematological and solid tumors (4-20). Regarding this, we and others have shown preclinical anti-tumor activity of BET inhibitors in B and T cell lymphomas (5,7-9,11,14,16,20-23). Importantly, the early clinical trials with BET inhibitors have reported clear signs of anti-tumor activity (24-26). Here, in lymphoma models, we characterized the anti-tumor activity of three novel BET inhibitors, BAY-7575 and BAY-5627 and, in particular, BAY 1238097, a molecule with preferential binding to BRD4 compared to BRD2 or BRD3, which, due to a pharmacological and pharmacokinetic favorable profile (27), entered the early clinical evaluation (NCT02369029)(28).

Material and Methods

Cell lines and molecules

Established human cell lines derived from 27 diffuse large B-cell lymphoma (twenty GCB-DLBCL: FARAGE, OCI-LY-1, OCI-LY-2, OCI-LY-7, OCI-LY-8, OCI-LY-18, OCI-LY-19, RCK8, VAL, SU-DHL-4, SU-DHL-5, SU-DHL-6, SU-DHL-8, SU-DHL-10, SU-DHL-16, KARPAS422, WSU-DLCL2, DOHH2, Pfeiffer, TOLEDO; seven ABC-DLBCL: RI-1 (RIVA), HBL-1, TMD8, U2932, SU-DHL-2, OCI-LY-3, OCI-LY-10), ten mantle cell lymphoma (MCL: GRANTA-519, JeKo-1, JVM-2, MAVER-1, MINO, REC-1, SP-49, SP-53, UPN-1 and Z-138), three splenic marginal zone lymphoma (SMZL: KARPAS1718, VL51, SSK41), nine anaplastic large T cell lymphoma (ALCL: JB6, Ki-JK, KARPAS-299, L-82, SUP-M2, SU-DHL-1, TS, FEPD, MAC-1), one pro-lymphocytic leukemia (MEC-1) and one primary mediastinal large cell lymphoma (KARPAS1106P) were cultured in culture media as previously indicated (29). Cell lines has been authenticated for cell identity and for Interspecies contamination (IDEXX BioResearch, Ludwigsburg, Germany). BAY 1238097 (patent application WO2014026997, example 127.1), BAY-7575 (patent application BHC WO2015004075, example 28) and BAY-5627 (patent application WO2015004075, example 25) were provided by Bayer AG (Berlin, Germany) and dissolved in dimethyl sulphoxide (DMSO) to obtain a stock concentration of 10 mM. Other compounds used were: ibrutinib, GSK126, everolimus (Selleckchem, Houston, TX, USA), and DZNep (Sigma Aldrich).

Cell proliferation, cell death, cell cycle analysis

The anti-proliferative activity of BAY-7575 and BAY-5627, and of BAY 1238097 was assessed using 3-(4,5-dimethylthiazol-2-yl)-2,5-diphenyltetrazolium bromide (MTT), and the doses corresponding to the IC50 (50%-inhibitory concentration) and the LC50 (50%-lethal concentration) were estimated as previously described (30). Apoptosis and cell cycle distribution were evaluated on cells treated with DMSO or different doses of compounds, as previously reported (29).

Western blotting analysis

Protein extraction, separation and immunoblotting were performed as previously described (29). The following antibodies were used: anti-BRD4 (A301-985A100, Bethyl), anti-MYC (13987, Cell Signaling Technology, Danvers, MA, USA), anti-αGAPDH (MAB374, Millipore), anti-Histone H3 (ab1791, AbCam), anti-Histone H3K27me3 (9733, Cell Signaling Technology), anti-EZH2 (3147, Cell Signaling Technology), anti-AKT (9272, Cell Signaling Technology), anti- phospho-AKT Ser 473 (4060, Cell Signaling Technology), anti-phospho-mTOR Ser 2481 (2974, Cell Signaling Technology).

Chromatin immunoprecipitation

Data mining of the publicly available ChIP-Seq dataset SRP043524 (31) and chromatin immunoprecipitation were performed as previously described (5). Quantitative real-time polymerase chain reaction (PCR) of ChIP-DNA was performed using primers specific for a locus of BRD4 binding in the upstream regulatory region of EZH2 (chr7:148,502,464-148,583,441) as determined by analyzing the ChIP-Seq dataset SRP043524 (31); primers specific for human alpha-satellite were used as a negative control (sequences available upon request).

Real-time polymerase chain reaction (PCR)

RNA was extracted using the RNeasy kit (Qiagen AG, Hombrechtikon, CH). Real-time PCR was performed as previously described (29) (primer sequences available upon request).

Gene expression profiling

Gene expression profiling (GEP) was performed with the HumanHT-12 v4 Expression BeadChip (Illumina, San Diego, CA), as previously described (32). For GEP comparison after exposure to the compound or DMSO, probes presenting a false discovery rate (FDR), controlled by the Benjamini-Hochberg algorithm, < 0.05 and a log ratio > |1| were considered differentially expressed using the empirical Bayes (paired) moderated t-test as implemented in the LIMMA R-package (33). Gene set enrichment was defined with GSEA (34) on pre-ranked lists using the MSigDB 5.2 (34) and the SignatureDB collection (35) applying a threshold based on FDR < 0.1.

For exploratory analyses performed on baseline gene expression profiles of cell lines with different degrees of sensitivity to compounds, probes presenting a P < 0.05 and a log ratio > |1| were defined differentially expressed using the empirical Bayes (paired) moderated t-test as implemented in CARMAweb 1.6 (36). Gene set enrichment was defined with GSEA (34) applying a threshold based on FDR < 0.1. All GEP raw data will be available at the National Center for Biotechnology Information Gene Expression Omnibus (http:// www.ncbi.nlm.nih.gov/geo) database.

In vivo experiments

Animal experiments were approved by the relevant regulatory agency of the federal state of Berlin (Landesamt für Gesundheit und Soziales Berlin). Animals were housed according to institutional guidelines with access to food (pelleted diet) and water *ad libitum*. SCID female mice, 9-12 weeks old were inoculated subcutaneously into the right flank with $5x10^6$ SU-DHL-8 cells/mouse suspended in 0.1 mL of matrigel or with OCI-LY-3 tumor fragments (3x3 mm). BAY 1238097 was prepared as a solution in NaCl 0.9% in water, pH 4 and administered orally under 10 mL/kg. Treatments with BAY 1238097 or vehicle control were initiated on day 4 post tumor inoculation for the SU-DHL-8 model (8 mice/group). BAY 1238097 was applied daily for 12 days at its maximal tolerated dose (MTD) of 15 mg/kg. Treatment of the OCI-LY-3 tumors started on day 21 post tumor inoculation, mice being randomized with a median tumor size per group of of-98mm^3 for the BAY 1238097 treated group (n=7) and 93 mm3 for the vehicle control group (n=8). BAY 1238097 was applied at the MTD of 45 mg/kg using an intermittent schedule, twice a week, for 4 weeks.

Tumors were measured twice a week using a caliper and volume was calculated using the formula: tumor volume = [length x width x width]/2. Treated/control ratio was calculated at the end of the study as follows: T/C = (median tumor volume in the treated group/median tumor volume in the vehicle control group)x100. A T/C≤ 42% was declared active in agreement with NCI criteria. Differences in tumor volumes were calculated using the Wilcoxon rank-sum test (Stata/SE 12.1 for Mac, Stata Corporation, College Station, TX). The P-value (P) for significance was < 0.05. Mice body weight was determined on a daily basis and body weight loss ≥ 20%, compared to the first day of therapy, was judged excessive and the dose considered as toxic.

Drug combinations and evaluation of synergism

Drug combination evaluation was performed as previously described (5). Combinations were defined to be

synergistic if the Chou-Talalay Combination Index (CI) was < 0.9, additive if the CI was between 0.9 and 1.1 and antagonistic/no benefit, if the CI was > 1.1 (37).

Results

BAY 1238097, BAY-7575 and BAY-5627 have *in vitro* anti-tumor activity in lymphoma models

We evaluated the anti-proliferative activity of three novel BET inhibitors - BAY 1238097, BAY-7575 and BAY-5627 - in a panel of cell lines derived from activated B-cell type diffuse large B-cell lymphoma (ABC DLBCL; n.=7), germinal center B-cell type DLBCL (GCB DLBCL; n.=20), mantle cell lymphoma (MCL; n.=10); splenic marginal zone lymphoma (SMZL; n.=3), primary mediastinal large cell lymphoma (PMBCL, n.=1), chronic lymphocytic leukemia (CLL, n.=1) and anaplastic large T cell lymphoma (ALCL, n.=9). As assessed by MTT assays performed after 72 hours of drug exposure, BAY 1238097, BAY-7575 and BAY-5627 were active in a dose-dependent manner in almost all the cell lines (Figure 1A) with median IC50 values of 231 nM (95%CI, 161-280 nM), 103 nM (95% CI, 76-122 nM) and 71 nM (95% CI, 55-89 nM), respectively. The three compounds had higher activity in B cell than in T cell models (P<0.001), while no differences were observed among B-cell tumor types (DLBCL, MCL, SMZL) or DLBCL subtypes (ABC, GCB).

BAY 1238097, BAY-7575 and BAY-5627 had highly correlated patterns of activity (R values > 0.8, P < 0.0001) (Figure S1). We also compared the activity of BAY 1238097, BAY-7575 and BAY-5627 with the results we had previously obtained using the BET inhibitor OTX015 (MK-8628) (5). The three novel compounds presented a similar pattern of activity with OTX015, which was higher for BAY-7575 (R=0.430; P=0.01) and BAY-5627 (R=0.392; P=0.01) than for BAY 1238097 (R=0.197; P > 0.05), and higher for all of them when focusing on B cell derived lymphomas (R=0.739, P<0.0001; R=0.638, P=0.0001; R=0.424, P=0.02; R=0.739, P<0.0001).

The anti-tumor activity of BAY 1238097, BAY-7575 and BAY-5627 was mainly cytostatic as indicated by the distribution of LC50 values, which were higher than 1 μM in 86% (44/51) of the cells exposed to BAY-7575 and BAY-5627 and in 84% (43/51) of those exposed to BAY 1238097. Figure 1B and S2A shows the validation in the eight cell lines with an LC50 <1 μM with all the three BET inhibitors, and in one with higher LC50 value (U2932). Time-dependent apoptosis was observed in the eight cell lines treated for 72 or 96 hours with a dose of 500 nM. The cytostatic activity was shown by treating six DLBCL cell lines (Farage, DOHH-2, Toledo, KARPAS-422, SU-DHL-4 and WSU-DLCL2) with BAY 1238097 (500 nM, 72 hours), which induced cell cycle arrest in G1 with decreased G2/M phase (Figure 1C and S2B).

BAY 1238097 has *in vivo* anti-tumor activity in lymphoma models

We then focused on BAY 1238097 which had been characterized extensively with regard to its pharmacological and pharmacokinetic properties, using different schedules and routes of administration *in vivo,* had a very favorable overall profile (27), thus entering the early clinical evaluation (28). We assessed its *in vivo* ability to reduce tumor growth in two DLBCL models implanted in SCID female mice. The first model was obtained by engraftment of a GCB-DLBCL cell line (SU-DHL-8) (Figure 2A, S3A). BAY 1238097, given at the MTD of 15 mg/kg (p.o. using a daily schedule), significantly affected tumor growth in comparison with control group, with a T/C of 15 % on day 14 post tumor inoculation (P < 0.001). The second model was obtained by engraftment of an ABC-DLBCL cell line (OCI-LY-3) (Figure 2B, S3B). The treatment with BAY 1238097 at the MTD of 45 mg/kg (p.o. with a twice weekly schedule) significantly inhibited tumor growth as well, with a T/C of 23 % on day 48 post tumor inoculation (P < 0.001). BAY 1238097 treatments were overall well tolerated with a maximal mean body weight loss of 6% on day 9 in the SU-DHL-8 study an 9% on day 45 in the OCI-LY-3 model.

BAY 1238097 affects the gene expression of GCB DLBCL cells

To understand the mechanism of action of BAY 1238097 in DLBCL, we performed a gene expression profiling study on the cell line DOHH-2 exposed to DMSO or BAY 1238097 (500 nM) for 8, 12 or 24 hours (Figure 3A-B and Supplementary Table 1). We first looked at the genome-wide changes induced by the compound. BAY 1238097 decreased target genes of Myc, Notch and E2F, members of the NFKB/MYD88 and mTOR/AKT signaling. The upregulated transcripts were mainly represented by histones. The GEP signatures highly overlapped with the signatures obtained with other BET inhibitors and partially overlapped with HDAC or mTOR inhibitors and demethylating agents. At the gene level, 143 probes (121 annotated transcripts) were downregulated and 71 (59 annotated transcripts) upregulated. BTK, CCDC86, CCND2, CD19, CD27, FAIM, FAIM3, IL7R, IRAK1, MAPK13, MYB, MYC, PDE4B, TNFRSF13B, TNFRSF17 were among the top downregulated genes. Beside histone-coding genes, the upregulated genes included CCL5, CDKN2C, CD69, JUN, and MKNK2.

BAY 1238097 downregulates EZH2 expression and synergizes with EZH2 inhibitors

Analysis of genomic alterations in the cell lines exposed to BAY 1238097 revealed that the presence of somatic mutations in the *EZH2* gene was associated with higher sensitivity to the BET inhibitor (P=0.007), an association maintained when considering only the cell lines derived from GCB-DLBCL (P=0.025) (Figure 4A), in which mutations more frequently occur (38). An EZH2 signature obtained comparing series of follicular lymphomas with mutated *EZH2* versus wild type cases (39) appeared enriched in the transcripts high in GCB-DLBCL with higher sensitivity to BAY 1238097 (NES=1.6, P<0.01) (Figure 4B). Due to this association between EZH2 mutations and BAY 1238097 activity we evaluated whether EZH2 was regulated in a BET bromodomain dependent manner. We took advantage of publicly available ChIP-Seq data for the HBL1 DLBCL model treated with the BET inhibitor JQ1 (31). The *EZH2* upstream regulatory region presented binding of BRD4 and JQ1 treatment (500 nM, 3 hours) reduced the BET Bromodomain binding, indicating a direct effect of BET Bromodomain on the regulation of EZH2 expression (Figure 4C-D).

Based on these findings we assessed the possible therapeutic benefit of the dual inhibition of both BET Bromodomain and EZH2. To pursue this aim, we first exposed eight GCB-DLBCL cell lines (five mutated EZH2, three wild-type EZH2 protein) to BAY 1238097 and to the EZH2-inhibitor DZNep for 72 hours. Benefit was observed in three cell lines, all with mutated EZH2 (synergism in WSU-DLCL2 and KARPAS-422, additive effect in the SU-DHL-6) (Figure 5A). Similar results were obtained combining BAY 1238097 with a second, more selective, EZH2 inhibitor, GSK126: the same three *EZH2* mutated cell lines achieved a benefit from the combination treatment (Figure 5B).

Based on these data we assessed changes at protein levels of EZH2, total histone H3 and H3K27me3 after exposure to BAY 1238097 single agent and in combination with GSK126. BET inhibitor treatment was followed by a downregulation of EZH2, histone H3 and H3K27me3 levels. A stronger downregulation of H3K27me3 levels after the BAY 1238097/GSK126 combination was observed (Figure 5C). Similar results were obtained using DZNep (data not shown).

Baseline features are associated with response to BAY 1238097

The anti-proliferative activity of BAY 1238097 was not associated with *MYC*/*BCL2*/*BCL6* single/double translocations, *MLL2*, *MYD88, FOXO1* mutations, or *TP53* status. To identify genes and pathways that might predict sensitivity to the novel BET inhibitor, we compared the baseline gene expression profiles of cell lines with a BAY 1238097 IC50 lower than 500 nM versus those with a higher IC50. The analysis was limited to GCB DLBCL due to sample size. Transcripts with higher expression in the most sensitive GCB DLBCL cells (n.=10)

were enriched of genes involved in JAK/STAT, IFN and BCR signaling, while the less sensitive GCB DLBCL (n.=4) had higher expression of genes involved in cell cycle, chromatin structure, and E2F1 targets (Figure S4 and Supplementary Table 2).

BAY 1238097 shows *in vitro* synergism with the mTOR inhibitor everolimus

Based on the above-mentioned similarity between gene expression changes following exposure to BAY 1238097 and mTOR-inhibitors, BAY 1238097 was combined with the mTOR inhibitor everolimus, leading to a therapeutic benefit in 7/8 DLBCL cell lines: synergism in 2/2 ABC-DLBCL (U-2932, TMD8) and in 5/6 GCB-DLBCL (KARPAS-422, SU-DHL-6, DOHH-2, SU-DHL-8, Toledo) (Figure 3A). As shown in Figure 3B, the treatment of two DLBCL cell lines with only BAY 1238097 induced a downregulation of pAKT, which was maintained in the cell lines exposed to both compounds.

BAY 1238097 shows *in vitro* synergism with the BTK inhibitor ibrutinib

As mentioned above, a high expression of JAK/STAT and IFN signaling genes was positively associated with sensitivity to BAY 1238097, which also downregulated the NFKB/MYD88 pathway, including the BTK transcript. Among all cell lines exposed to the compound, the presence of the L265P-*MYD88* somatic mutation was associated with higher sensitivity to the BET inhibitor in ABC DLBCL cell lines (P=0.05). We assessed the combination of BAY 1238097 with the BTK-inhibitor ibrutinib and observed synergism in 2/2 ABC-DLBCL cell lines harboring the L265P *MYD88* mutation (OCI-LY-10, TMD8). No benefit was observed in the two ABC-DLBCL cell lines bearing a wild-type *MYD88* (SU-DHL-2, U-2932) (Figure 3C).

Discussion

We have evaluated the activity of three novel BET Bromodomain inhibitors BAY-7575 and BAY-5627, and BAY 1238097 in pre-clinical models of mature lymphoid tumors, focusing on the latter compound which entered clinical evaluation, and we found that: i) all three compounds had a wide anti-proliferative activity, which was mostly cytostatic; ii) BAY 1238097 affected cellular pathways relevant for the lymphoma cells; iii) sensitivity to BAY 1238097 was associated with phenotypic and genetic features; iv) BAY 1238097 reduced EZH2 expression and synergized with EZH2 inhibitors; v) BAY 1238097 synergized with mTOR and BTK inhibitors.

The anti-tumor activity of BAY-7575, BAY-5627 and BAY 1238097 was higher in cell lines derived from B than T cell lymphoma but it did not further differ based on lymphoma histotype or the presence of genetic lesions such as *MYC* gene translocation or TP53 inactivation. The three compounds shared a very similar pattern of activity across all the tested lymphoma models, which also partially correlated with what was previously observed with other BET inhibitors such as OTX015 and JQ1 (5,8). The anti-tumor activity of BAY 1238097 was furthermore confirmed in two *in vivo* DLBCL xenograft models where a strong efficacy was demonstrated when giving the compound orally using either a daily or a twice weekly schedule. As for other targeted agents (5,40), the activity was mostly cytostatic, with very few cell lines, derived from ABC DLBCL (as seen with OTX015 (5)), from GCB DLBCL and from MCL, undergoing apoptosis after 72 hours of drug exposure.

Baseline gene expression profiling is a strategy to identify mutations and features associated with response to a compound and to suggest possible combinatorial schemes. The cells with the highest sensitivity to BAY 1238097 had not only high expression levels of genes involved in the JAK/STAT, IFN and BCR signaling, but also higher incidence of somatic mutations in *EZH2* and *MYD88,* which could represent potential biomarkers. These data also suggested rational combinations to be further explored. Gain-of-function mutations of *EZH2* gene frequently occur in GCB DLBCL and follicular lymphomas (38,41). Here, both the mutation and an EZH2

gene expression signature derived from follicular lymphomas were associated with higher sensitivity to BAY 1238097 in GCB-DLBCL. This prompted us to look at the effect of BAY 1238097 on EZH2 expression and to possible therapeutic consequences. The analysis of publicly available ChIP-Seq data (31) indicated that in DLBCL EZH2 is indeed expressed in a BRD4-depenedent manner, and in accordance with the data reported by Zhao et al. (42), JQ1 can inhibit the binding. When we treated DLBCL cells with BAY 1238097 we observed a downregulation of EZH2 and, more importantly, of H3K27me3, the marker of EZH2 activity. Interestingly, this led to a synergism when we combined pharmacological inhibition of both BET Bromodomains and EZH2, suggesting that this combination of epigenetic drugs is worth further preclinical and clinical investigations.

Besides regulating EZH2 levels, BAY 1238097 decreased MYC, target genes of MYC, Notch and E2F, as well as members of the NFKB/MYD88 and mTOR/AKT signaling pathways, changes which are in line with what was seen previously with other BET inhibitors (8,11,43-45).

Finally, based on these expression changes and on data previously reported by us and others (5,21)(31,46-48), we evaluated the combination of BAY 1238097 with the BTK inhibitor ibrutinib and the mTOR inhibitor everolimus. Synergism was observed combining BAY 1238097 and the BTK inhibitor in the ibrutinib-sensitive ABC-DLBCL cell lines while no benefit was observed in ibrutinib-resistant ABC-DLBCL cells, suggesting that the addition of the BET inhibitor cannot overcome a genetically-driven resistance. In accordance to what was seen with the BET inhibitor OTX015 (5), the combination of BAY 1238097 with everolimus was highly beneficial both in ABC and in GCB DLBCL cells. Immunoblotting data suggested that the synergism could be due to decreased levels of pAKT after BET inhibitor treatment, which might attenuate the negative feedback observed after applying mTOR inhibitors alone (49).

In conclusion, the novel BET inhibitors BAY-7575 and BAY-5627, and BAY 1238097 showed a clear anti-lymphoma preclinical activity mediated by interfering with biologic processes driving the lymphoma cells. Our data also point to combination schemes targeting EZH2, mTOR and BTK alongside BET Bromodomains.

Acknowledgements

This work is lovingly dedicated to the memory of Pietro Gaudio, who died on March 11, 1996.

Authors´ Contribution

F.B, M.O. and B.H. discussed the original study design. S.S and N.S. designed and synthesized the BET inhibitors; E.B. and E.G. designed and performed experiments, interpreted data, co-wrote the manuscript; C.T. and A.A.M. performed experiments; P.L. designed and performed the *in vivo* experiments; A.R., performed gene expression profiling; I.K. and L.C., performed data mining; A.S., E.Z., M.O. and B.H. provided advice; F.B. directed the study, performed data mining, interpreted data, and co-wrote the manuscript. E.B. and E.G. equally contributed.

References

1. Filippakopoulos P, Picaud S, Mangos M, Keates T, Lambert JP, Barsyte-Lovejoy D*, et al.* Histone recognition and large-scale structural analysis of the human bromodomain family. Cell 2012;149(1):214-31.
2. Dawson MA, Kouzarides T, Huntly BJ. Targeting epigenetic readers in cancer. N Engl J Med 2012;367(7):647-57.
3. Hnisz D, Abraham BJ, Lee TI, Lau A, Saint-Andre V, Sigova AA*, et al.* Super-enhancers in the control of cell identity and disease. Cell 2013;155(4):934-47.
4. Mertz JA, Conery AR, Bryant BM, Sandy P, Balasubramanian S, Mele DA*, et al.* Targeting MYC dependence in cancer by inhibiting BET bromodomains. Proc Natl Acad Sci U S A 2011;108(40):16669-74.
5. Boi M, Gaudio E, Bonetti P, Kwee I, Bernasconi E, Tarantelli C*, et al.* The BET Bromodomain Inhibitor OTX015 Affects Pathogenetic Pathways in Preclinical B-cell Tumor Models and Synergizes with Targeted Drugs. Clin Cancer Res 2015;21(7):1628-38.

6. Dawson MA, Prinjha RK, Dittmann A, Giotopoulos G, Bantscheff M, Chan WI, *et al.* Inhibition of BET recruitment to chromatin as an effective treatment for MLL-fusion leukaemia. Nature 2011;478(7370):529-33.
7. Delmore JE, Issa GC, Lemieux ME, Rahl PB, Shi J, Jacobs HM, *et al.* BET bromodomain inhibition as a therapeutic strategy to target c-Myc. Cell 2011;146(6):904-17.
8. Chapuy B, McKeown MR, Lin CY, Monti S, Roemer MG, Qi J, *et al.* Discovery and characterization of super-enhancer-associated dependencies in diffuse large B cell lymphoma. Cancer Cell 2013;24(6):777-90.
9. Bhadury J, Nilsson LM, Muralidharan SV, Green LC, Li Z, Gesner EM, *et al.* BET and HDAC inhibitors induce similar genes and biological effects and synergize to kill in Myc-induced murine lymphoma. Proc Natl Acad Sci U S A 2014;111(26):E2721-30.
10. Bid HK, Phelps DA, Xaio L, Guttridge DC, Lin J, London C, *et al.* The Bromodomain BET Inhibitor JQ1 Suppresses Tumor Angiogenesis in Models of Childhood Sarcoma. Mol Cancer Ther 2016;15(5):1018-28.
11. Picaud S, Da Costa D, Thanasopoulou A, Filippakopoulos P, Fish PV, Philpott M, *et al.* PFI-1, a highly selective protein interaction inhibitor, targeting BET Bromodomains. Cancer Res 2013;73(11):3336-46.
12. Asangani IA, Wilder-Romans K, Dommeti VL, Krishnamurthy PM, Apel IJ, Escara-Wilke J, *et al.* BET Bromodomain Inhibitors Enhance Efficacy and Disrupt Resistance to AR Antagonists in the Treatment of Prostate Cancer. Mol Cancer Res 2016;14(4):324-31.
13. Liu S, Walker SR, Nelson EA, Cerulli R, Xiang M, Toniolo PA, *et al.* Targeting STAT5 in hematologic malignancies through inhibition of the bromodomain and extra-terminal (BET) bromodomain protein BRD2. Mol Cancer Ther 2014;13(5):1194-205.
14. Emadali A, Rousseaux S, Bruder-Costa J, Rome C, Duley S, Hamaidia S, *et al.* Identification of a novel BET bromodomain inhibitor-sensitive, gene regulatory circuit that controls Rituximab response and tumour growth in aggressive lymphoid cancers. EMBO Mol Med 2013;5(8):1180-95.
15. Lockwood WW, Zejnullahu K, Bradner JE, Varmus H. Sensitivity of human lung adenocarcinoma cell lines to targeted inhibition of BET epigenetic signaling proteins. Proc Natl Acad Sci U S A 2012;109(47):19408-13.
16. Puissant A, Frumm SM, Alexe G, Bassil CF, Qi J, Chanthery YH, *et al.* Targeting MYCN in neuroblastoma by BET bromodomain inhibition. Cancer Discov 2013;3(3):308-23.
17. Henssen A, Althoff K, Odersky A, Beckers A, Koche R, Speleman F, *et al.* Targeting MYCN-Driven Transcription By BET-Bromodomain Inhibition. Clin Cancer Res 2016;22(10):2470-81.
18. Vazquez R, Riveiro ME, Astorgues-Xerri L, Odore E, Rezai K, Erba E, *et al.* The bromodomain inhibitor OTX015 (MK-8628) exerts anti-tumor activity in triple-negative breast cancer models as single agent and in combination with everolimus. Oncotarget 2016.
19. Riveiro ME, Astorgues-Xerri L, Vazquez R, Frapolli R, Kwee I, Rinaldi A, *et al.* OTX015 (MK-8628), a novel BET inhibitor, exhibits antitumor activity in non-small cell and small cell lung cancer models harboring different oncogenic mutations. Oncotarget 2016.
20. Rhyasen GW, Hattersley MM, Yao Y, Dulak A, Wang W, Petteruti P, *et al.* AZD5153: A Novel Bivalent BET Bromodomain Inhibitor Highly Active against Hematologic Malignancies. Mol Cancer Ther 2016;15(11):2563-74.
21. Gaudio E, Tarantelli C, Ponzoni M, Odore E, Rezai K, Bernasconi E, *et al.* Bromodomain inhibitor OTX015 (MK-8628) combined with targeted agents shows strong in vivo antitumor activity in lymphoma. Oncotarget 2016.
22. Boi M, Todaro M, Vurchio V, Yang SN, Moon J, Kwee I, *et al.* Therapeutic efficacy of the bromodomain inhibitor OTX015/MK-8628 in ALK-positive anaplastic large cell lymphoma: an alternative modality to overcome resistant phenotypes. Oncotarget 2016.
23. Hogg SJ, Newbold A, Vervoort SJ, Cluse LA, Martin BP, Gregory GP, *et al.* BET Inhibition Induces Apoptosis in Aggressive B-Cell Lymphoma via Epigenetic Regulation of BCL-2 Family Members. Mol Cancer Ther 2016;15(9):2030-41.
24. Stathis A, Zucca E, Bekradda M, Gomez-Roca C, Delord JP, de La Motte Rouge T, *et al.* Clinical Response of Carcinomas Harboring the BRD4-NUT Oncoprotein to the Targeted Bromodomain Inhibitor OTX015/MK-8628. Cancer Discov 2016.
25. Berthon C, Raffoux E, Thomas X, Vey N, Gomez-Roca C, Yee K, *et al.* Bromodomain inhibitor OTX015 in patients with acute leukaemia: a dose-escalation, phase 1 study. Lancet Haematol 2016;3(4):e186-95.
26. Amorim S, Stathis A, Gleeson M, Iyengar S, Magarotto V, Leleu X, *et al.* Bromodomain inhibitor OTX015 in patients with lymphoma or multiple myeloma: a dose-escalation, open-label, pharmacokinetic, phase 1 study. Lancet Haematol 2016;3(4):e196-204.
27. Lejeune P, Sugawara T, Gelato KA, Ellinger-Ziegelbauer H, Fernandez-Montalvan AE, Schmees N, *et al.* BAY 1238097, a novel BET inhibitor with strong efficacy in hematological tumor models. Cancer Res 2015;75:(3524).
28. Postel-Vinay S, Herbschleb K, Massard C, Woodcock V, Ocker M, Wilkinson G, *et al.* First-in-human phase I dose escalation study of the Bromodomain and Extra-Terminal motif (BET) inhibitor BAY 1238097 in subjects with advanced malignancies. Eur J Cancer 2016;68(Supplement 1):S7-S8.

29. Boi M, Rinaldi A, Kwee I, Bonetti P, Todaro M, Tabbo F*, et al.* PRDM1/BLIMP1 is commonly inactivated in anaplastic large T-cell lymphoma. Blood 2013;122(15):2683-93.
30. Mensah AA, Kwee I, Gaudio E, Rinaldi A, Ponzoni M, Cascione L*, et al.* Novel HDAC inhibitors exhibit pre-clinical efficacy in lymphoma models and point to the importance of CDKN1A expression levels in mediating their anti-tumor response. Oncotarget 2015;6(7):5059-71.
31. Ceribelli M, Kelly PN, Shaffer AL, Wright GW, Xiao W, Yang Y*, et al.* Blockade of oncogenic IkappaB kinase activity in diffuse large B-cell lymphoma by bromodomain and extraterminal domain protein inhibitors. Proc Natl Acad Sci U S A 2014;111(31):11365-70.
32. Boi M, Gaudio E, Bonetti P, Kwee I, Bernasconi E, Tarantelli C*, et al.* The BET Bromodomain Inhibitor OTX015 Affects Pathogenetic Pathways in Preclinical B-cell Tumor Models and Synergizes with Targeted Drugs. Clinical cancer research : an official journal of the American Association for Cancer Research 2015;21(7):1628-38.
33. Smyth GK. Linear models and empirical Bayes methods for assessing differential expression in microarray experiments. Stat Appl Genet Mol Biol 2004;3:Article3.
34. Subramanian A, Tamayo P, Mootha VK, Mukherjee S, Ebert BL, Gillette MA*, et al.* Gene set enrichment analysis: a knowledge-based approach for interpreting genome-wide expression profiles. Proc Natl Acad Sci U S A 2005;102(43):15545-50.
35. Shaffer AL, Wright G, Yang L, Powell J, Ngo V, Lamy L*, et al.* A library of gene expression signatures to illuminate normal and pathological lymphoid biology. Immunol Rev 2006;210:67-85.
36. Rainer J, Sanchez-Cabo F, Stocker G, Sturn A, Trajanoski Z. CARMAweb: comprehensive R- and bioconductor-based web service for microarray data analysis. Nucleic Acids Res 2006;34(Web Server issue):W498-503.
37. Chou TC. Drug combination studies and their synergy quantification using the Chou-Talalay method. Cancer Res 2010;70(2):440-6.
38. Testoni M, Zucca E, Young KH, Bertoni F. Genetic lesions in diffuse large B-cell lymphomas. Ann Oncol 2015;26(6):1069-80.
39. Guo S, Chan JK, Iqbal J, McKeithan T, Fu K, Meng B*, et al.* EZH2 mutations in follicular lymphoma from different ethnic groups and associated gene expression alterations. Clin Cancer Res 2014;20(12):3078-86.
40. Ezell SA, Mayo M, Bihani T, Tepsuporn S, Wang S, Passino M*, et al.* Synergistic induction of apoptosis by combination of BTK and dual mTORC1/2 inhibitors in diffuse large B cell lymphoma. Oncotarget 2014;5(13):4990-5001.
41. Chase A, Cross NC. Aberrations of EZH2 in cancer. Clin Cancer Res 2011;17(9):2613-8.
42. Wu X, Liu D, Tao D, Xiang W, Xiao X, Wang M*, et al.* BRD4 Regulates EZH2 Transcription through Upregulation of C-MYC and Represents a Novel Therapeutic Target in Bladder Cancer. Mol Cancer Ther 2016;15(5):1029-42.
43. Gupta SS, Maetzig T, Maertens GN, Sharif A, Rothe M, Weidner-Glunde M*, et al.* Bromo- and extraterminal domain chromatin regulators serve as cofactors for murine leukemia virus integration. J Virol 2013;87(23):12721-36.
44. Cheng Z, Gong Y, Ma Y, Lu K, Lu X, Pierce LA*, et al.* Inhibition of BET bromodomain targets genetically diverse glioblastoma. Clin Cancer Res 2013;19(7):1748-59.
45. Adhikary G, Grun D, Balasubramanian S, Kerr C, Huang JM, Eckert RL. Survival of skin cancer stem cells requires the Ezh2 polycomb group protein. Carcinogenesis 2015;36(7):800-10.
46. Lee DH, Qi J, Bradner JE, Said JW, Doan NB, Forscher C*, et al.* Synergistic effect of JQ1 and rapamycin for treatment of human osteosarcoma. Int J Cancer 2015;136(9):2055-64.
47. Vázquez R, Astorgues-Xerri L, Riveiro ME, Beltrame L, Marchini S, Bertoni F*, et al.* Abstract 3526: OTX015 effects in triple-negative breast cancer (TNBC) models are independent of hypoxia conditions and synergistic with other anticancer agents. Cancer Res 2015;75(15 Supplement):3526-.
48. Sun B, Shah B, Fiskus W, Qi J, Rajapakshe K, Coarfa C*, et al.* Synergistic activity of BET protein antagonist-based combinations in mantle cell lymphoma cells sensitive or resistant to ibrutinib. Blood 2015;126(13):1565-74.
49. Gupta M, Ansell SM, Novak AJ, Kumar S, Kaufmann SH, Witzig TE. Inhibition of histone deacetylase overcomes rapamycin-mediated resistance in diffuse large B-cell lymphoma by inhibiting Akt signaling through mTORC2. Blood 2009;114(14):2926-35.

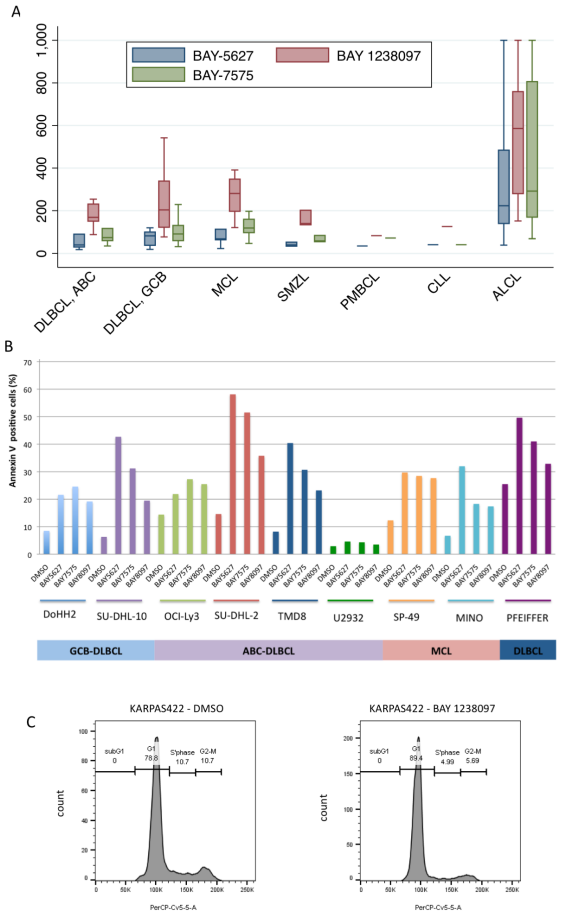

Figure 1. BAY-7575, BAY-5627 and BAY 1238097 have anti-proliferative activity *in vitro* and *in vivo* in models of B-cell lymphomas. (A) IC50 value distribution in 51 lymphoma cell lines. In each box-plot, the line in the middle of the box represents the median and the box extends from the 25th to the 75th percentile (interquartile range, IQ); the whiskers extend to the upper and lower adjacent values (i.e., ±1.5 IQ); outside values have been omitted from the figure. Y-axis, IC50 values in nM. "DLBCL, ABC", activated B-cell type diffuse large B-cell lymphoma (n.=7); "DLBCL, GCB", germinal center B-cell type diffuse large B-cell lymphoma (n.=20); "MCL", mantle cell lymphoma (n.=10); "SMZL", splenic marginal zone lymphoma (n.=3); "PMBCL", primary mediastinal large cell lymphoma (n.=1); "CLL", chronic lymphocytic leukemia (n.=1); "ALCL", anaplastic large T cell lymphoma (n.=9). Y-axis, IC50 values in nM. **(B)** Apoptosis was evaluated by Annexin-V/7-AAD staining in several cell lines exposed to 500 nM of each compounds for 72 hours. **(C)** Cell cycle analysis of cells treated with BAY 1238097 (500 nM for 72 hours).

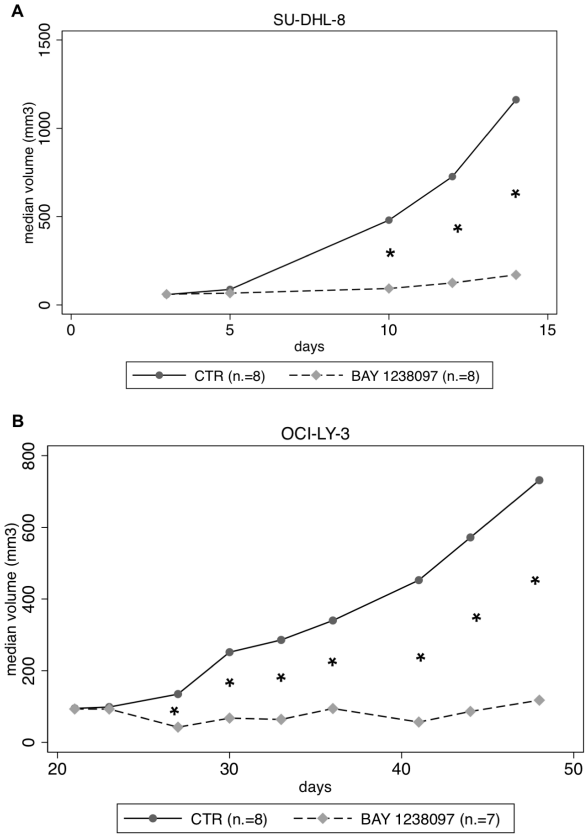

Figure 2. BAY 1238097 has *in vivo* anti-proliferative activity in models of diffuse large B-cell lymphoma. (A) SCID mice subcutaneously inoculated with the GCB DLBCL SU-DHL-8 cell line and treated with BAY 1238097 (n.=8) or vehicle control (n.=8): tumor volumes differences between treated and control mice were statistically significant starting on day 10. *, P < 0.05. Y-axis: median tumor volumes. X-axis, days post inoculation **(B)**. SCID mice subcutaneously inoculated with the ABC DLBCL OCI-LY-3 cell line and treated with BAY 1238097 (n.=7) or vehicle control (n.=8): tumor volumes differences between treated and control mice were statistically significant starting on day 27. *, P < 0.05. Y-axis: median tumor volumes. X-axis, days post inoculation.

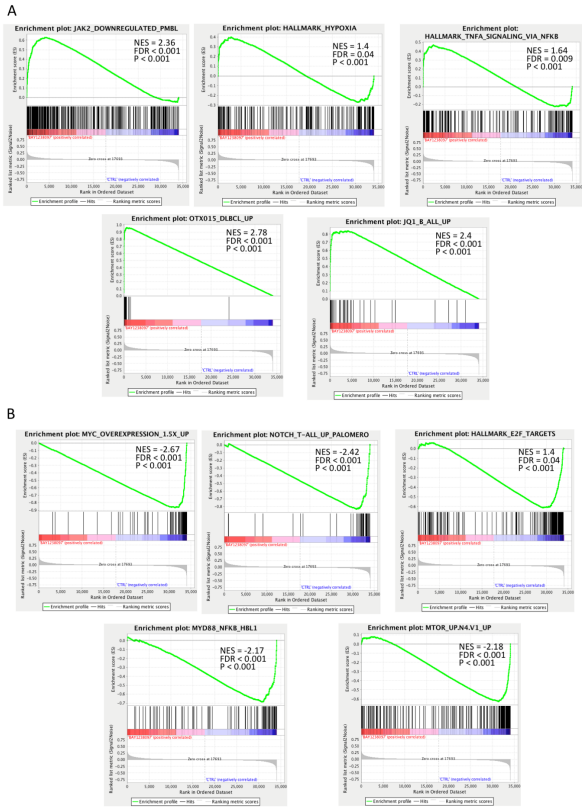

Figure 3. BAY 1238097 affects the gene expression of GCB DLBCL cells. Representative GSEA plots illustrating the gene-set enrichment in genes upregulated **(A)** and downregulated **(B)** in DOHH-2 cell line after BAY 1238097 exposure. FDR, false discovery rate; NES, normalized enrichment score.

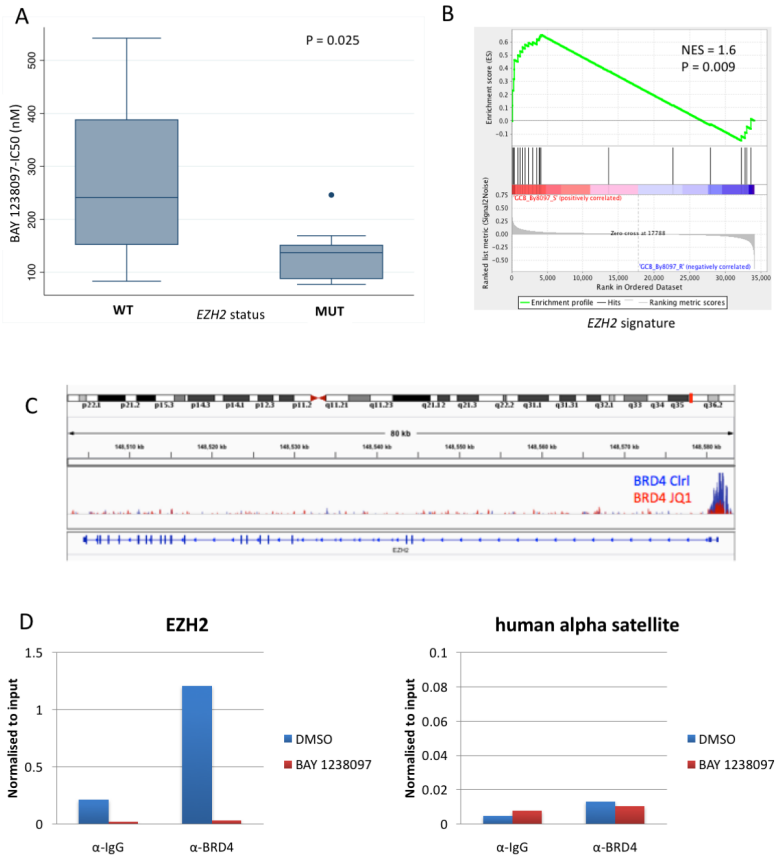

Figure 4. *EZH2* mutational status is associated with sensitivity to BAY 1238097 and both JQ1 and BAY 1238097 decrease BRD4 binding to EZH2 promoter region. (A) *EZH2* mutation in GCB-DLBCL was associated with higher sensitivity to BAY 1238097. Box-plots present the distribution of IC50 values in ten *EZH2* wild-type vs. seven mutated GCB cell lines. **(B)** EZH2 signature from follicular lymphomas with or without *EZH2* mutation was associated with higher sensitivity in GCB-DLBCL cell lines. **(C)** Decreased BRD4 binding to the upstream regulatory regions of *EZH2* in HBL1 ABC-DLBCL cells following treatment with JQ1: ChIP-Seq reads at the *EZH2* gene locus showing BRD4 binding in HBL1 ABC-DLBCL cells exposed to DMSO (blue) or 500 nM JQ1 (red) for 3 hours. The red and blue tracks have been overlaid to better show the reduction in BRD4 binding after JQ1 exposure. The lower panel shows the *EZH2* gene structure. **(D)** Decreased BRD4 binding to the upstream regulatory regions of *EZH2* in DOHH-2 GCB-DLBCL cells following treatment with BAY 1238097 (500 nM for 3 hours). Cells were fixed with formaldehyde and subjected to the Chromatin Immunoprecipitation (ChIP) assay. Anti-IgG served as a negative control for the ChIP assay. Quantitative real-time PCR showed the enrichment of BRD4 binding in the upstream regulatory regions of *EZH2*, which decreased following treatment with BAY 1238097. Amplification of the centromeric human alpha satellite sequence served as a negative control. For each primer set, results were normalized to total input chromatin DNA samples.

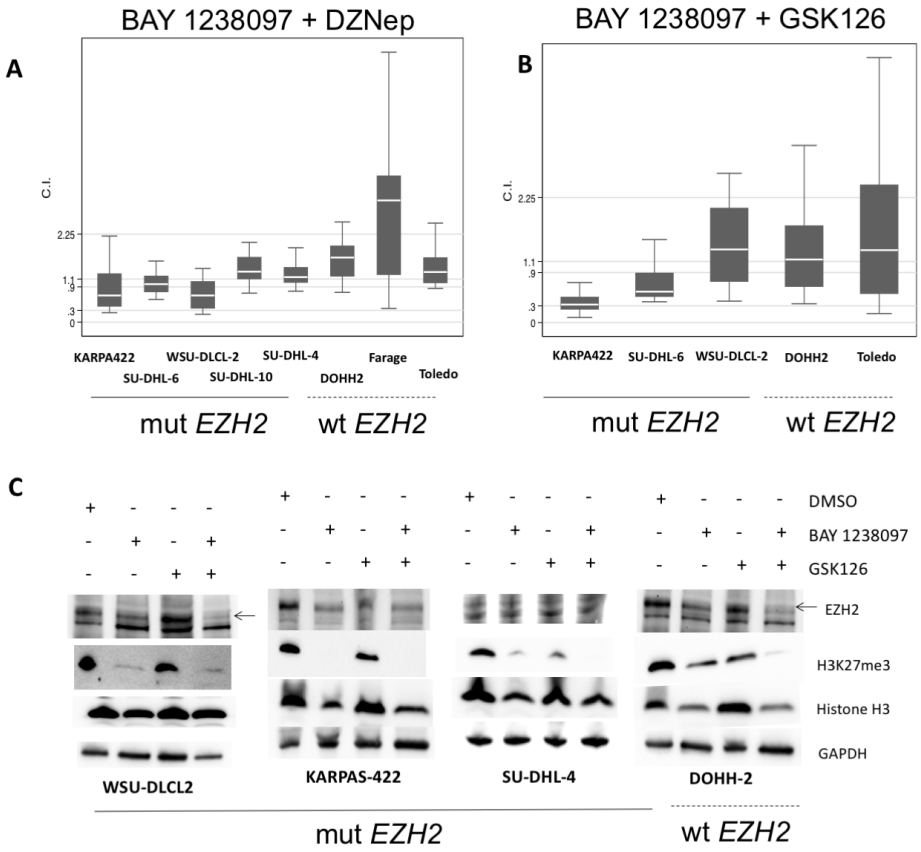

Figure 5. BAY 1238097 shows *in vitro* synergism with EZH2 inhibitors with a decrease in EZH2 protein levels and H3K27me3. BAY 1238097 was tested in combination with the EZH2 inhibitor DZNep **(A)** or with GSK126 **(B)** in *EZH2* mutant and *EZH2* wild-type GCB-DLBCL cell lines. In each box-plot, the line in the middle of the box represents the median and the box extends from the 25th to the 75th percentile (interquartile range, IQ); the whiskers extend to the upper and lower adjacent values (i.e., ±1.5 IQ); outside values have been omitted from the figure. Y-axis: combination index (CI) values (<0.3, strong synergism; 0.3-0.9, synergism; 0.9-1.1, additive effect; > 1.1, no benefit/antagonism. **(C)** Four GCB-DLBCL cells lines (1 wild-type, 3 mutated *EZH2*) were treated with 500 nM BAY 1238097 or with an EZH2 inhibitor (DZNep and GSK126, both used at the concentration of 500 nM) as single agents and combination for 72 hours. The arrow indicates the EZH2 correct band. DMSO alone was added as negative control cells. Membranes were hybridized with antibodies against EZH2, H3K27me3, histone H3 and GAPDH.

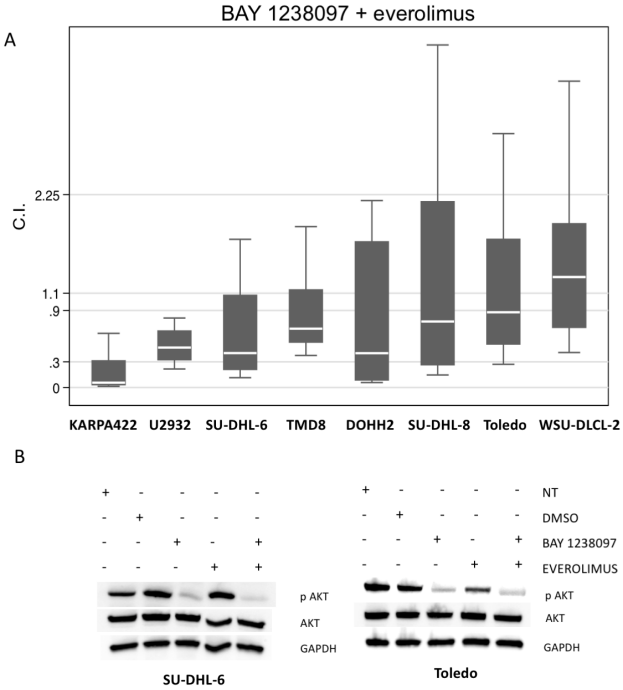

Figure 6. BAY 1238097 shows *in vitro* synergism with the mTOR inhibitor everolimus. (A) BAY 1238097 was tested in combination with the mTOR inhibitor everolimus in ABC-DLBCL and GCB-DLBCL cell lines. **(B)** Two GCB-DLBCL cell lines were treated with 500 nM BAY 1238097 or with 100 nM everolimus as single agents and in combination for 72 hours. Untreated cells and DMSO-treated cells were added as negative controls. Membranes were hybridized with antibodies against phospho-mTOR, phospho-AKT, AKT, or GAPDH. Y-axis: combination index (CI) values (<0.3, strong synergism; 0.3-0.9, synergism; 0.9-1.1, additive effect; > 1.1, no benefit/antagonism). In each box-plot, the line in the middle of the box represents the median and the box extends from the 25th to the 75th percentile (interquartile range, IQ); the whiskers extend to the upper and lower adjacent values (i.e., 1.5 IQ) and outside values have been omitted from the figure.